Eidgenössische Technische Hochschule Zürich
Swiss Federal Institute of Technology Zurich

The Essence of Matrix Converters

Johann W. Kolar and Thomas Friedli

Swiss Federal Institute of Technology (ETH) Zurich
Power Electronic Systems Laboratory
www.pes.ee.ethz.ch

Outline

- Review of Conventional AC-AC Converters

- Derivation of MC Topologies
- Indirect MC - IMC

- Direct (Conventional) MC - CMC
- Extended MC Topologies

- 

- Comparative Evaluation of AC-AC Converters
- Conclusions / Discussion

Classification of Three-Phase AC-AC Converters

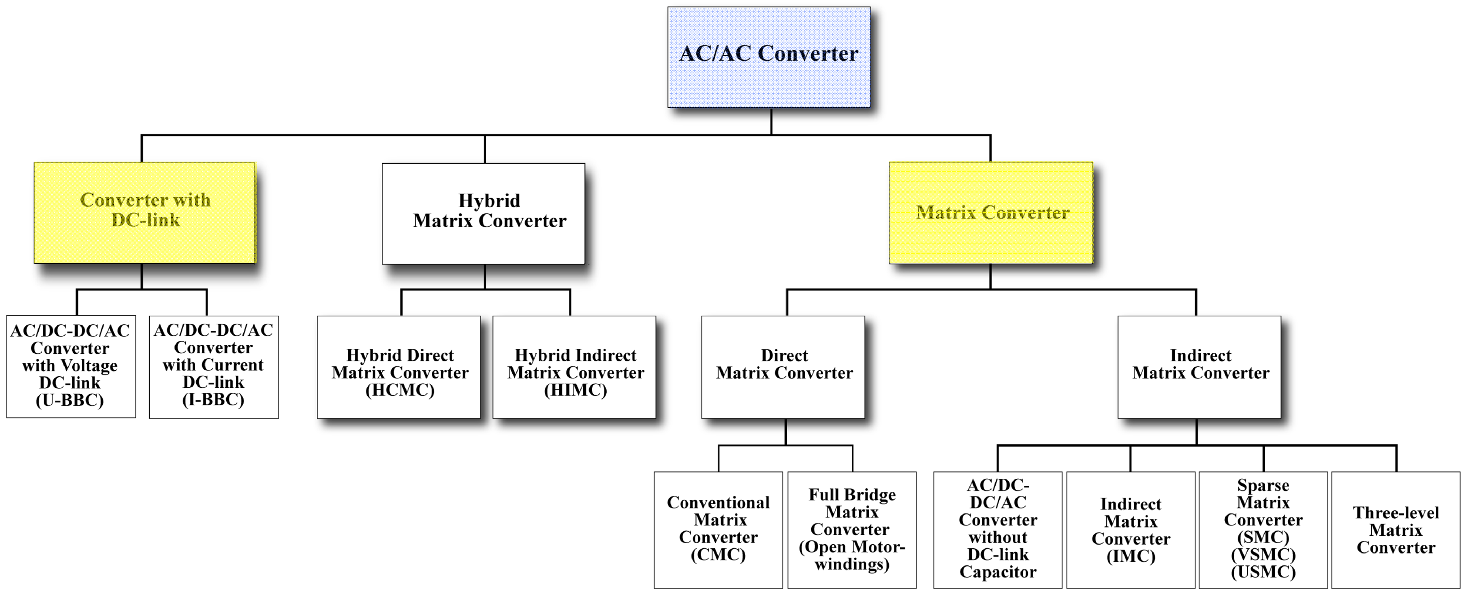

- *Converters with DC-link*
- *Hybrid Converters*
- *Indirect / Direct Matrix Converters*

DC-link AC-AC Converter Topologies

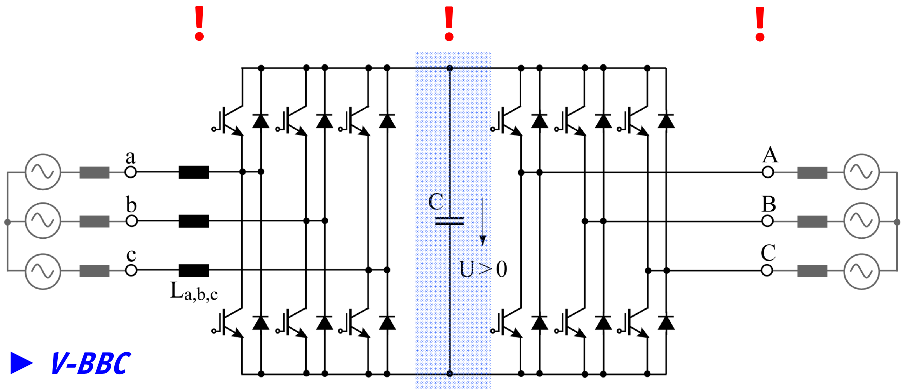

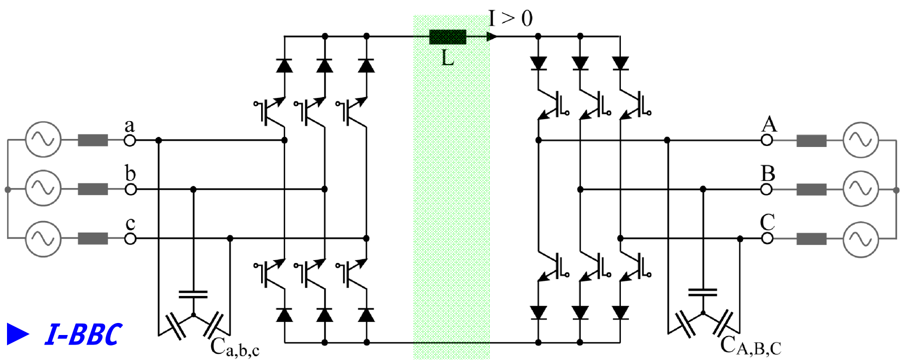

$$P = \frac{3}{2}\hat{U}_1 \cdot \hat{I}_1 \cos\Phi_1$$

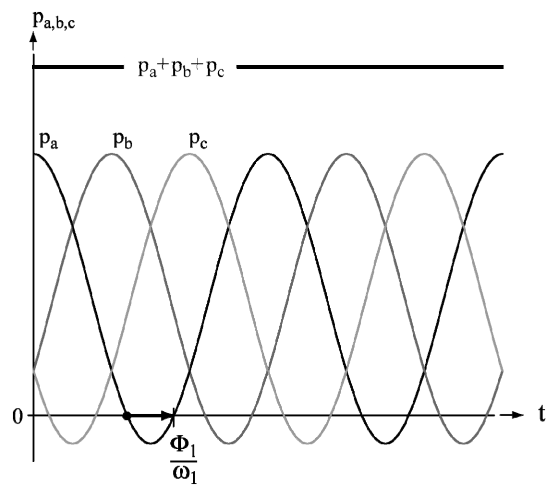

Symmetric Three-Phase Mains

Phase Voltages

$$u_a = \hat{U}_1 \cos(\omega_1 t)$$
$$u_b = \hat{U}_1 \cos\left(\omega_1 \left(t - \frac{T}{3}\right)\right)$$
$$u_c = \hat{U}_1 \cos\left(\omega_1 \left(t + \frac{T}{3}\right)\right)$$

Phase Currents

$$i_a = \hat{I}_1 \cos(\omega_1 t - \Phi_1)$$
$$i_b = \hat{I}_1 \cos\left(\omega_1 \left(t - \frac{T}{3}\right) - \Phi_1\right)$$
$$i_c = \hat{I}_1 \cos\left(\omega_1 \left(t + \frac{T}{3}\right) - \Phi_1\right)$$

Instantaneous Power

$$p(t) = u_a i_a + u_b i_b + u_c i_c = \frac{P}{3}(1 + \cos 2\omega_1 t) + \frac{Q}{3}\sin 2\omega_1 t + \frac{P}{3}\left(1 + \cos 2\omega_1 \left(t - \frac{T}{3}\right)\right) + \frac{Q}{3}\sin 2\omega_1 \left(t - \frac{T}{3}\right) + \frac{P}{3}\left(1 + \cos 2\omega_1 \left(t + \frac{T}{3}\right)\right) + \frac{Q}{3}\sin 2\omega_1 \left(t + \frac{T}{3}\right)$$

$$P = \frac{3}{2}\hat{U}_1 \cdot \hat{I}_1 \cos \Phi_1$$
$$Q = \frac{3}{2}\hat{U}_1 \cdot \hat{I}_1 \sin \Phi_1$$

$$p(t) = \frac{P}{3}(1 + \cos 2\omega_1 t) + \frac{P}{3}\left(1 + \cos 2\omega_1 \left(t - \frac{T}{3}\right)\right) + \frac{P}{3}\left(1 + \cos 2\omega_1 \left(t + \frac{T}{3}\right)\right) = 3\frac{P}{3} = P$$

All-SiC JFET I-BBC Prototype

- P_{out} = 2.9 kVA
- f_S = 200 kHz
- 2.4 kVA / liter (42 W/in^3)
- 230 x 80 x 65 mm^3

200V/div
5A/div

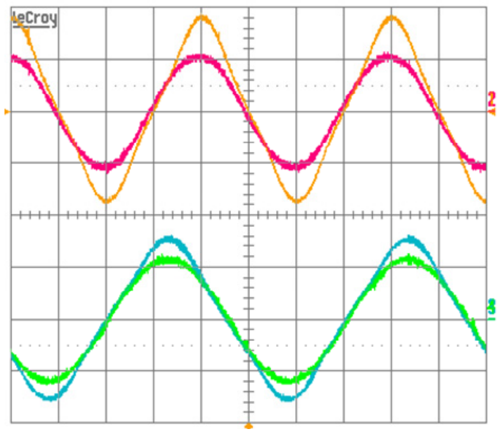

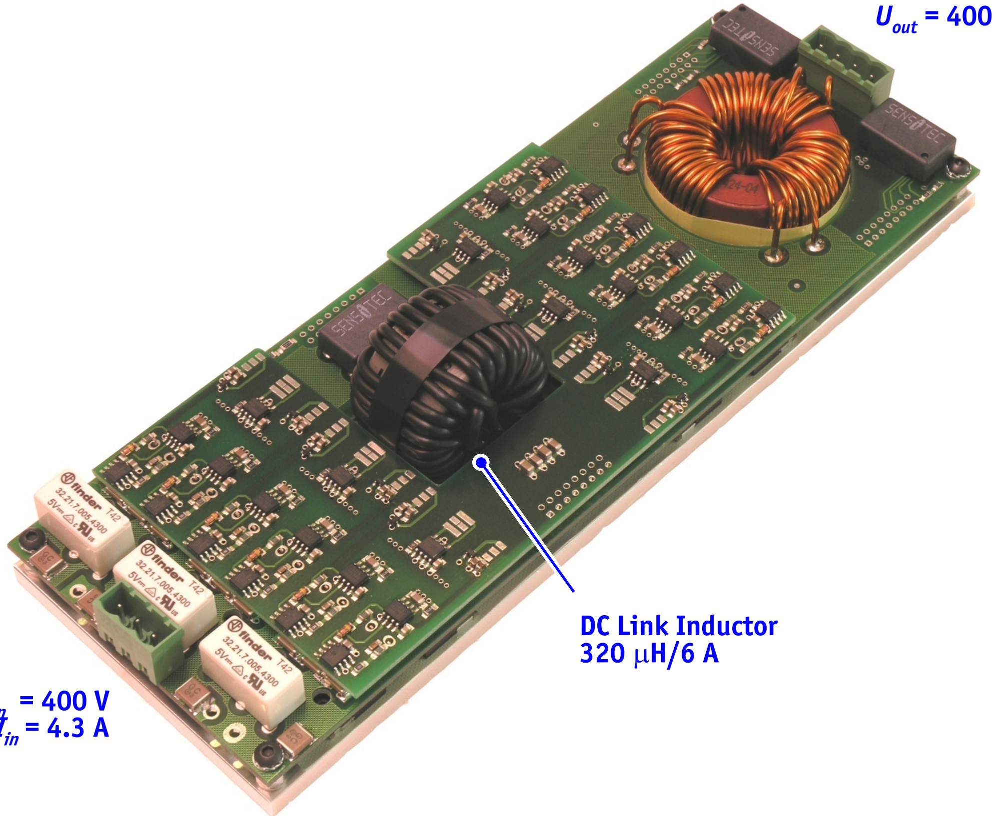

Basic Matrix Converter Topologies

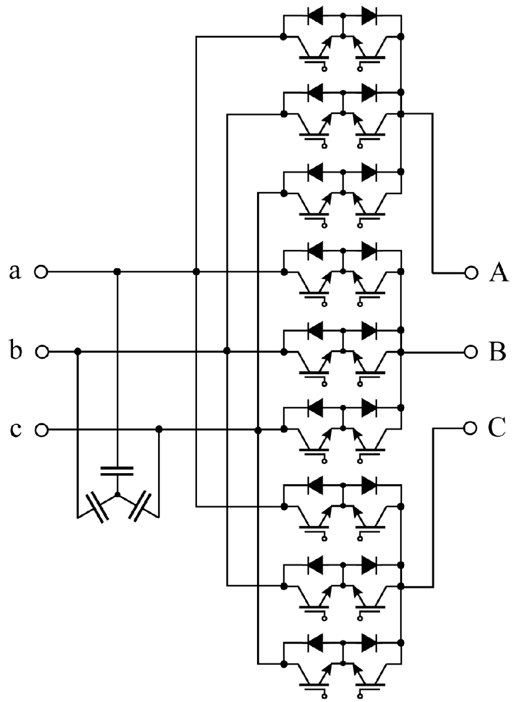

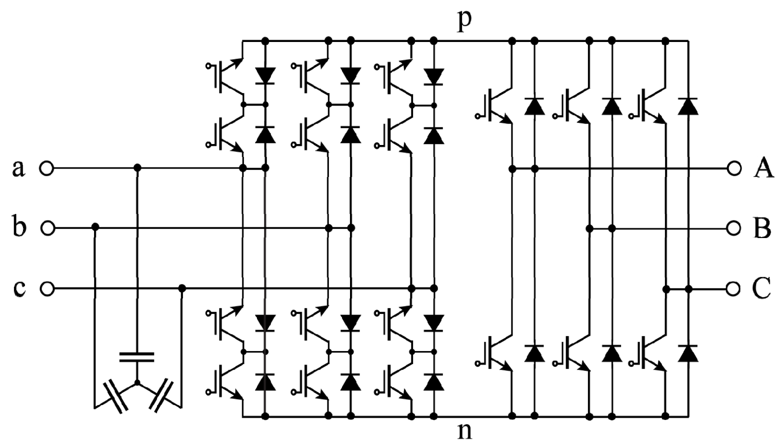

$$\frac{Q}{3}\left(\sin 2\omega_1 t + \sin 2\omega_1\left(t - \frac{T}{3}\right) + \sin 2\omega_1\left(t + \frac{T}{3}\right)\right) \equiv 0$$

V-BBC

Voltage Space Vectors
Modulation
DC Link Current

VSI Space Vector Modulation (1)

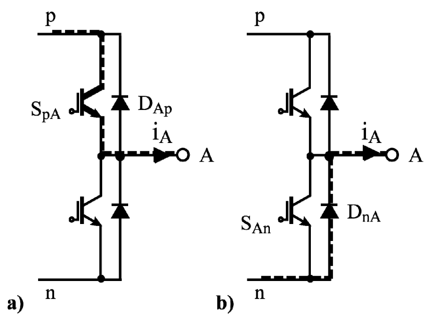

$$\vec{u}_{2,j} = \frac{2}{3}\left(u_{A,j} + \underline{a}u_{B,j} + \underline{a}^2 u_{C,j}\right)$$

$$u_{0,j} = \frac{1}{3}\left(u_{A,j} + u_{B,j} + u_{C,j}\right)$$

Output Voltage Reference Value

$$\vec{u}_2^* = \hat{U}_2^* \mathrm{e}^{j\varphi_{\vec{u}_2^*}} = \hat{U}_2^* \mathrm{e}^{j\omega_2^* t}$$

$$M_2 = \frac{\hat{U}_2^*}{U/2}$$

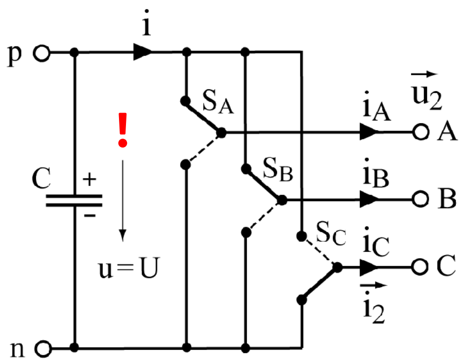

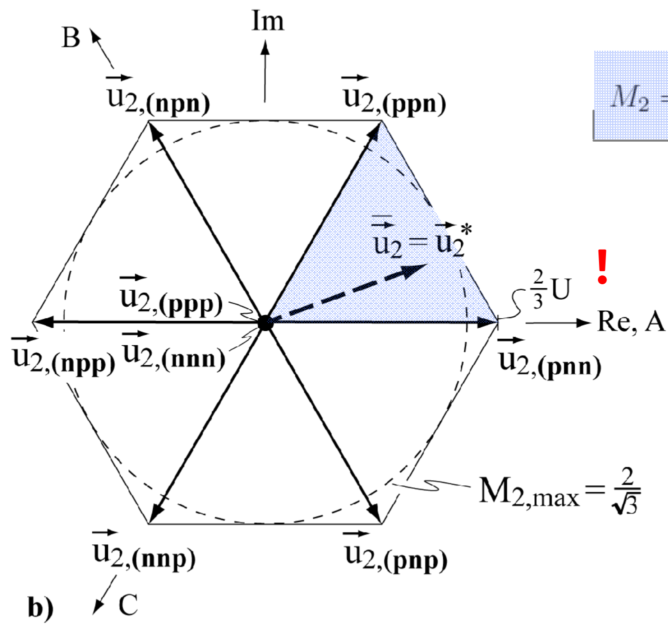

VSI Space Vector Modulation (2)

$$M_{2,\max} = \frac{\hat{U}^*_{2,\max}}{U/2} = \frac{2}{\sqrt{3}}$$

Switching State Sequence

$$\ldots \Big|_{t_\mu = 0} \quad (nnn) - (pnn) - (ppn) - (ppp) \Big|_{t_\mu = T_P/2}$$

$$(ppp) - (ppn) - (pnn) - (nnn) \Big|_{t_\mu = T_P} \quad \ldots$$

Formation of the Output Voltage

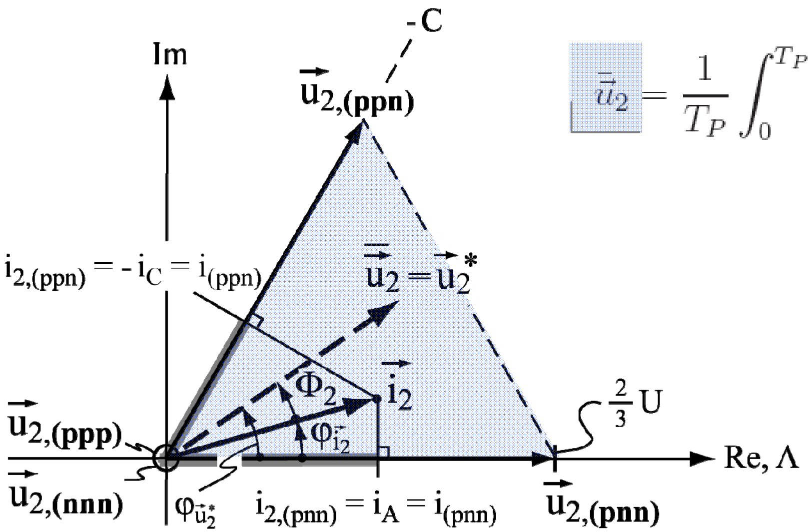

$$\bar{\vec{u}}_2 = \frac{1}{T_P}\int_0^{T_P} \vec{u}_{2,j}\, \mathrm{d}t_\mu = d_{(pnn)} \cdot \vec{u}_{2,(pnn)} + d_{(ppn)} \cdot \vec{u}_{2(ppn)}$$

$$= d_{(pnn)} \frac{2}{3} U + d_{(ppn)} \frac{2}{3} U \mathrm{e}^{j\pi/3}$$

$$= \vec{u}_2^*$$

Relative On-times

$$d_{(ppn)} = \frac{\sqrt{3}}{2} M_2 \sin\left(\varphi_{\vec{u}_2^*}\right)$$

$$d_{(pnn)} = \frac{\sqrt{3}}{2} M_2 \sin\left(\frac{\pi}{3} - \varphi_{\vec{u}_2^*}\right)$$

VSI Space Vector Modulation (3)

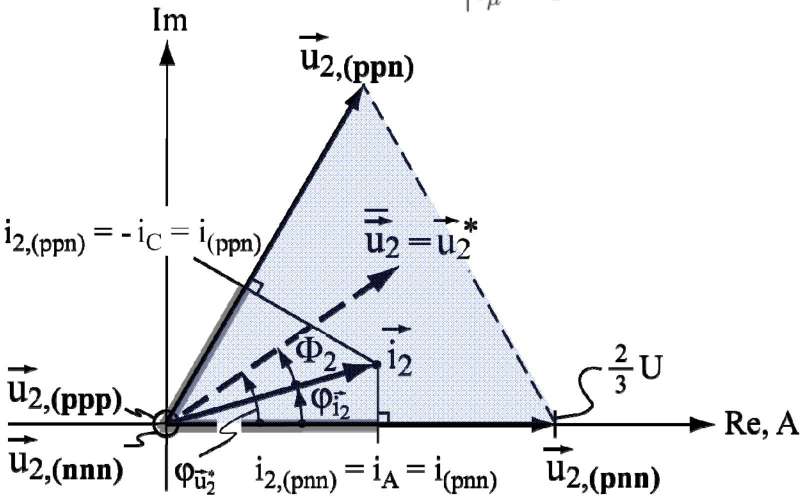

Freewheeling On-time

$$d_{(nnn)} + d_{(ppp)} = 1 - (d_{(ppn)} + d_{(pnn)})$$

Discontinuous Modulation

$$\cdots \Big|t_\mu = 0\ (p\underline{n}n) - (\underline{p}pn) - (\underline{p}pp) \Big|t_\mu = T_P/2\ (\underline{p}pp) - (\underline{p}pn) - (\underline{p}nn) \Big|t_\mu = T_P \cdots$$

$$\cdots \Big|t_\mu = 0\ (pp\underline{n}) - (pn\underline{n}) - (nn\underline{n}) \Big|t_\mu = T_P/2\ (nn\underline{n}) - (pn\underline{n}) - (pp\underline{n}) \Big|t\mu = T_P \cdots$$

Space Vector Orientation

$$\frac{d_{(ppn)}}{d_{(pnn)}} = \frac{\sin\left(\varphi_{\vec{u}_2^*}\right)}{\sin\left(\frac{\pi}{3} - \varphi_{\vec{u}_2^*}\right)}$$

Modulation Limit

$$M_{2,\max} = \frac{\hat{U}^*_{2,\max}}{U/2} = \frac{2}{\sqrt{3}}$$

VSI Space Vector Modulation (4)

DC-link Current Shape

$$i_j = i_{2,j}$$

$$i_{(nnn)} = 0$$
$$i_{(nnp)} = i_C$$
$$i_{(npn)} = i_B$$
$$i_{(npp)} = i_B + i_C = -i_A$$
$$i_{(pnn)} = i_A$$
$$i_{(pnp)} = i_A + i_C = -i_B$$
$$i_{(ppn)} = i_A + i_B = -i_C$$
$$i_{(ppp)} = 0$$

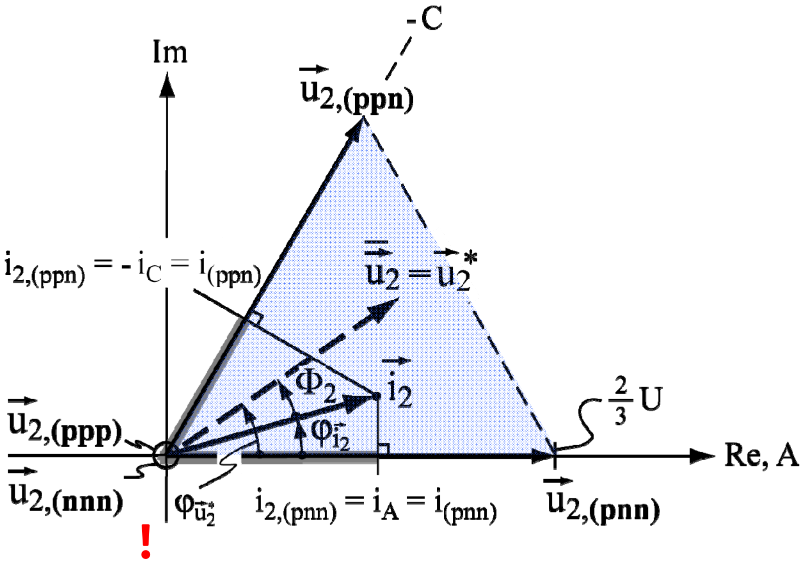

Local Average Value

$$\bar{i} = \frac{1}{T_P}\int_0^{T_P} i_j \, \mathrm{d}t_\mu$$

$$\bar{i} = -i_C d_{(ppn)} + i_A d_{(pnn)}$$

VSI Space Vector Modulation (5)

Local DC-link Current Shape

$$\bar{i} = I = \frac{3}{4} M_2 \hat{I}_2 \cos \Phi_2$$

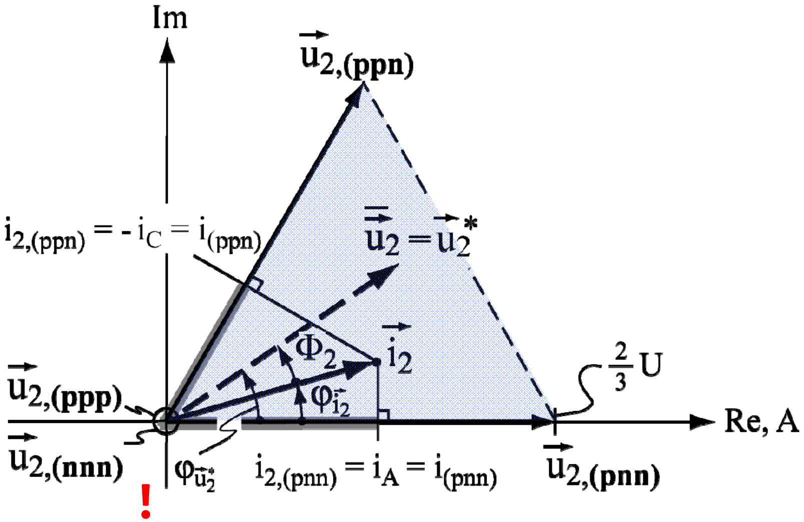

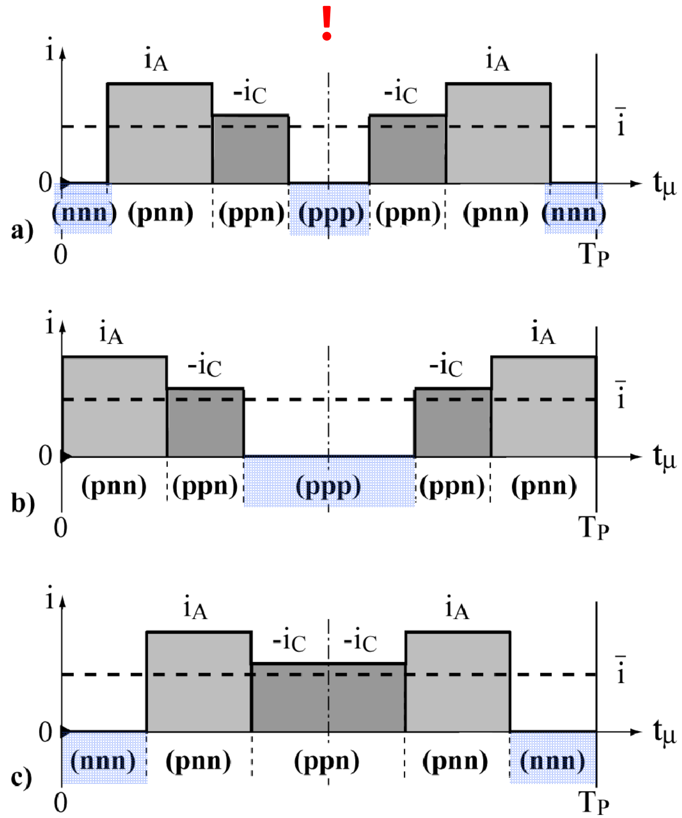

VSI DC-link Current Waveform

Influence of Output Voltage Phase Displacement Φ_2 on DC-link Current Waveform

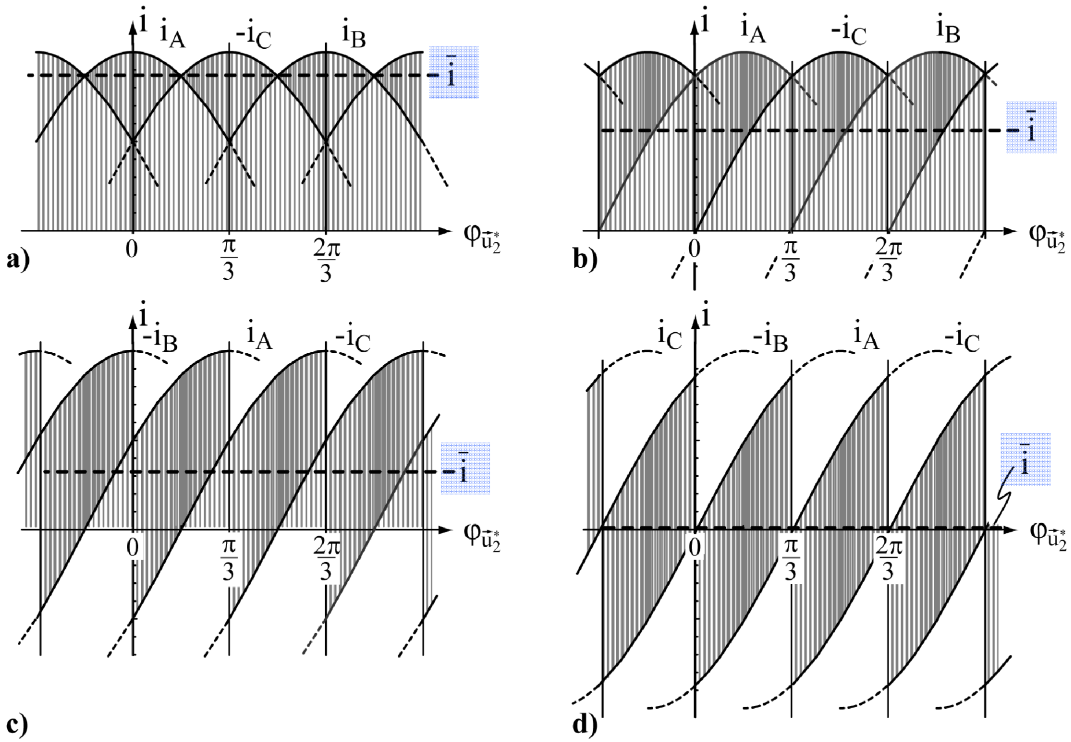

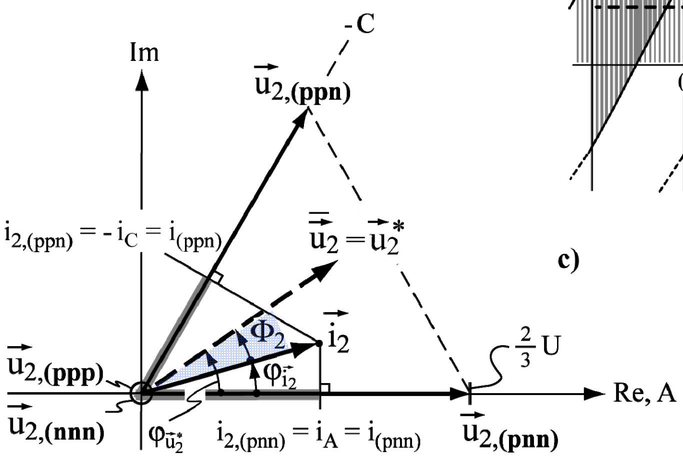

$$\bar{i} = I = \frac{3}{4} M_2 \hat{I}_2 \cos \Phi_2 \qquad M_2 = 2/\sqrt{3}$$

VSI Functional Equivalent Circuit

Voltage Conversion

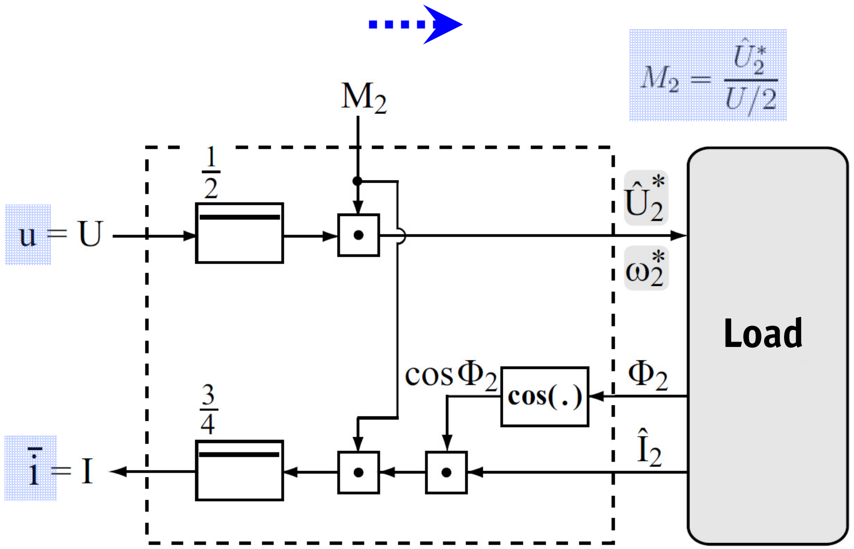

$$M_2 = \frac{\hat{U}_2^*}{U/2}$$

$$\bar{i} = I = \frac{3}{4} M_2 \hat{I}_2 \cos \Phi_2$$

Current Conversion

I-BBC

Current Space Vectors
Modulation
DC Link Voltage

CSR Commutation & Equivalent Circuit

Forced Commutation

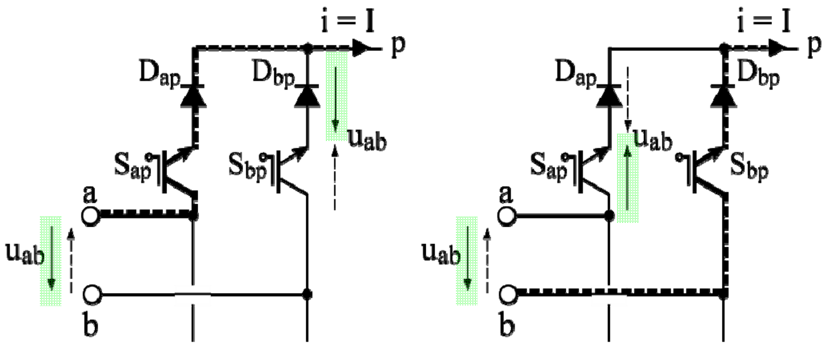

Natural Commutation

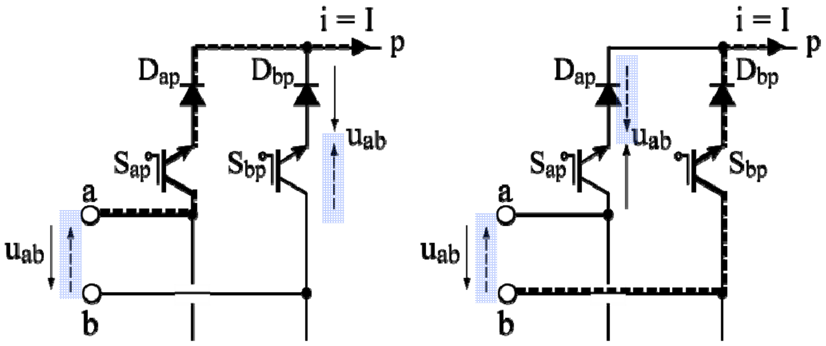

Equivalent Circuit

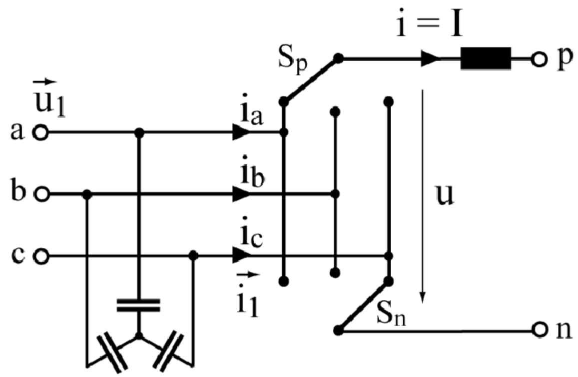

CSR Space Vector Modulation (1)

$$\vec{i}_k = \frac{2}{3}\left(i_{a,k} + \underline{a}\, i_{b,k} + \underline{a}^2\, i_{c,k}\right) \qquad \underline{a} = \mathrm{e}^{j2\pi/3}$$

Input Current Reference Value

$$\vec{i}_1^{\,*} = \hat{I}_1^*\mathrm{e}^{j\varphi_{\vec{i}_1^*}} = \hat{I}_1^*\mathrm{e}^{j(\omega_1 t - \Phi_1^*)}$$

$$M_1 = \frac{\hat{I}_1^*}{I}$$

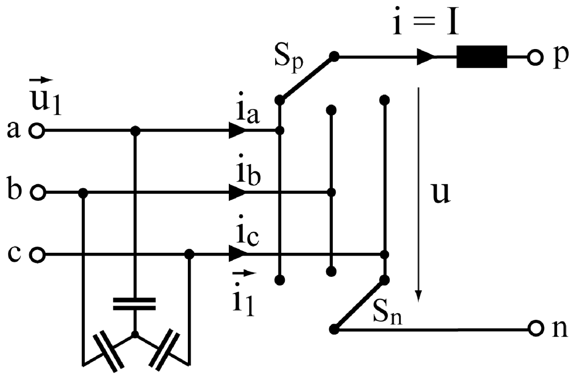

a)

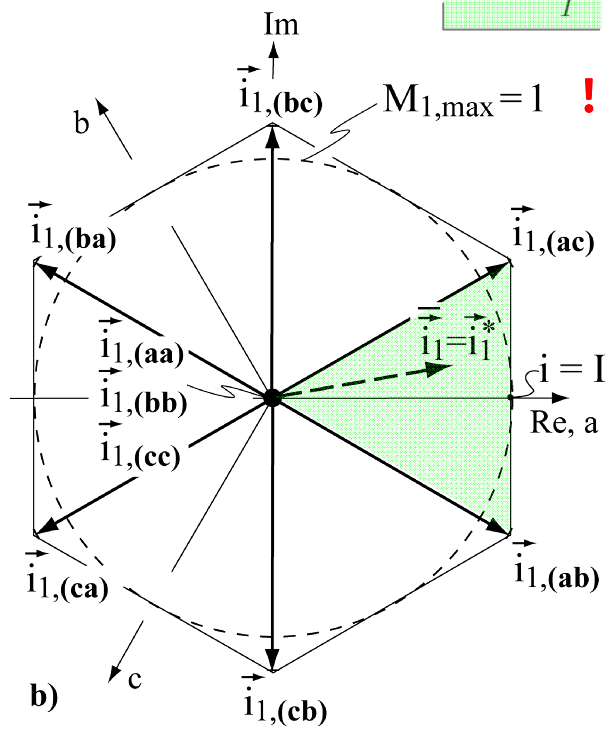

b)

CSR Space Vector Modulation (2)

Formation of the Input Current

$$|\vec{i}_{1,k}| = i_{1,k} = 2/\sqrt{3} \cdot I$$

$$\vec{i}_1 = \frac{1}{T_P}\int_0^{T_P} \vec{i}_{1,k}\, \mathrm{d}t_\mu = d_{(ac)} \cdot \vec{i}_{1,(ac)} + d_{(ab)} \cdot \vec{i}_{1,(ab)} = \vec{i}_1^*$$

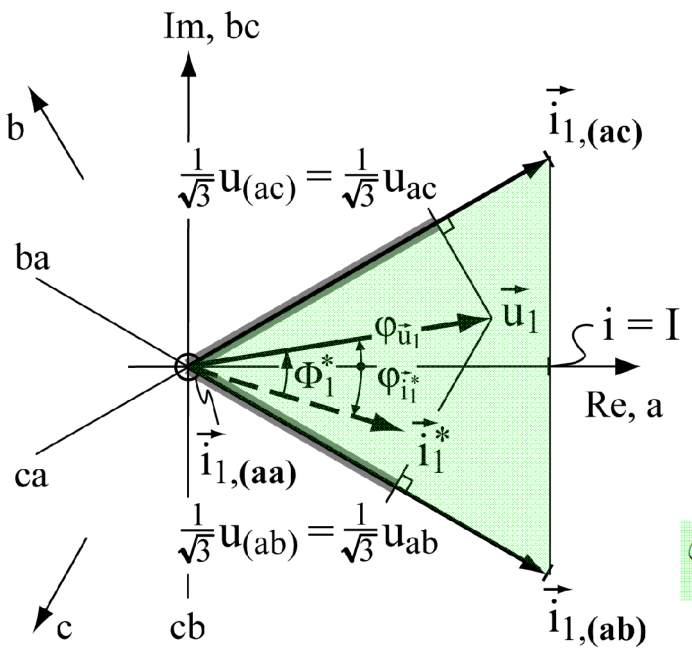

$$\varphi_{\vec{i}_1^*} = \varphi_{\vec{u}_1} - \Phi_1^*$$

Relative On-times

$$d_{(ac)} = M_1 \sin\left(\frac{\pi}{6} + \varphi_{\vec{i}_1^*}\right)$$

$$d_{(ab)} = M_1 \sin\left(\frac{\pi}{6} - \varphi_{\vec{i}_1^*}\right)$$

$$d_{(aa)} = 1 - \left(d_{(ac)} + d_{(ab)}\right)$$

Space Vector Orientation

$$\frac{d_{(ac)}}{d_{(ab)}} = \frac{\sin\left(\frac{\pi}{6} + \varphi_{\vec{i}_1^*}\right)}{\sin\left(\frac{\pi}{6} - \varphi_{\vec{i}_1^*}\right)}$$

CSR Space Vector Modulation (3)

Switching State Sequence

$$\cdots\Big|_{t_\mu=0}\ (\underline{a}b)-(\underline{a}c)-(\underline{a}a)\Big|_{t_\mu=T_P/2}\ (\underline{a}a)-(\underline{a}c)-(\underline{a}b)\Big|_{t_\mu=T_P}\cdots$$

$$\cdots\Big|_{t_\mu=0}\ (\underline{a}c)-(\underline{a}b)-(\underline{a}a)\Big|_{t_\mu=T_P/2}\ (\underline{a}a)-(\underline{a}b)-(\underline{a}c)\Big|_{t_\mu=T_P}\cdots$$

$$\cdots\Big|_{t_\mu=0}\ (\underline{a}c)-(\underline{a}a)-(\underline{a}b)\Big|_{t_\mu=T_P/2}\ (\underline{a}b)-(\underline{a}a)-(\underline{a}c)\Big|_{t_\mu=T_P}\cdots$$

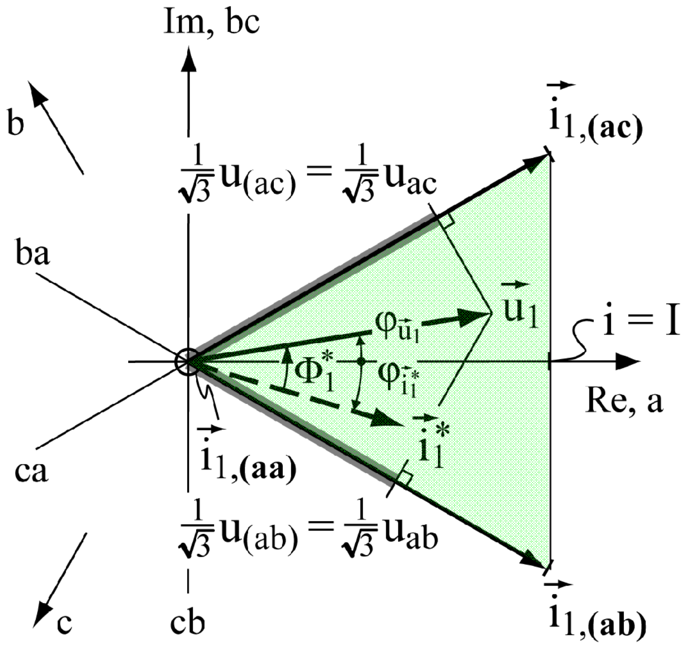

DC-link Voltage Formation

$$u_{(ab)} = u_a - u_b = u_{ab}$$
$$u_{(ba)} = u_b - u_a = u_{ba} = -u_{ab}$$
$$u_{(bc)} = u_b - u_c = u_{bc}$$
$$u_{(cb)} = u_c - u_b = u_{cb} = -u_{bc}$$
$$u_{(ca)} = u_c - u_a = u_{ca}$$
$$u_{(ac)} = u_a - u_c = u_{ac} = -u_{ca}$$
$$u_{(aa)} = u_{(bb)} = u_{(cc)} = 0$$

$$u_k = \sqrt{3}\cdot u_{1,k} \qquad \bar{u} = u_{ab}d_{(ab)} + u_{ac}d_{(ac)}$$

CSR Space Vector Modulation (4)

Local DC-link Voltage Shape

$$\bar{u} = \frac{3}{2} M_1 \hat{U}_1 \cos \Phi_1^*$$

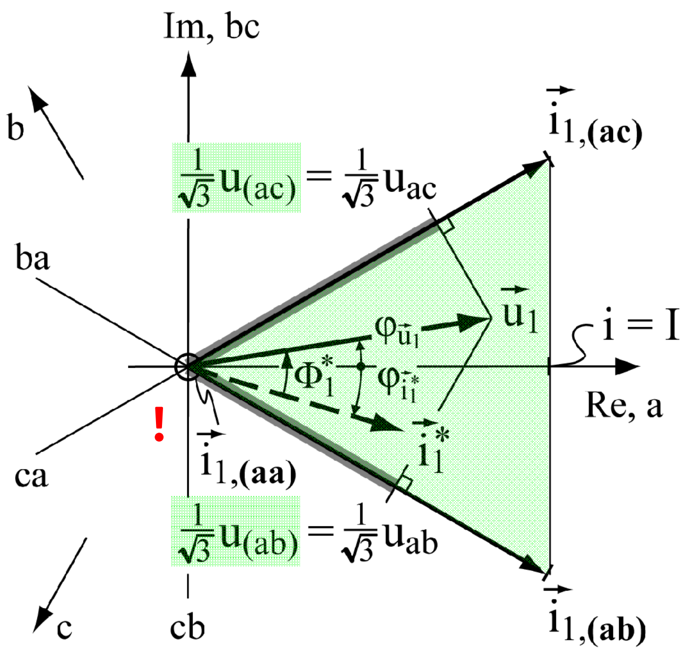

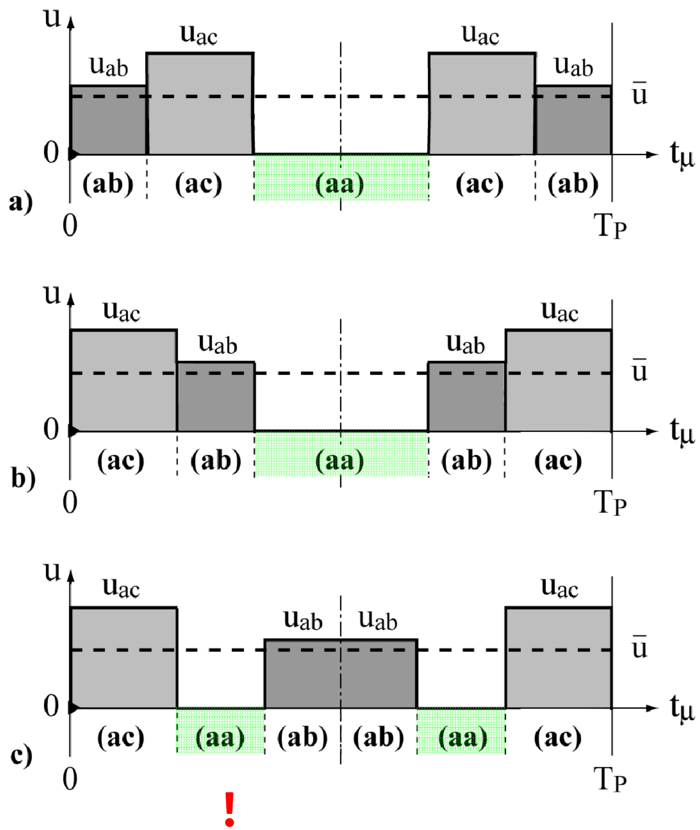

CSR DC-link Voltage Waveform

Influence of Input Current Phase Displacement Φ_1 on DC-link Voltage Waveform

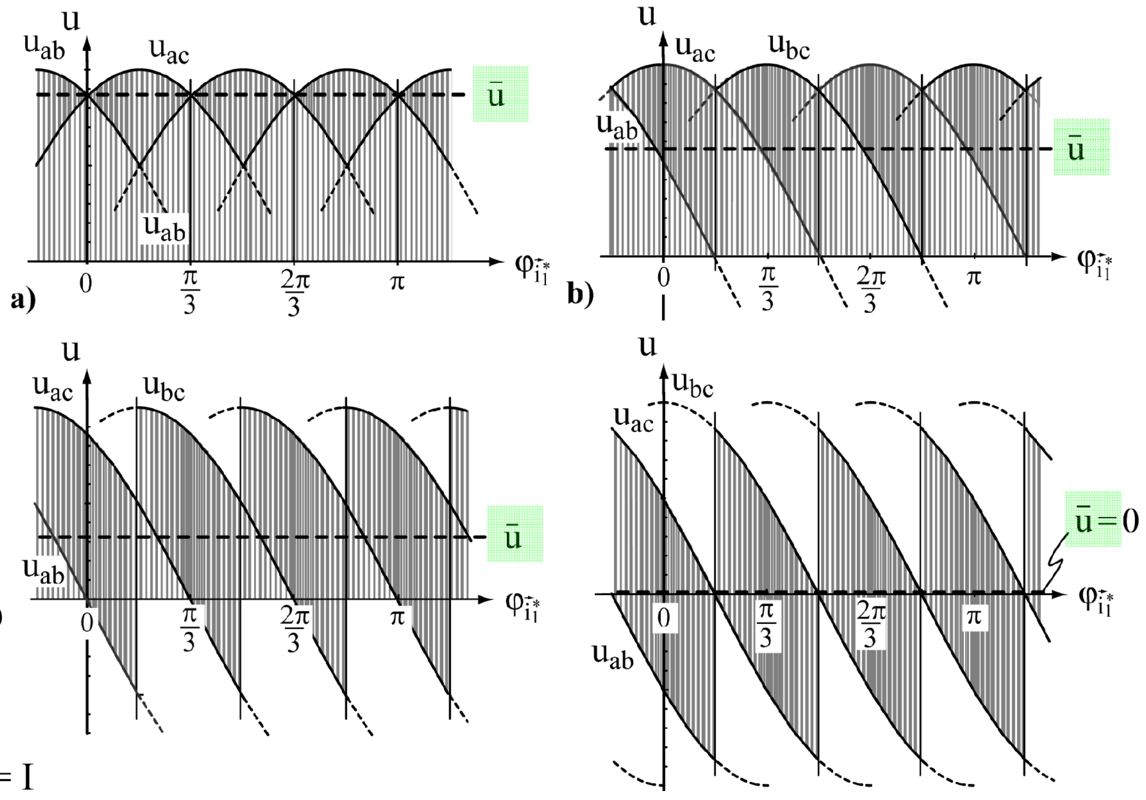

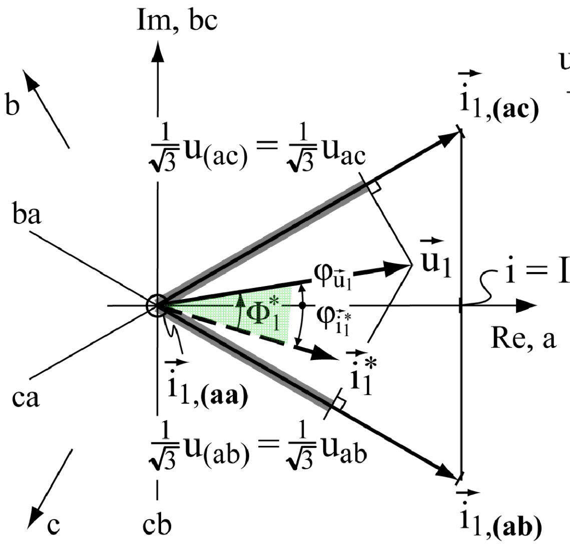

$$M_1 = \frac{\hat{I}_1^*}{I}$$

!

$$\bar{u} = \frac{3}{2} M_1 \hat{U}_1 \cos \Phi_1^*$$

CSR Functional Equivalent Circuit

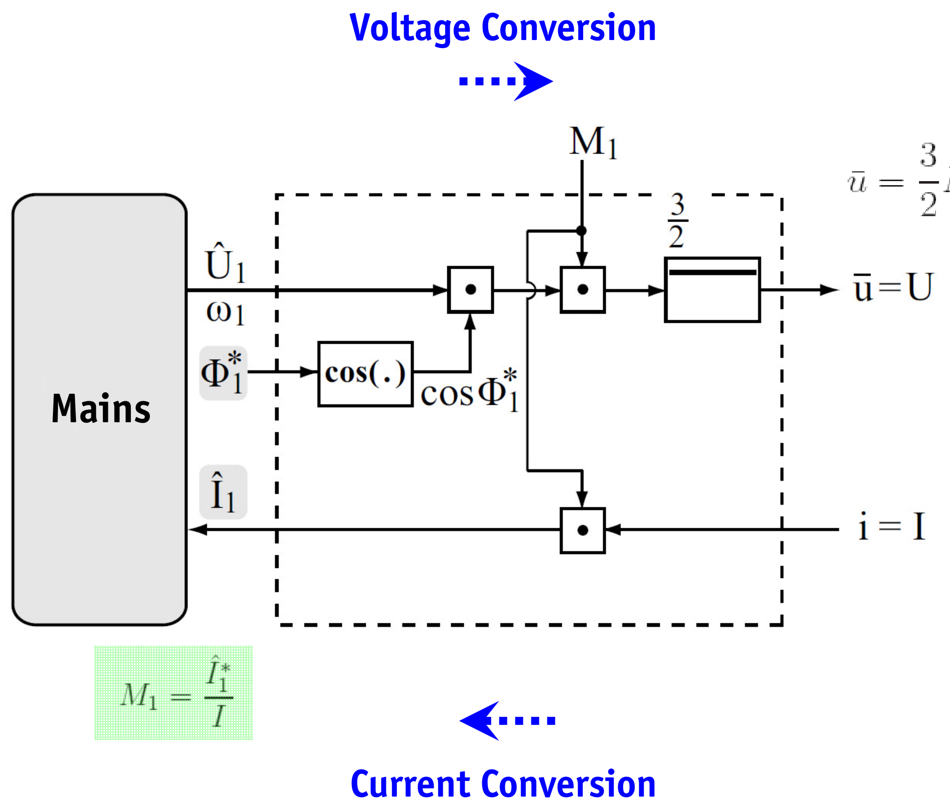

$$\bar{u} = \frac{3}{2} M_1 \hat{U}_1 \cos\Phi_1^*$$

$$M_1 = \frac{\hat{I}_1^*}{I}$$

Derivation of MC Topologies

Fundamental Frequency Front End

F^3E

Classification of Three-Phase AC-AC Converters

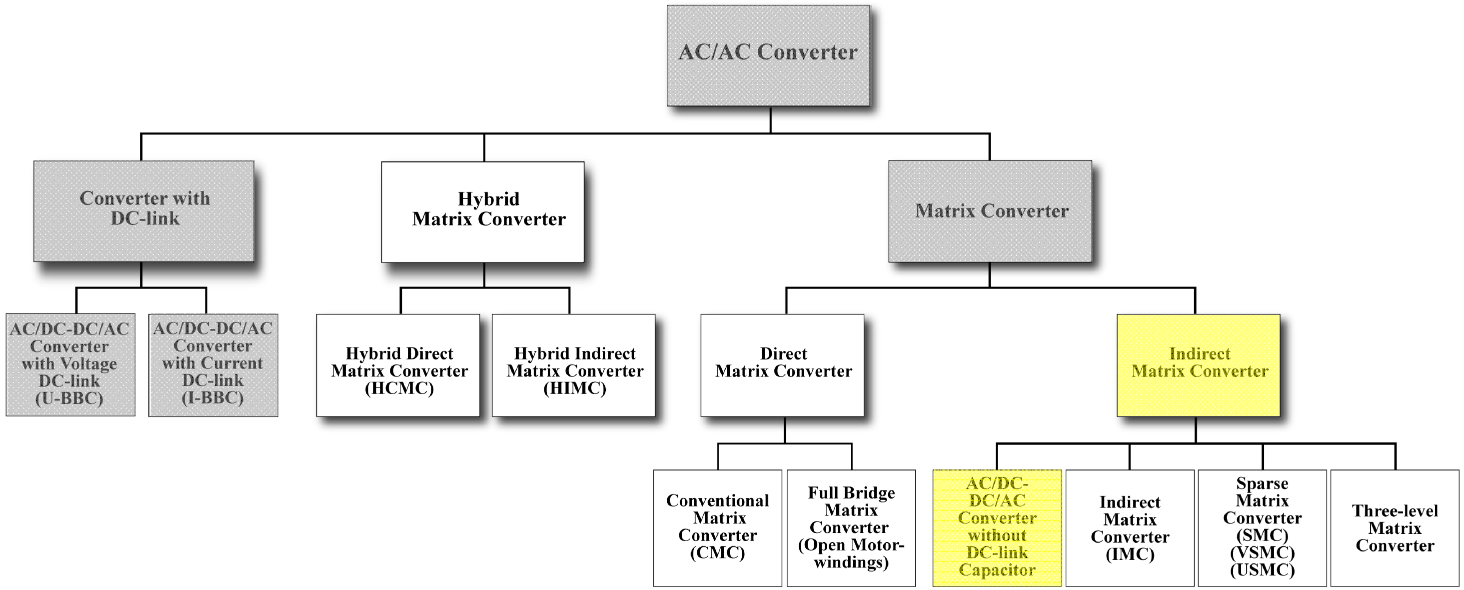

- *Converter without DC-link Capacitor*

F^3E Topology / Mains Behavior

$$u_{\min} = \frac{3}{2}\hat{U}_1$$

!

$$\hat{U}_2^* < \frac{\sqrt{3}}{2} \cdot \hat{U}_1 \approx 0.86\,\hat{U}_1$$

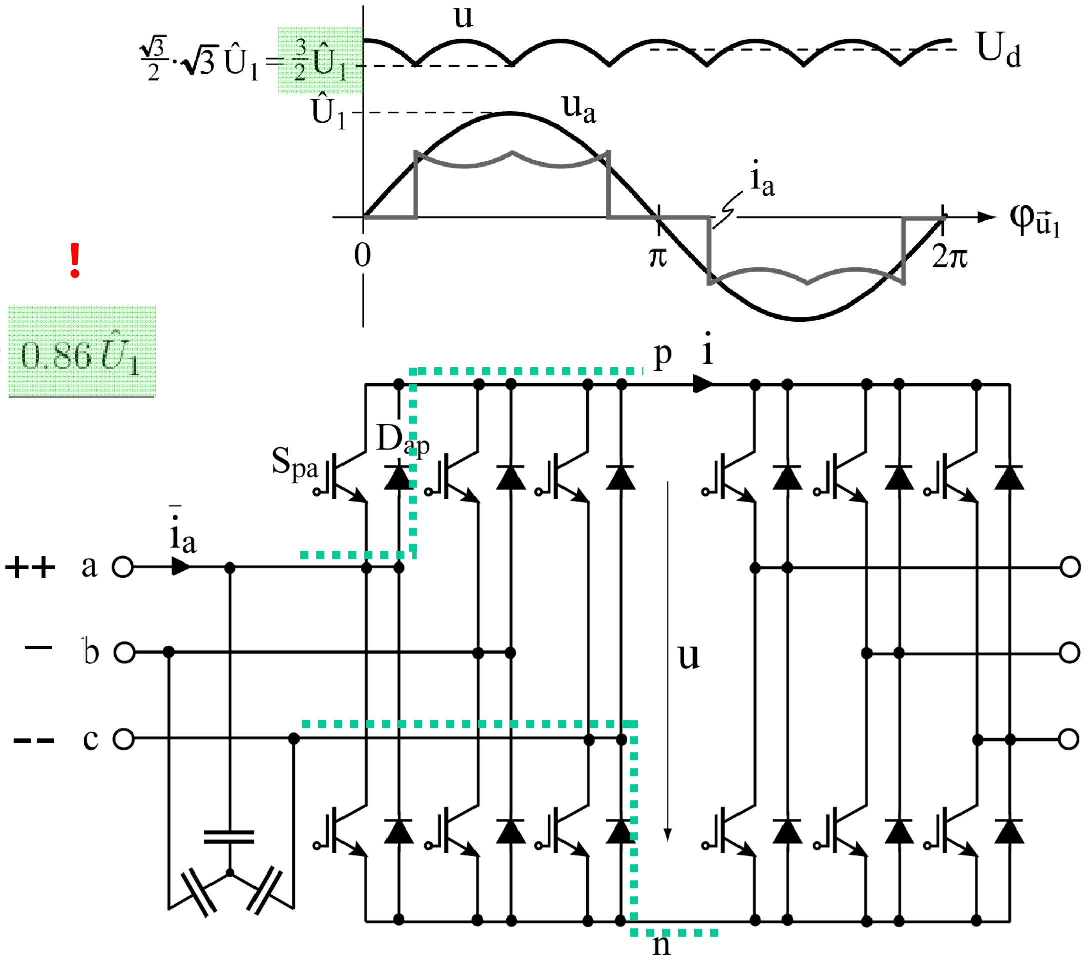

P. Ziogas [12]
T. Lipo [13, 18, 20]
B. Piepenbreier [15]

F^3E Topology Extension

- ***Sinusoidal Mains Current***

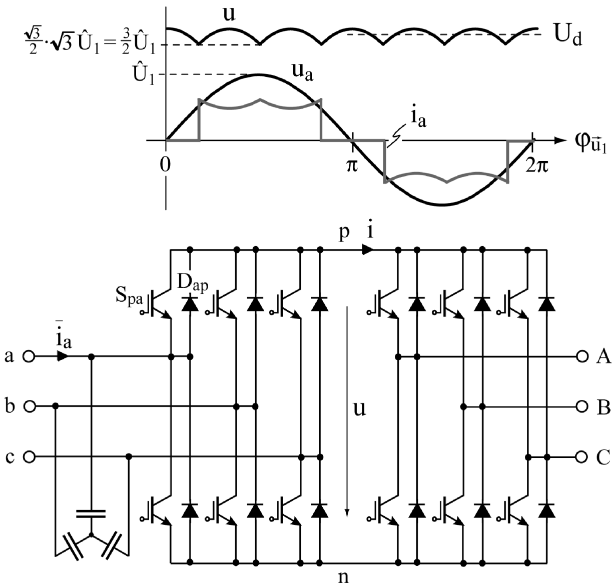

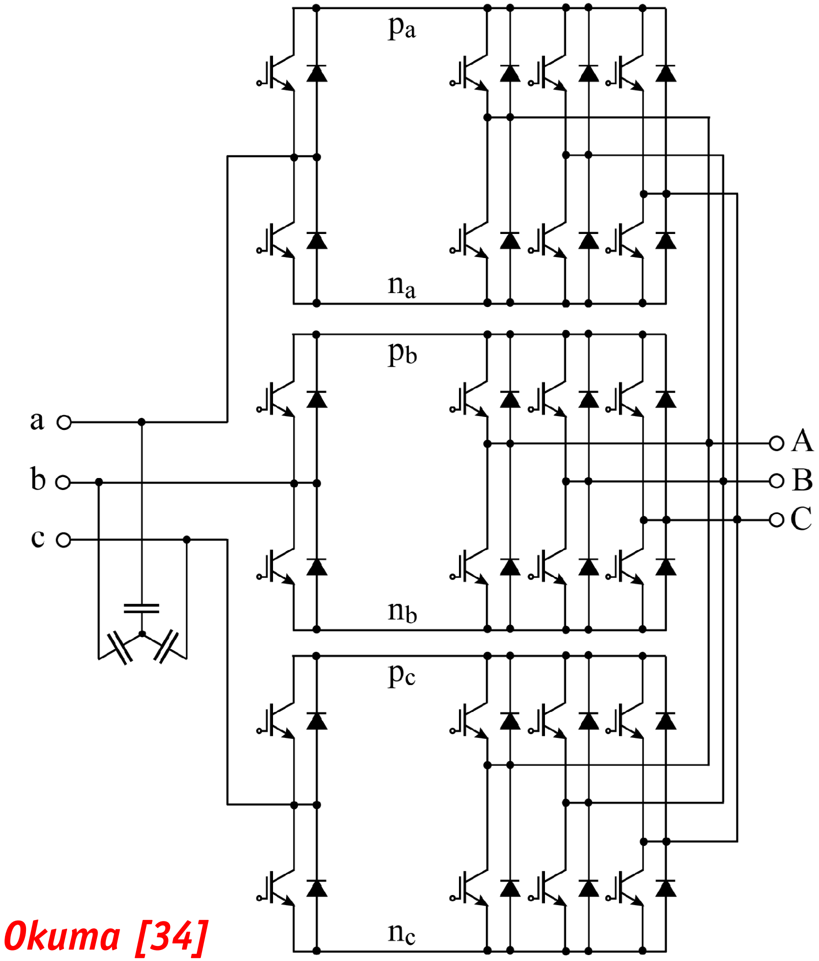

Y. Okuma [34]

Indirect Matrix Converter – IMC

Space Vectors
Modulation
Simulation
Experimental Results

Classification of Three-Phase AC-AC Converters

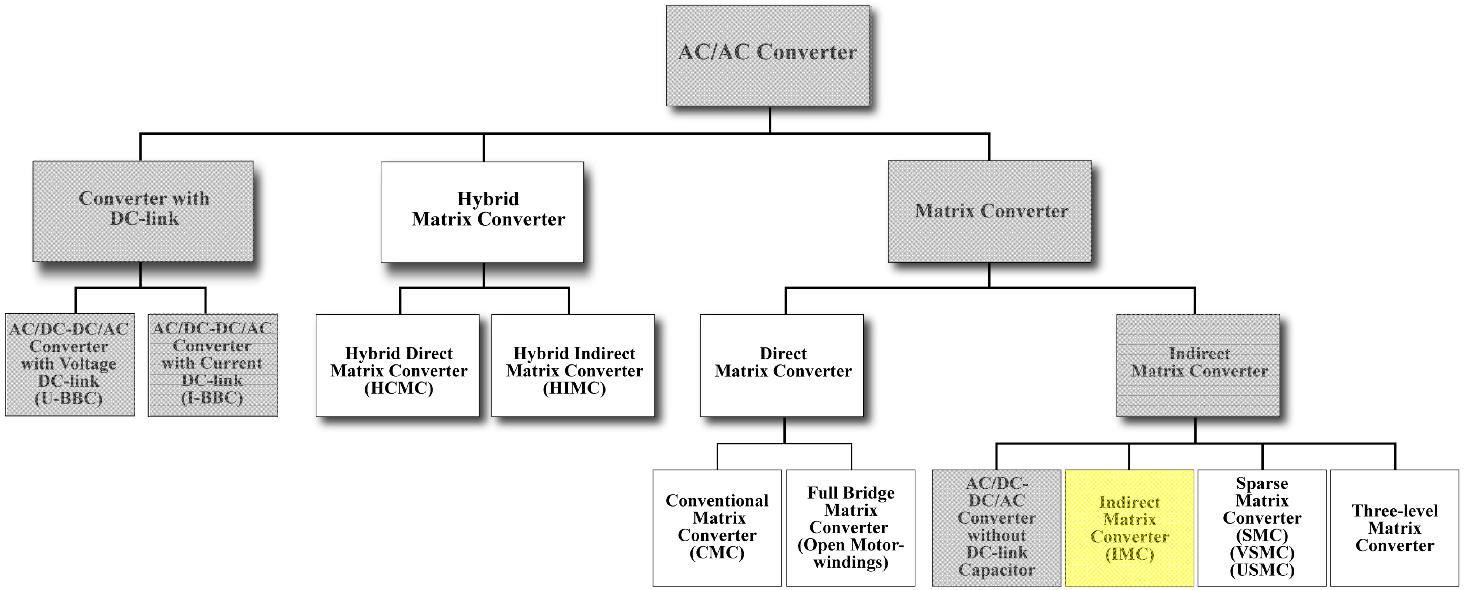

- ***Indirect Matrix Converter***

IMC Topology Derivation

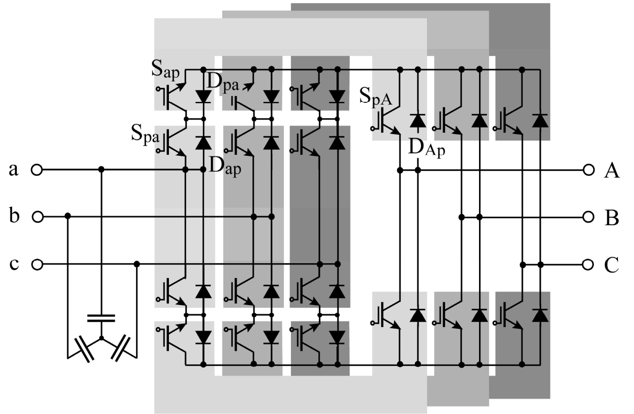

- *Extension of F^3E-Topology*
- *Bidirectional CSR Mains Interface* **!**

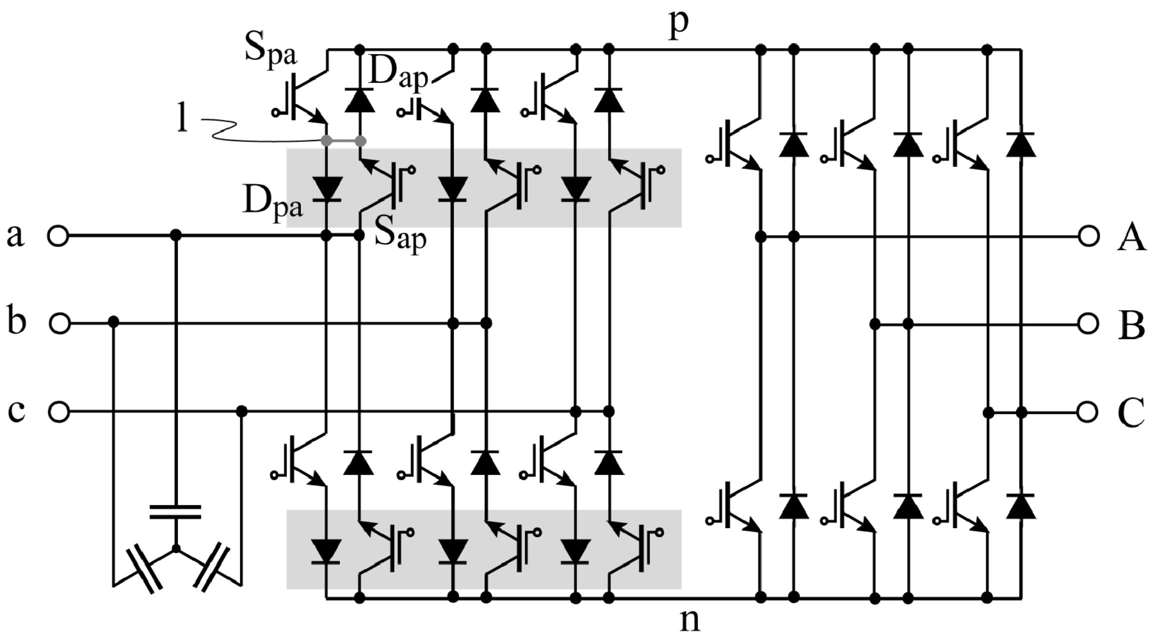

J. Holtz [16]
K. Shinohara [17]

IMC Properties

► ***Positive DC-link Voltage Required*** **!**

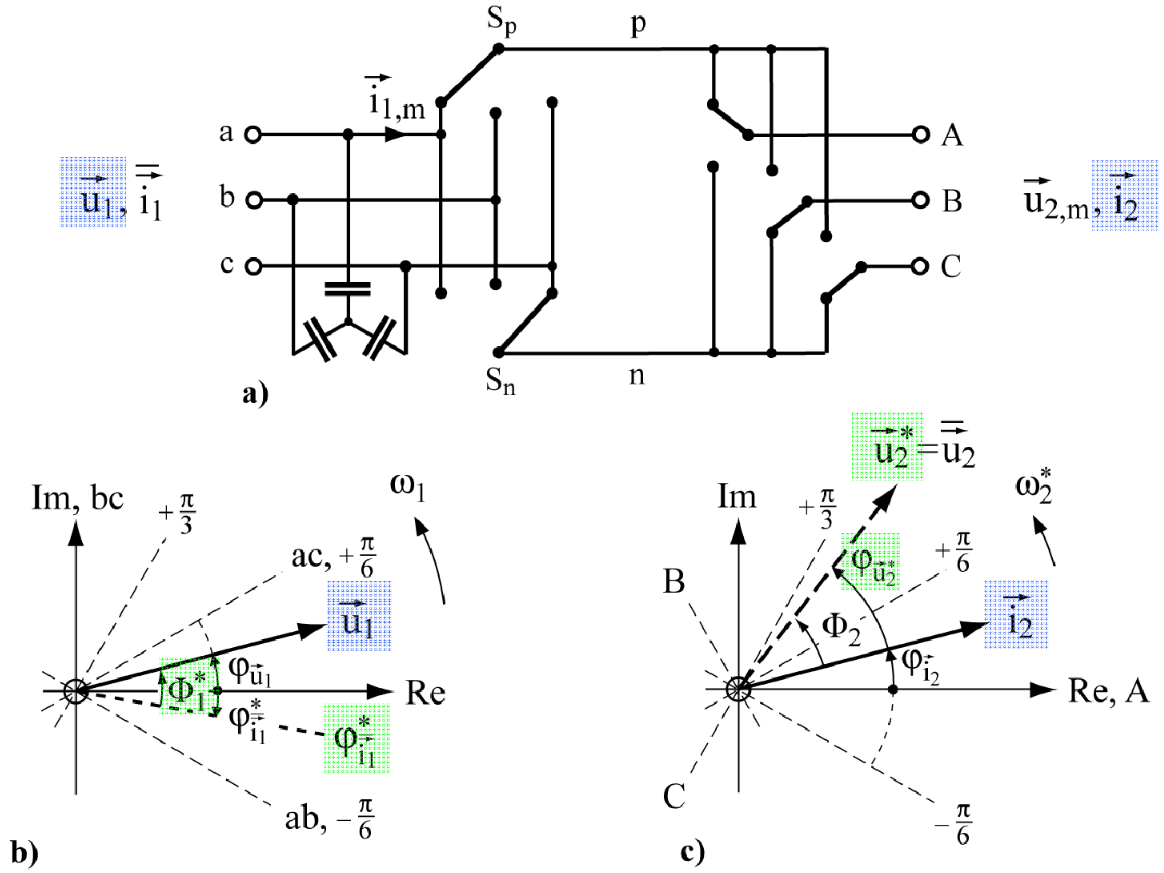

IMC Voltage and Current Space Vectors

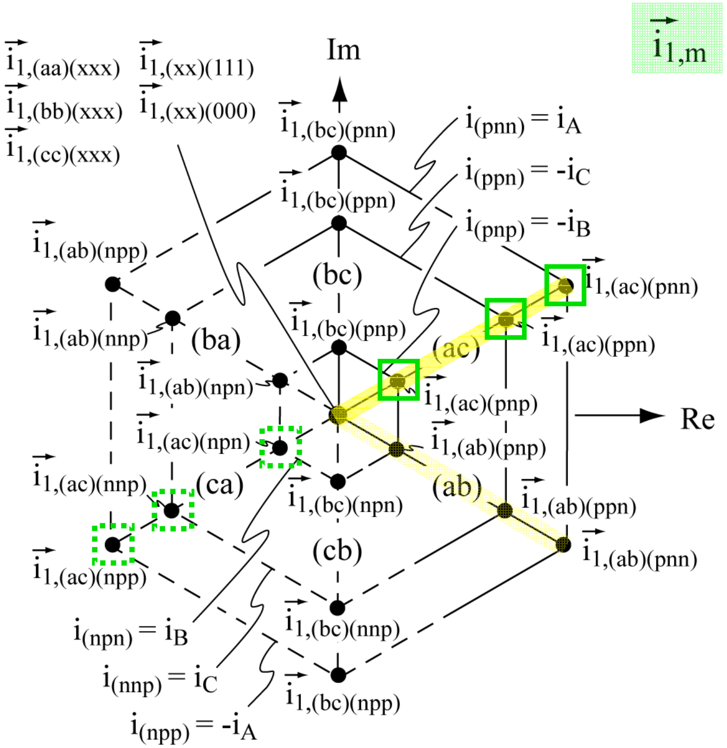

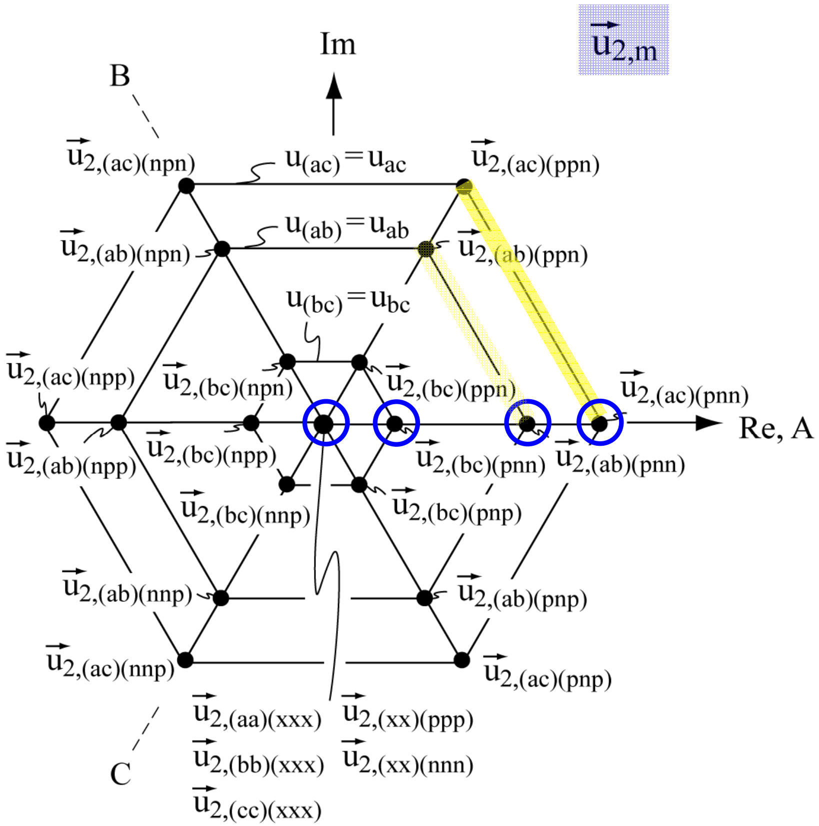

IMC Space Vector Modulation (1)

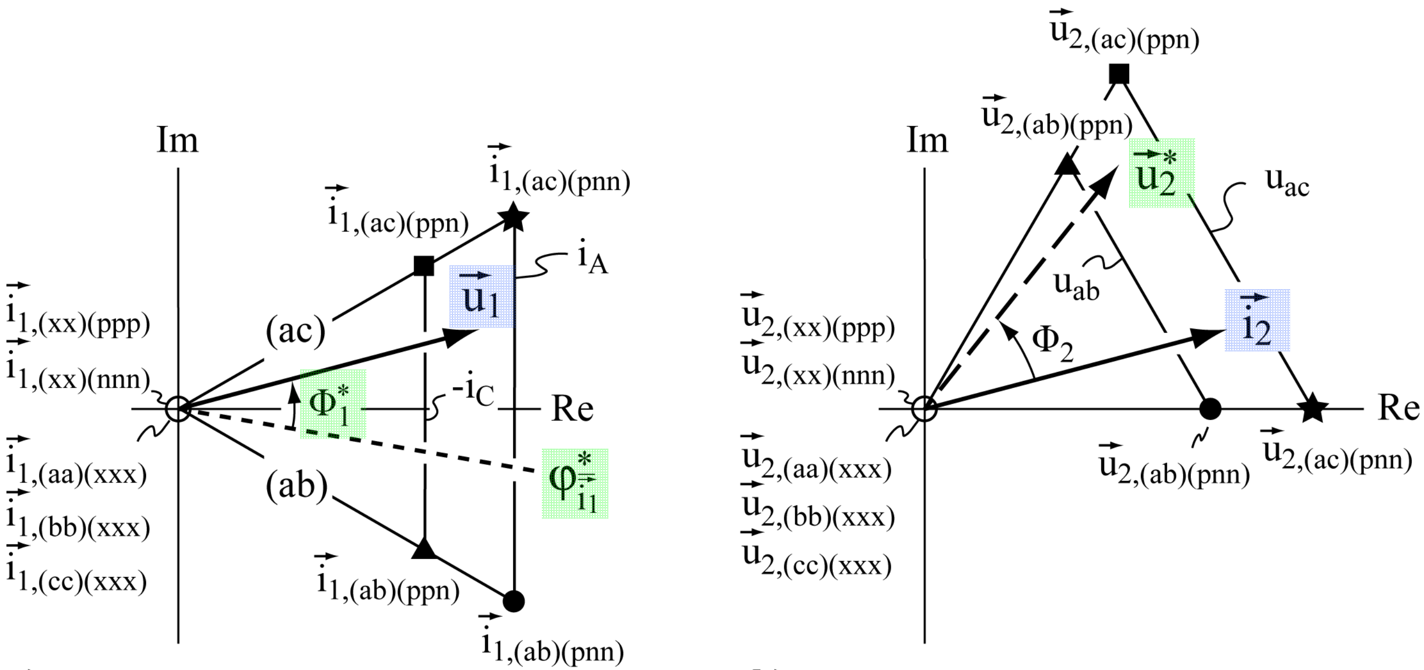

a) **b)**

$$\vec{u}_1 = \hat{U}_1 e^{j\varphi_{\vec{u}_1}} = \hat{U}_1 e^{j\omega_1 t} \qquad \vec{i}_1 = \hat{I}_1 e^{j\varphi^*_{\vec{i}_1}}$$

$$\vec{u}_2^* = \hat{U}_2^* e^{j\varphi_{\vec{u}_2^*}} = \hat{U}_2^* e^{j\omega_2^* t}$$

$$\vec{i}_2 = \hat{I}_2 e^{j\varphi_{\vec{i}_2}} = \hat{I}_2 e^{j\left(\varphi_{\vec{u}_2^*} - \Phi_2\right)}$$

IMC Space Vector Modulation (2)

- *Zero Current Commutation* **!**
- *Zero Voltage Commutation*

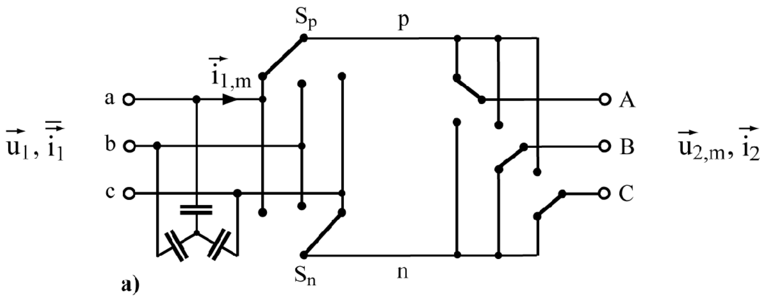

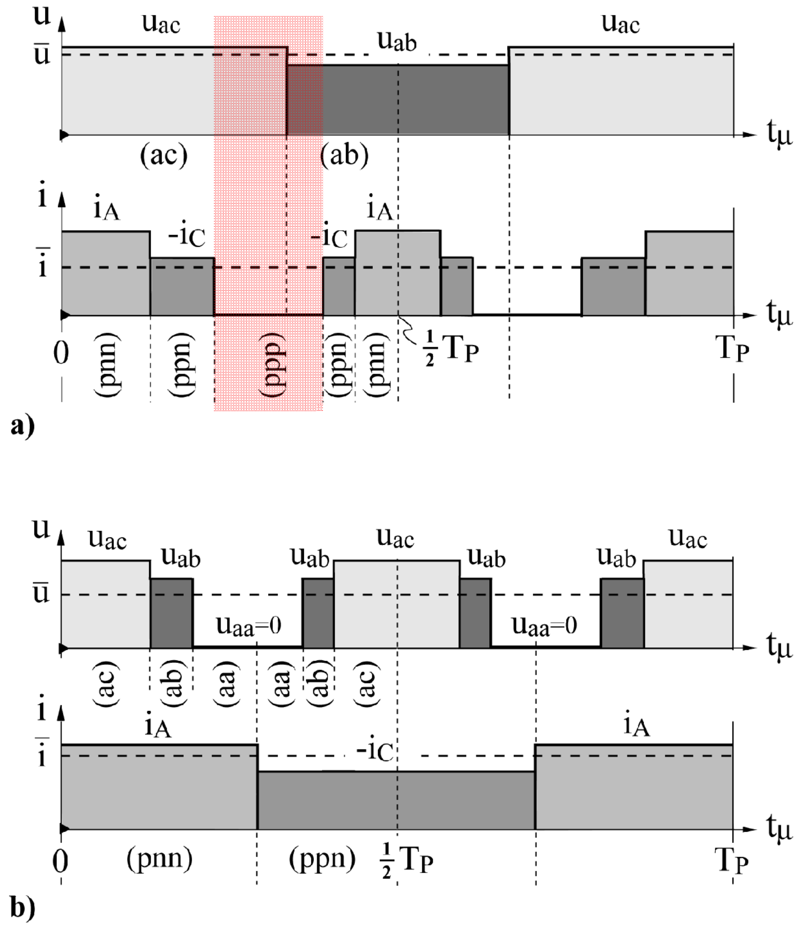

IMC Zero DC-link Current Commutation (1)

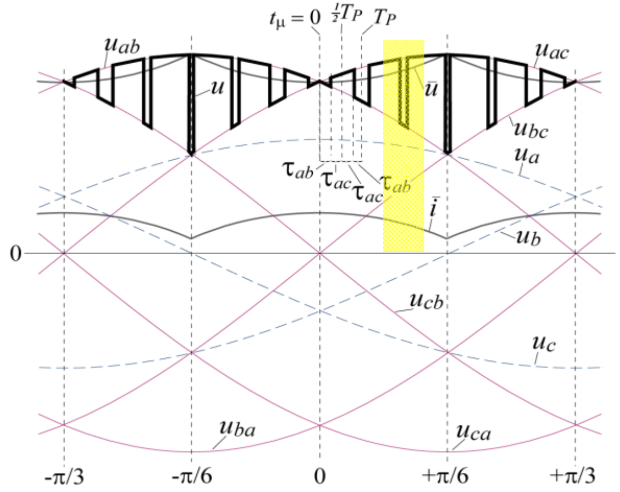

120° of Mains Period

DC-link Voltage $u = u_{ac}$
DC-link Current $i = i_A$

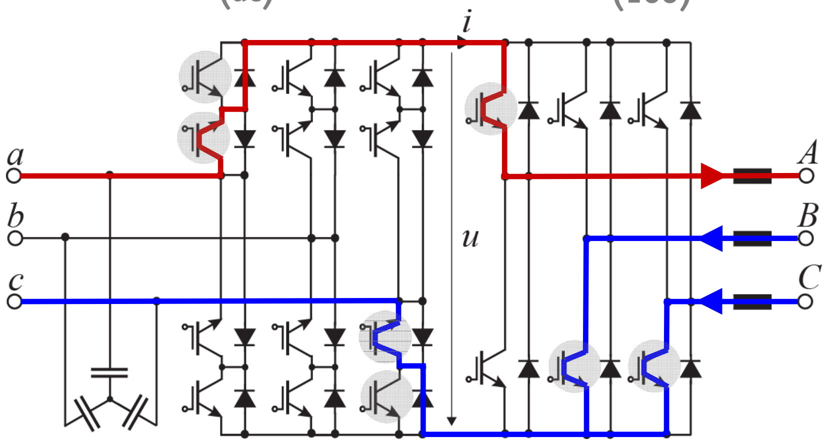

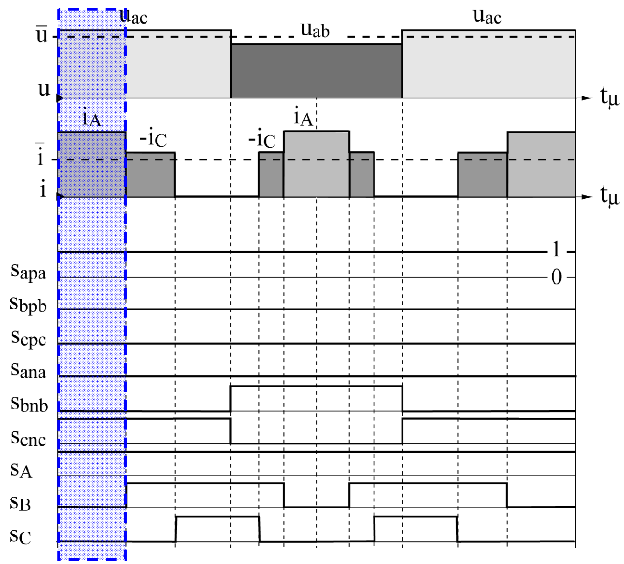

DC link Voltage & Current

PWM Pattern

IMC Zero DC-link Current Commutation (2)

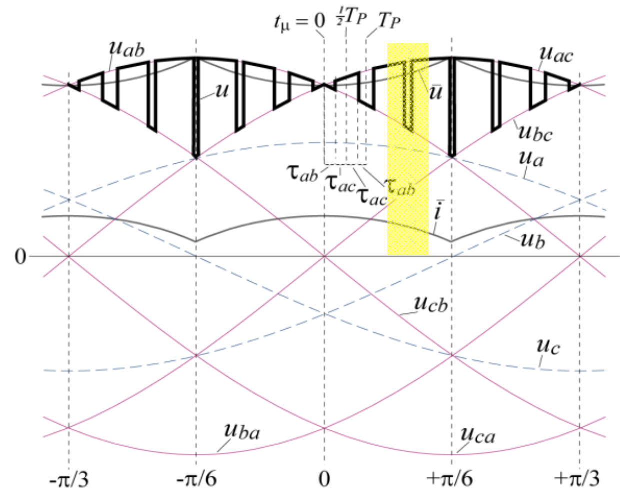

120° of Mains Period

DC-link Voltage $u = u_{qc}$
DC-link Current $i = - i_C$

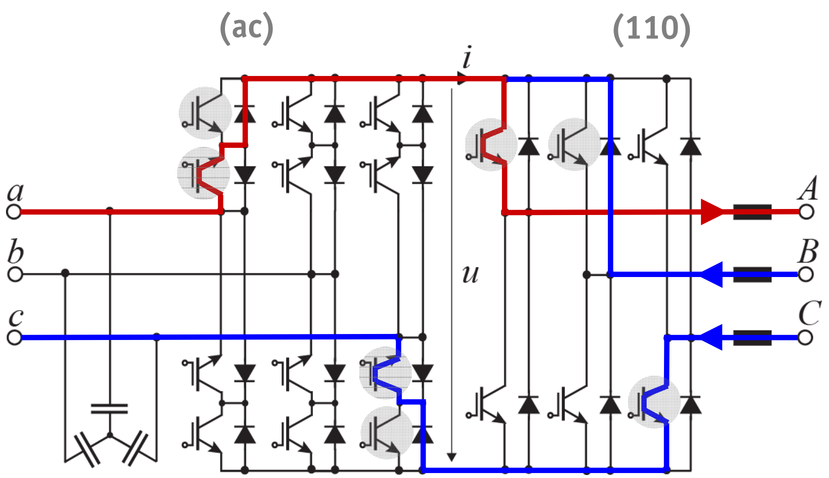

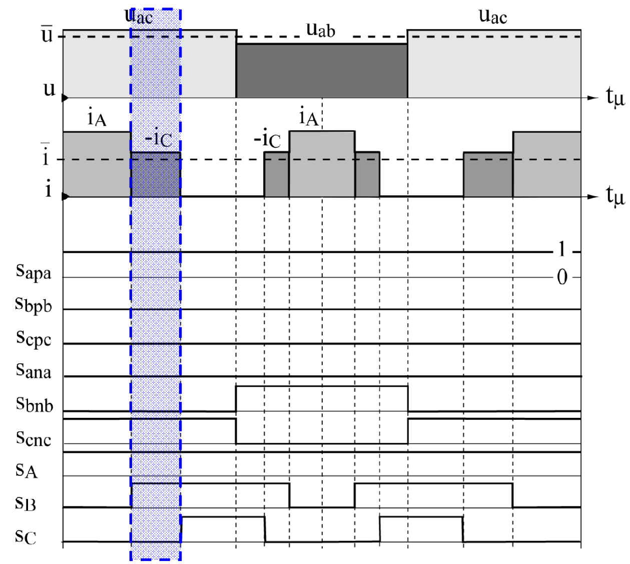

DC link Voltage & Current

PWM Pattern

IMC Zero DC-link Current Commutation (3)

DC-link Voltage $u = u_{ac}$
DC-link Current $i = 0$

(ac) (111)

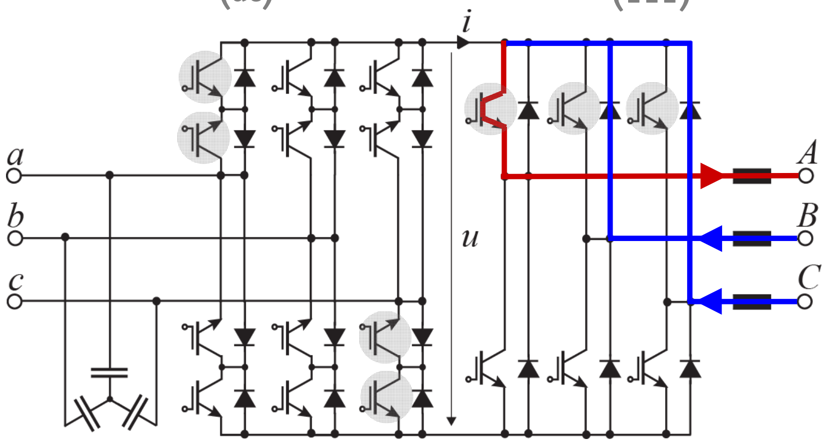

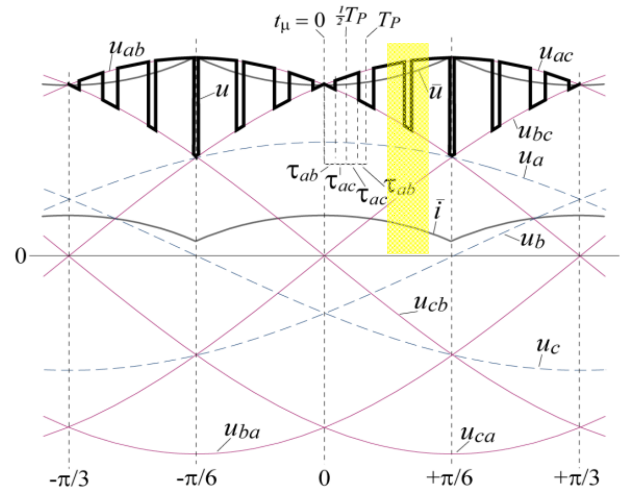

120° of Mains Period

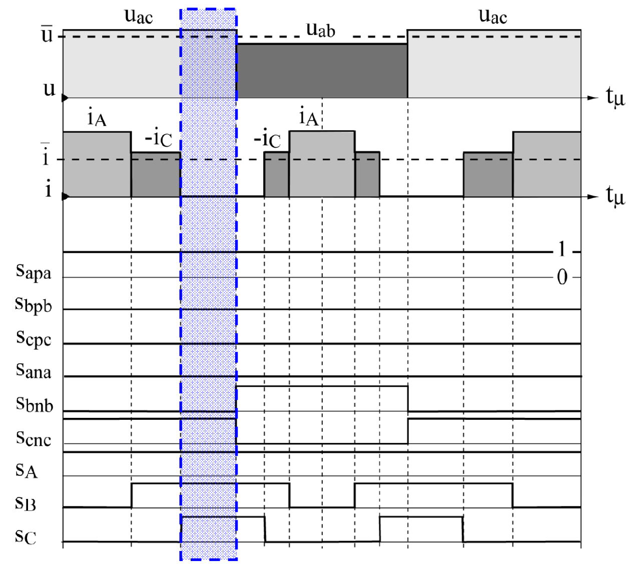

DC link Voltage & Current

PWM Pattern

IMC Zero DC-link Current Commutation (4)

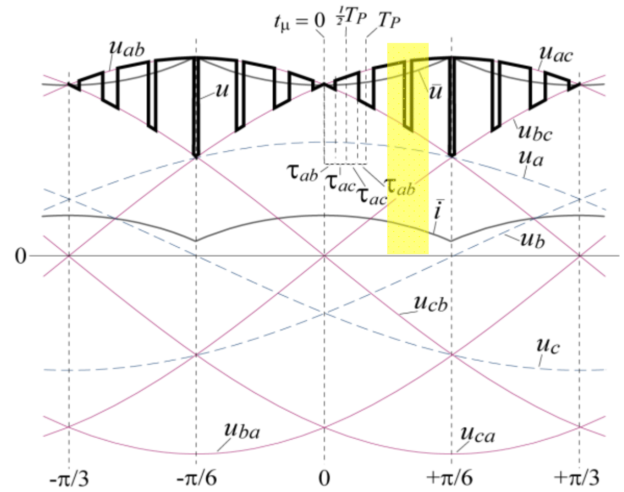

120° of Mains Period

DC-link Voltage $u = u_{ab}$
DC-link Current $i = 0$

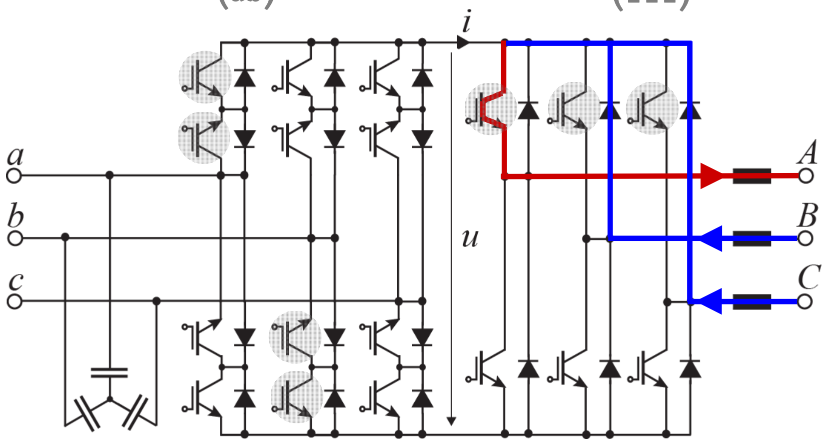

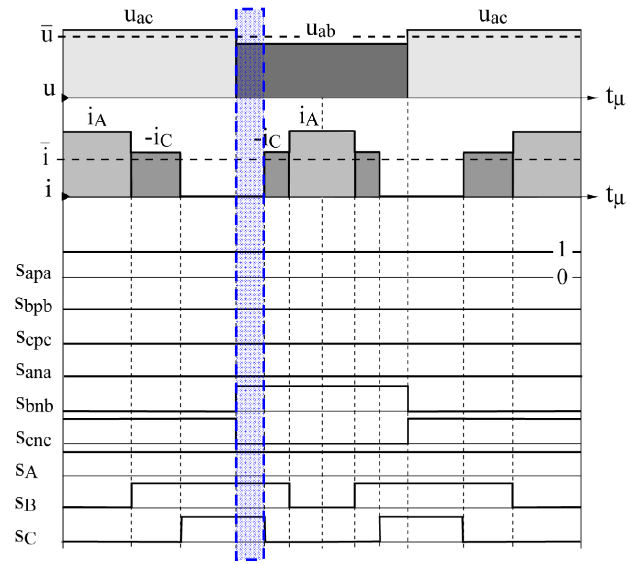

DC link Voltage & Current

PWM Pattern

IMC Zero DC-link Current Commutation (5)

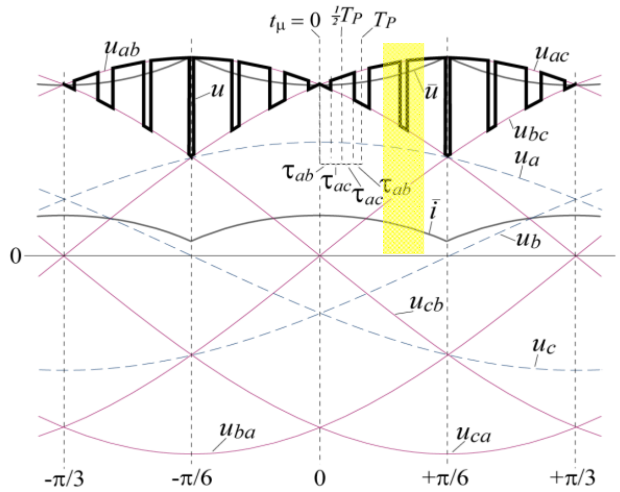

120° of Mains Period

DC-link Voltage $u = u_{qb}$
DC-link Current $i = -i_C$

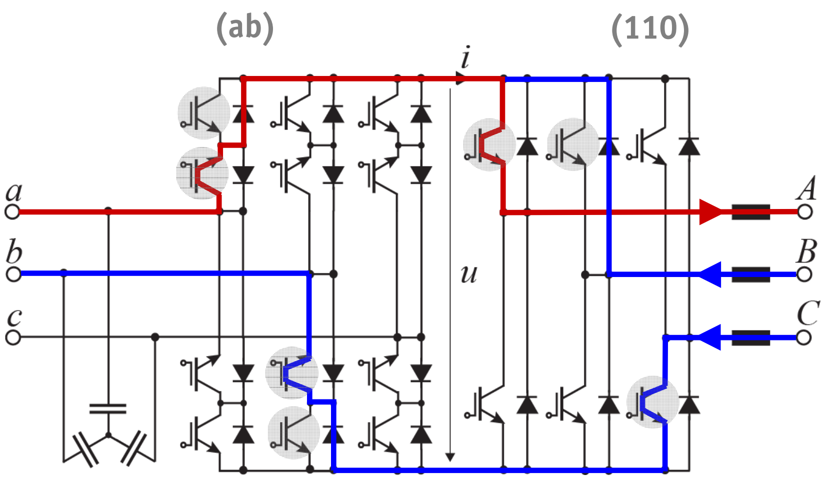

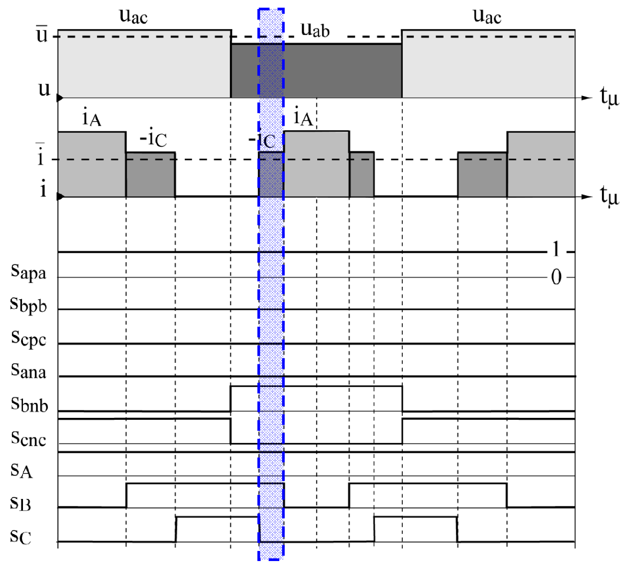

DC link Voltage & Current

PWM Pattern

IMC Zero DC-link Current Commutation (6)

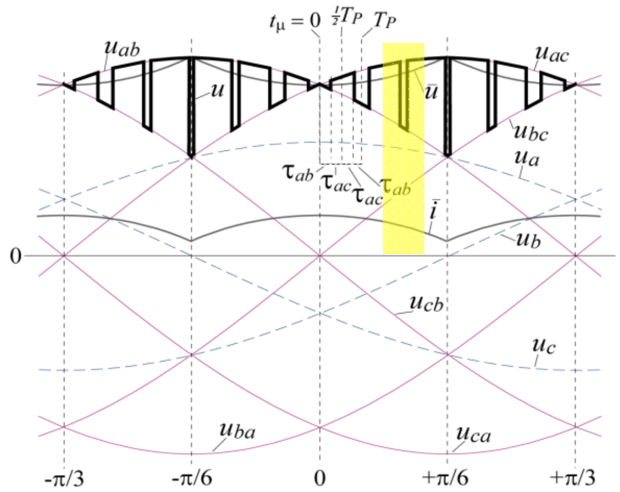

120° of Mains Period

DC-link Voltage $u = u_{ab}$

DC-link Current $i = i_A$

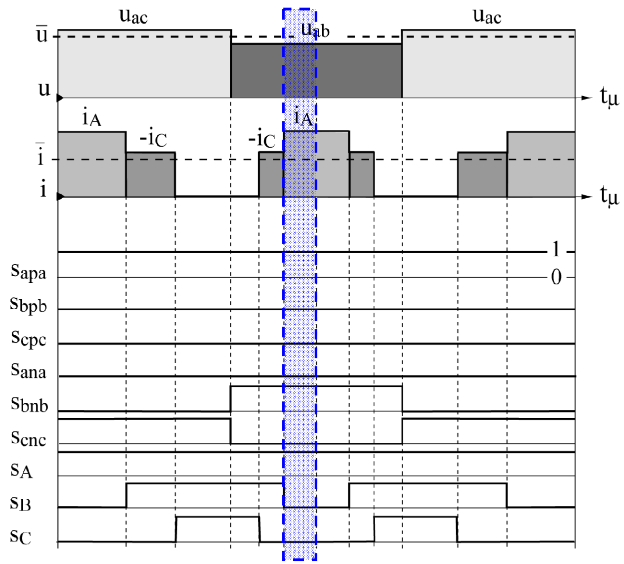

DC link Voltage & Current

PWM Pattern

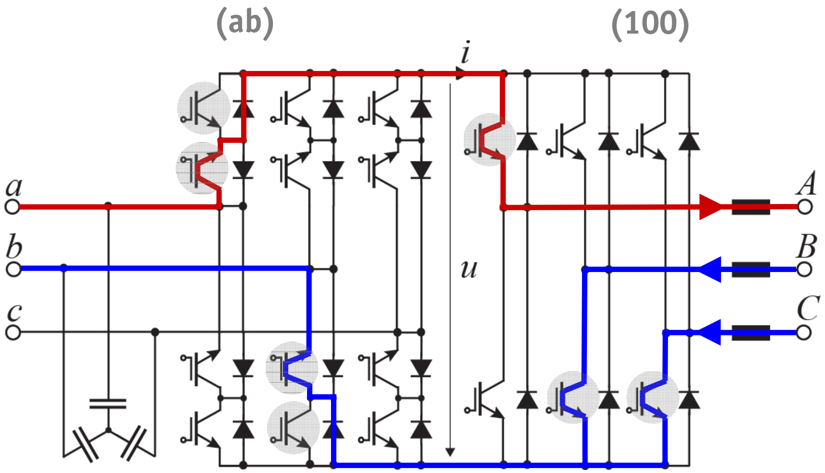

IMC Zero DC-link Current Commutation (7)

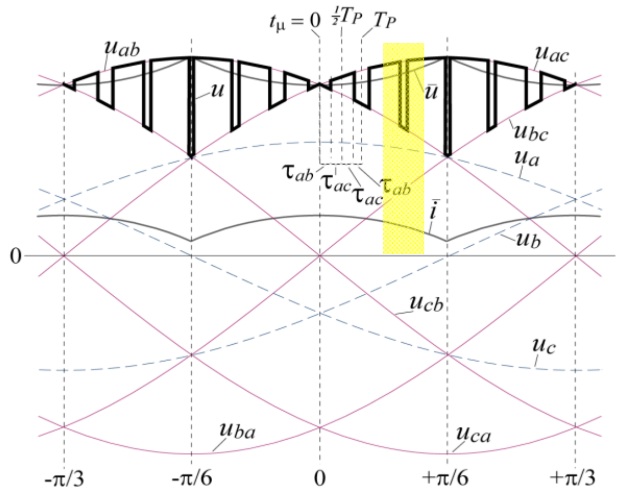

120° of Mains Period

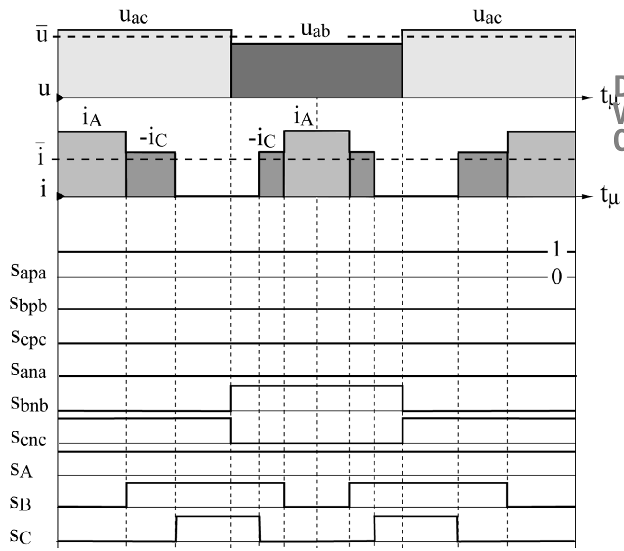

DC link Voltage & Current

PWM Pattern

Summary

- **Simple and Robust** Modulation Scheme Independent of Commutation Voltage Polarity or Current Flow Direction
- **Negligible Rectifier Stage Switching Losses** Due to Zero Current Commutation

IMC Space Vector Modulation (3)

Output Voltage Ref. Value $\vec{u}_2^* = \hat{U}_2^* e^{j\varphi_{\vec{u}_2^*}} = \hat{U}_2^* e^{j\omega_2^* t}$

Input Current Ref. Angle $\varphi^*_{\vec{i}_1}$ $\vec{i}_1 = \hat{I}_1 e^{j\varphi^*_{\vec{i}_1}}$ $\varphi^*_{\vec{i}_1} = \varphi_{\vec{u}_1} - \Phi_1^*$

Mains Voltage $\vec{u}_1 = \hat{U}_1 e^{j\varphi_{\vec{u}_1}} = \hat{U}_1 e^{j\omega_1 t}$

Load Behavior $\vec{i}_2 = \hat{I}_2 e^{j\varphi_{\vec{i}_2}} = \hat{I}_2 e^{j\left(\varphi_{\vec{u}_2^*} - \Phi_2\right)}$

Assumptions

$\varphi_{\vec{u}_1} \in \left[0, \frac{\pi}{6}\right]$

$\varphi_{\vec{u}_2^*} \in \left[0, \frac{\pi}{3}\right]$

$\varphi^*_{\vec{i}_1} \in \left[-\frac{\pi}{6}, \frac{\pi}{6}\right]$

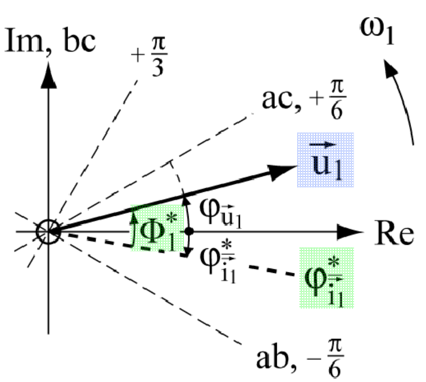

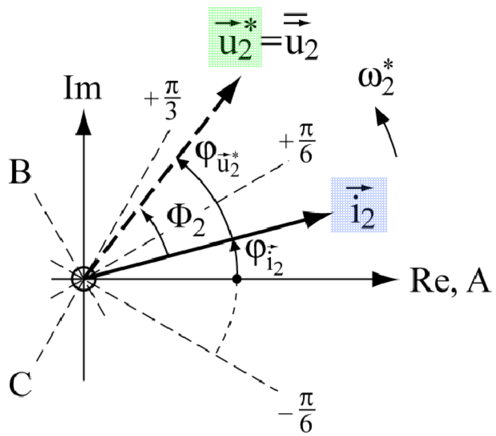

PWM Pattern is Specific for each Combination of Input Current and Output Voltage Sectors

Freewheeling Limited to Output Stage

$$d_{(ab)} + d_{(ac)} = 1$$

Input Current Formation

$$\bar{i}_a = \left(d_{(ab)} + d_{(ac)}\right)\bar{i} = \bar{i}$$
$$\bar{i}_b = -d_{(ab)}\,\bar{i}$$
$$\bar{i}_c = -d_{(ac)}\,\bar{i}$$

Desired Input Current

$$\bar{i}_a = \hat{I}_1 \cos\varphi^*_{\vec{i}_1}$$
$$\bar{i}_b = \hat{I}_1 \cos\left(\varphi^*_{\vec{i}_1} - \frac{2\pi}{3}\right)$$
$$\bar{i}_c = \hat{I}_1 \cos\left(\varphi^*_{\vec{i}_1} + \frac{2\pi}{3}\right)$$

Resulting Rectifier Stage Relative On-Times

$$d_{(ab)} = \frac{\sin\left(\frac{\pi}{6} - \varphi^*_{\vec{i}_1}\right)}{\cos\varphi^*_{\vec{i}_1}} \qquad d_{(ac)} = \frac{\sin\left(\frac{\pi}{6} + \varphi^*_{\vec{i}_1}\right)}{\cos\varphi^*_{\vec{i}_1}}$$

Absolute On-Times

$$\tau_{(ab)} = d_{(ab)}\frac{T_P}{2} \qquad \tau_{(ac)} = d_{(ac)}\frac{T_P}{2}$$

Mains Voltage

$$u_a = \hat{U}_1 \cos\left(\varphi_{\vec{u}_1}\right)$$

$$u_b = \hat{U}_1 \cos\left(\varphi_{\vec{u}_1} - \frac{2\pi}{3}\right)$$

$$u_c = \hat{U}_1 \cos\left(\varphi_{\vec{u}_1} + \frac{2\pi}{3}\right)$$

Available DC Link Voltage Values

$$u_{(ab)} = u_{ab} = u_a - u_b = \sqrt{3} \cdot \hat{U}_1 \cos\left(\varphi_{\vec{u}_1} + \frac{\pi}{6}\right)$$

$$u_{(ac)} = u_{ac} = u_a - u_c = \sqrt{3} \cdot \hat{U}_1 \cos\left(\varphi_{\vec{u}_1} - \frac{\pi}{6}\right)$$

Select Identical Duty Cycles of Inverter Switching States (100), (110) in τ_{ac} and τ_{ab} for Maximum Modulation Range

$$\delta_{(ac)(pnn)} = \frac{\tau_{(ac)(pnn)}}{\tau_{(ac)}} = \delta_{(ab)(pnn)} = \frac{\tau_{(ab)(pnn)}}{\tau_{(ab)}} = \delta_{(pnn)}$$

$$\delta_{(ac)(ppn)} = \frac{\tau_{(ac)(ppn)}}{\tau_{(ac)}} = \delta_{(ab)(ppn)} = \frac{\tau_{(ab)(ppn)}}{\tau_{(ab)}} = \delta_{(ppn)}$$

Switch Conducting
the Largest Current is Clamped
(over π/3-wide Interval)

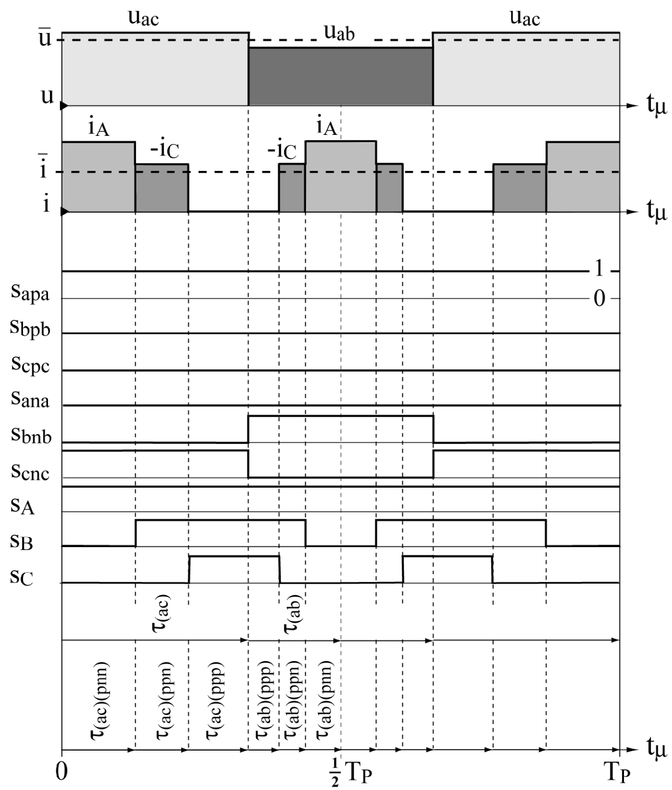

Voltage Space Vectors Related to Active Inverter Switching States

$$\vec{u}_{2,(pnn)} = \frac{2}{3} u$$

$$\vec{u}_{2,(ppn)} = \frac{2}{3} u \, \mathrm{e}^{j\pi/3}$$

Output Voltage Formation

$$\begin{aligned}
\bar{\vec{u}}_2 &= \frac{2/3}{T_P/2}\Big(\delta_{(ac)(pnn)}\tau_{(ac)}u_{ac} + \delta_{(ab)(pnn)}\tau_{(ab)}u_{ab} \\
&\quad + \delta_{(ac)(ppn)}\tau_{(ac)}u_{ac}\mathrm{e}^{j\pi/3} + \delta_{(ab)(ppn)}\tau_{(ab)}u_{ab}\mathrm{e}^{j\pi/3}\Big) \\
&= \delta_{(pnn)}\frac{2}{3}\left(\frac{\tau_{(ac)}}{T_P/2}u_{ac} + \frac{\tau_{(ab)}}{T_P/2}u_{ab}\right) + \delta_{(ppn)}\frac{2}{3}\left(\frac{\tau_{(ac)}}{T_P/2}u_{ac} + \frac{\tau_{(ab)}}{T_P/2}u_{ab}\right)\mathrm{e}^{j\pi/3} \\
&= \delta_{(pnn)}\frac{2}{3}\left(d_{(ac)}u_{ac} + d_{(ab)}u_{ab}\right) + \delta_{(ppn)}\frac{2}{3}\left(d_{(ac)}u_{ac} + d_{(ab)}u_{ab}\right)\mathrm{e}^{j\pi/3}
\end{aligned}$$

Local DC-link Voltage Average Value

$$\overline{u} = d_{(ac)}u_{ac} + d_{(ab)}u_{ab}$$

$$\bar{\vec{u}}_2 = \delta_{(pnn)}\frac{2}{3}\overline{u} + \delta_{(ppn)}\frac{2}{3}\overline{u}\,\mathrm{e}^{j\pi/3} \qquad \bar{\vec{u}}_2 = \vec{u}_2^*$$

Calculation of the Inverter Active Switching State On-Times can be directly based on $\bar{u}$!

DC-link Voltage Local Average Value

$$\overline{u} = \frac{3}{2} \cdot \hat{U}_1 \frac{\cos\left(\varphi_{\vec{u}_1} - \varphi^*_{\vec{i}_1}\right)}{\cos\left(\varphi^*_{\vec{i}_1}\right)} = \frac{3}{2} \cdot \hat{U}_1 \frac{\cos\left(\Phi^*_1\right)}{\cos\left(\varphi^*_{\vec{i}_1}\right)}$$

Minimum of DC-link Voltage Local Average Value

$$\overline{u}_{\min} = \frac{3}{2}\hat{U}_1 \cos\Phi^*_1$$

Resulting IMC Output Voltage Limit

$$\hat{U}^*_{2,\max} \leq \frac{\sqrt{3}}{2} \cdot \hat{U}_1 \cos\Phi^*_1$$

Simulation of DC-link Voltage and Current Time Behavior

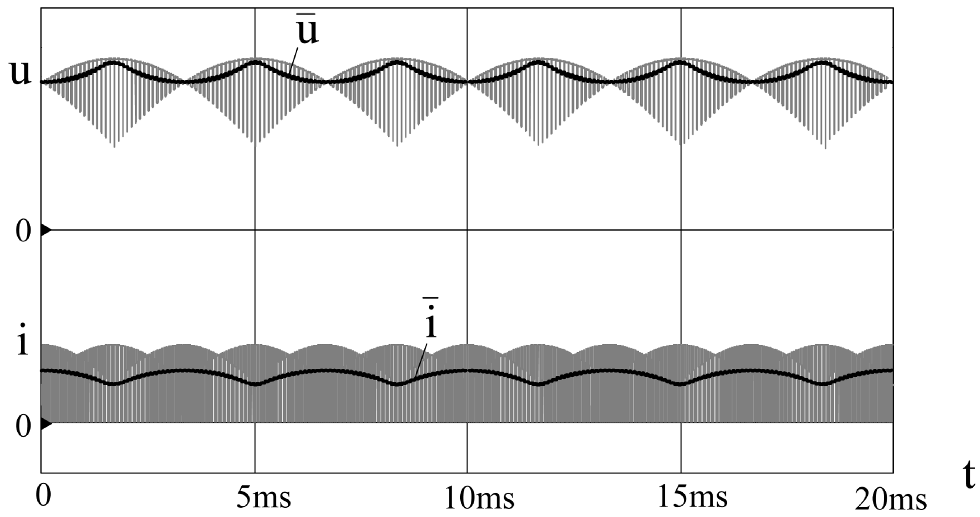

Resulting Inverter Stage Relative On-Times

$$\delta_{(ppn)} = \frac{\sqrt{3}}{2} \cdot \frac{\hat{U}_2^*}{\overline{u}/2} \sin\left(\varphi_{\vec{u}_2^*}\right)$$

$$\delta_{(pnn)} = \frac{\sqrt{3}}{2} \cdot \frac{\hat{U}_2^*}{\overline{u}/2} \cos\left(\varphi_{\vec{u}_2^*} + \frac{\pi}{6}\right)$$

Resulting Inverter Stage Absolute On-Times

$$\tau_{(ac)(pnn)} = \frac{1}{2} T_P d_{(ac)} \delta_{(pnn)} = \frac{1}{2} T_P \frac{2}{\sqrt{3}} \frac{\hat{U}_2^*}{\hat{U}_1} \frac{1}{\cos \Phi_1^*} \sin\left(\frac{\pi}{6} + \varphi_{\vec{i}_1}^*\right) \cos\left(\varphi_{\vec{u}_2^*} + \frac{\pi}{6}\right)$$

$$\tau_{(ac)(ppn)} = \frac{1}{2} T_P d_{(ac)} \delta_{(ppn)} = \frac{1}{2} T_P \frac{2}{\sqrt{3}} \frac{\hat{U}_2^*}{\hat{U}_1} \frac{1}{\cos \Phi_1^*} \sin\left(\frac{\pi}{6} + \varphi_{\vec{i}_1}^*\right) \sin\left(\varphi_{\vec{u}_2^*}\right)$$

$$\tau_{(ab)(pnn)} = \frac{1}{2} T_P d_{(ab)} \delta_{(pnn)} = \frac{1}{2} T_P \frac{2}{\sqrt{3}} \frac{\hat{U}_2^*}{\hat{U}_1} \frac{1}{\cos \Phi_1^*} \sin\left(\frac{\pi}{6} - \varphi_{\vec{i}_1}^*\right) \cos\left(\varphi_{\vec{u}_2^*} + \frac{\pi}{6}\right)$$

$$\tau_{(ab)(ppn)} = \frac{1}{2} T_P d_{(ab)} \delta_{(ppn)} = \frac{1}{2} T_P \frac{2}{\sqrt{3}} \frac{\hat{U}_2^*}{\hat{U}_1} \frac{1}{\cos \Phi_1^*} \sin\left(\frac{\pi}{6} - \varphi_{\vec{i}_1}^*\right) \sin\left(\varphi_{\vec{u}_2^*}\right)$$

DC-link Voltage Local Average Value

$$\bar{i}_{(ac)} = \frac{1}{\tau_{(ac)}}\left(i_A \delta_{(pnn)} \tau_{(ac)} - i_C \delta_{(ppn)} \tau_{(ac)}\right) = i_A \delta_{(pnn)} - i_C \delta_{(ppn)}$$

$$\bar{i}_{(ab)} = \frac{1}{\tau_{(ab)}}\left(i_A \delta_{(pnn)} \tau_{(ab)} - i_C \delta_{(ppn)} \tau_{(ab)}\right) = i_A \delta_{(pnn)} - i_C \delta_{(ppn)}$$

Equal DC-link Current Local Average Values for Inverter Active Switching States

$$\bar{i} = \bar{i}_{(ac)} = \bar{i}_{(ab)} = \hat{I}_2 \frac{\hat{U}_2^*}{\hat{U}_1} \frac{\cos \Phi_2}{\cos \Phi_1^*} \cos \varphi^*_{\vec{i}_1}$$

Local Average Value of Input Current in *a*

$$\bar{i}_a = \bar{i} = \hat{I}_1 \cos \varphi^*_{\vec{i}_1}$$

Resulting Input Phase Current Amplitude

$$\hat{I}_1 = \hat{I}_2 \frac{\hat{U}_2^*}{\hat{U}_1} \frac{\cos \Phi_2}{\cos \Phi_1^*}$$

Power Balance of Input and Output Side

$$\bar{p} = P = \bar{u}\,\bar{i} = \frac{3}{2} \hat{U}_1 \hat{I}_1 \cos \Phi_1^* = \frac{3}{2} \hat{U}_2^* \hat{I}_2 \cos \Phi_2$$

IMC Simulation Results

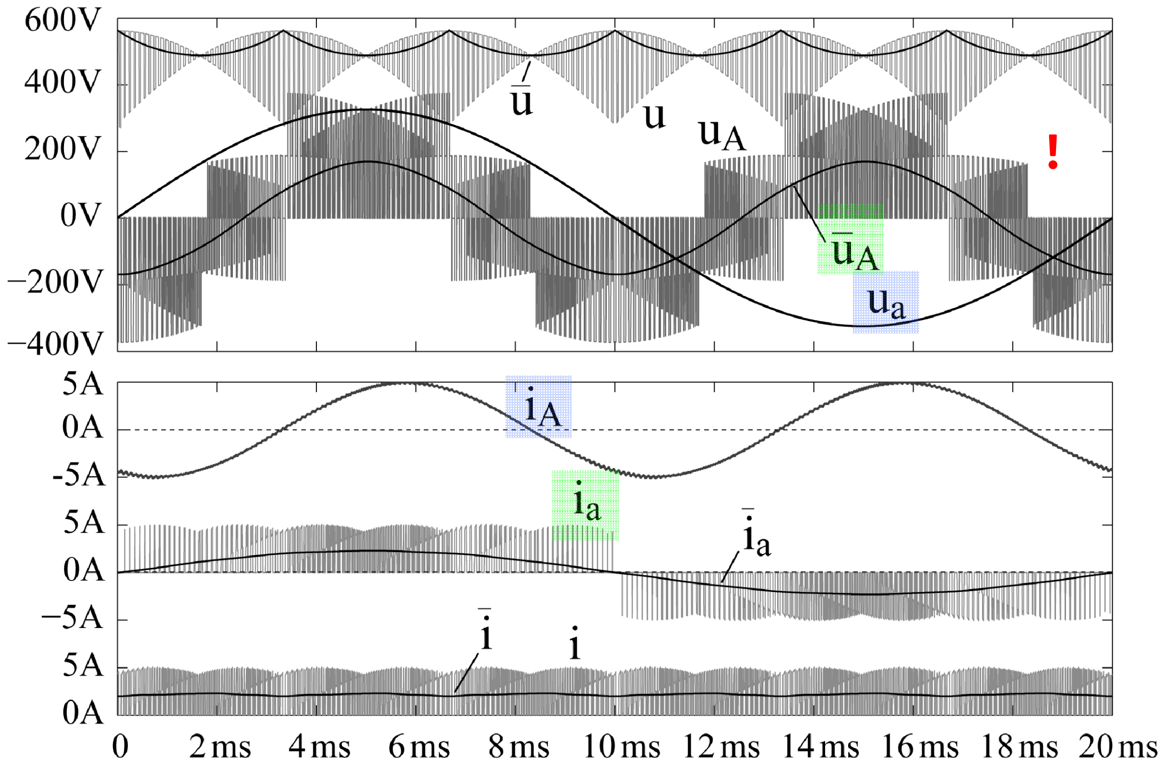

RB-IGBT IMC Experimental Results (1)

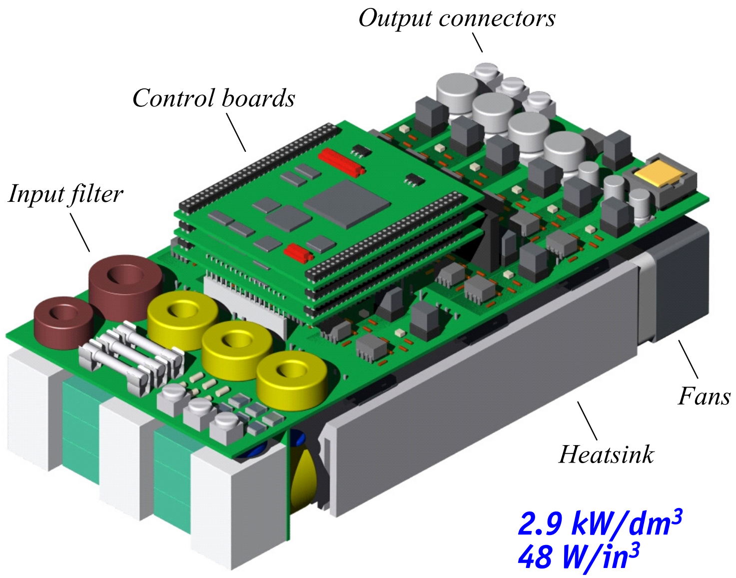

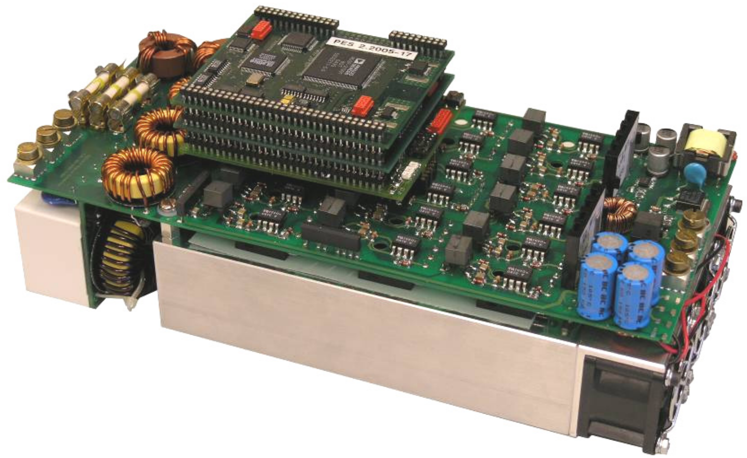

2.9 kW/dm^3
48 W/in^3

Input RMS voltage	400V
Output Power	6.8 kVA
Rectifier Switching Frequency	12.5 kHz
Inverter Switching Frequency	25 kHz

Efficiency 95.5%

RB-IGBT IMC Experimental Results (2)

U_1 = 400V
P_{out} = 1.5 kW
f_{out} = 120 Hz

f_S = 12.5 kHz / 25kHz

DC Link Voltage

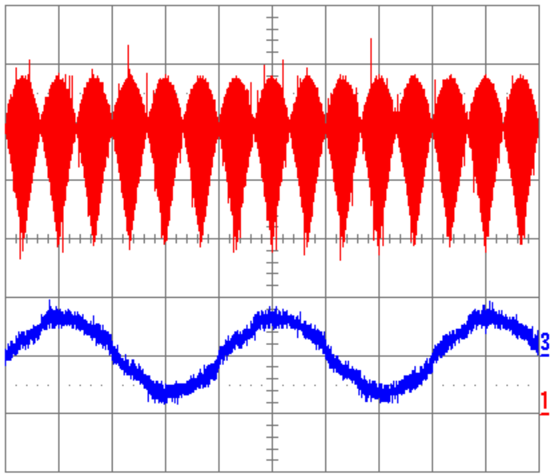

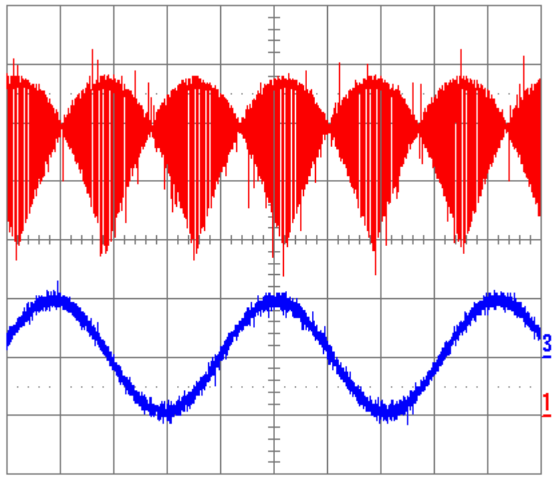

Input Current

Output Current

100 V/div
5A/div

Alternative Modulation Schemes (1)

▶ Conventional Modulation (HV)

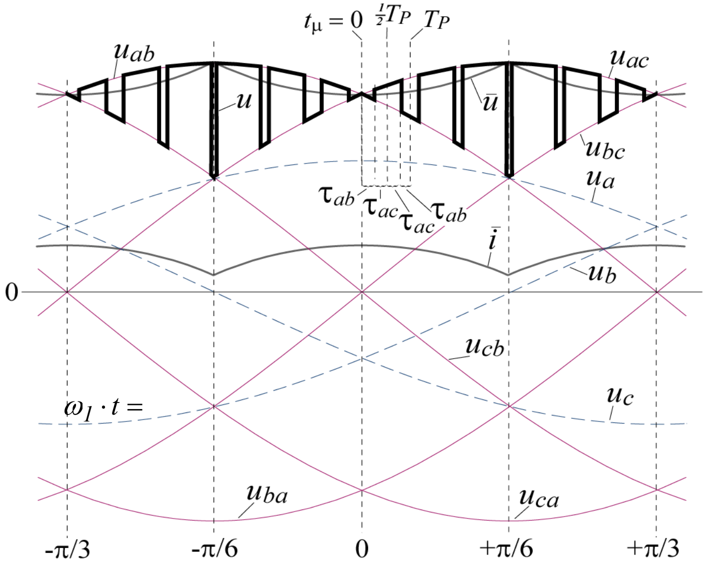

DC-link Voltage: *Largest and Medium Line-to-Line Mains Voltage*

$$\hat{U}_{2,max,I} = \frac{\sqrt{3}}{2}\hat{U}_1 \approx 0.86 \cdot \hat{U}_1$$

▶ Low Output Voltage Modulation (LV)

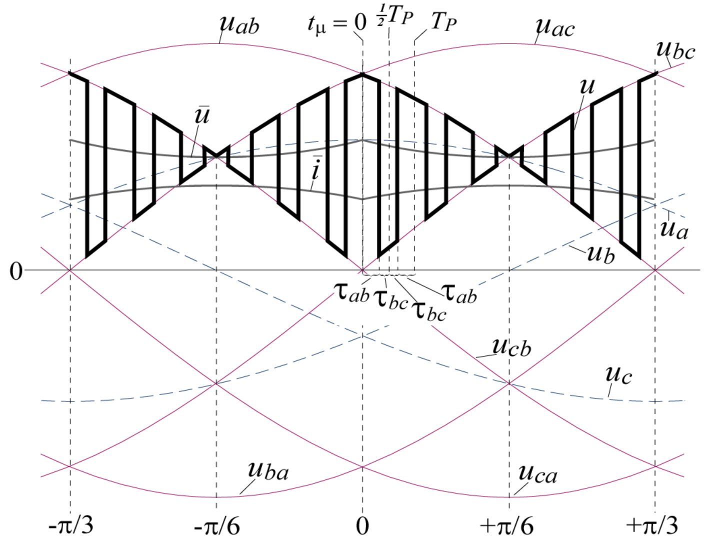

DC-link Voltage: *Medium and Smallest Line-to-Line Mains Voltage*

$$\hat{U}_{2,max,II} = \frac{1}{2}\hat{U}_1 = 0.5 \cdot \hat{U}_1$$

Alternative Modulation Schemes (2)

▶ Low Output Voltage Modulation

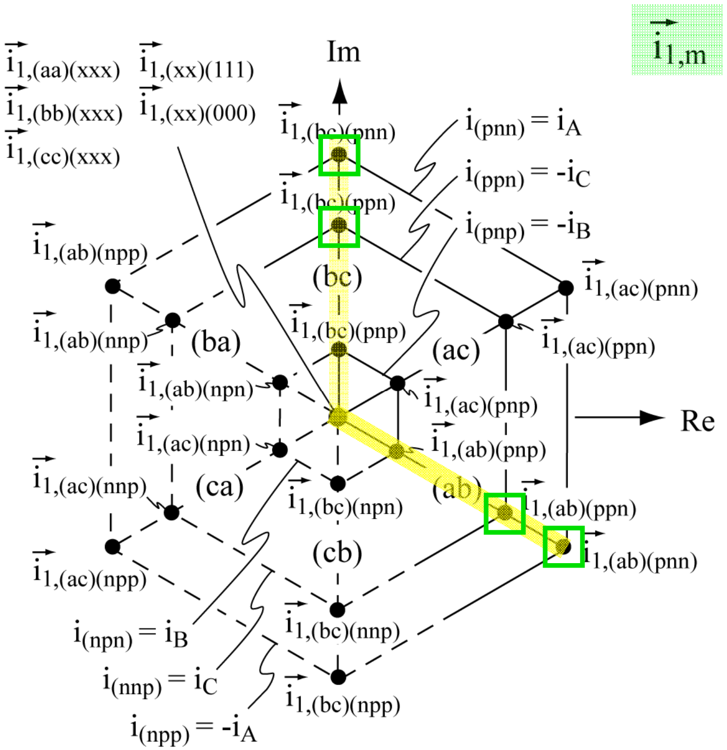

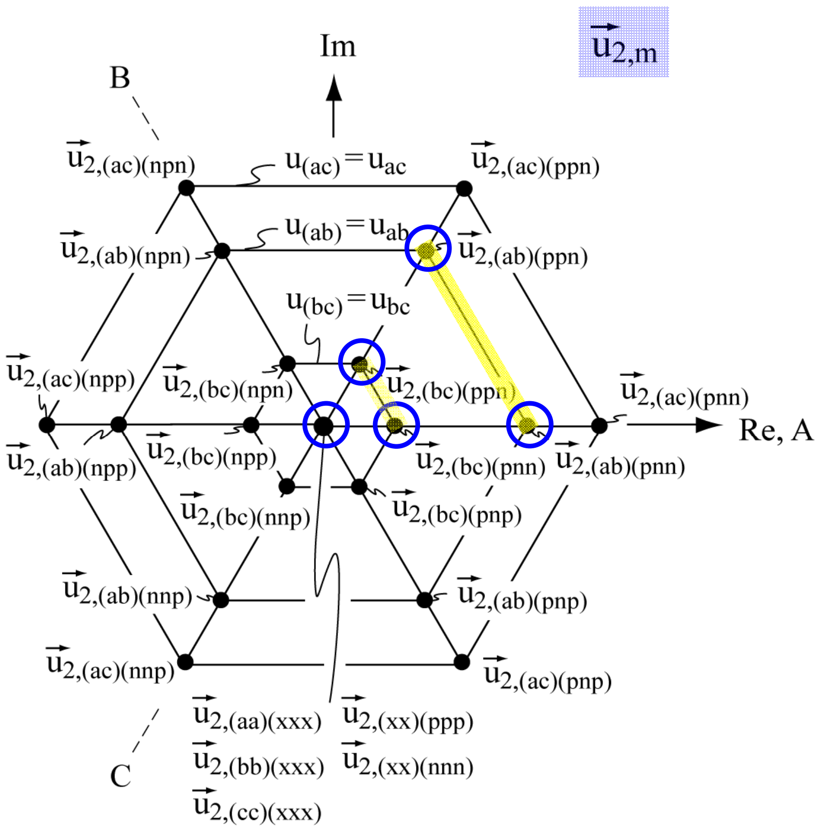

Alternative Modulation Schemes (3)

► LV vs. HV Modulation

Output Voltage Generation

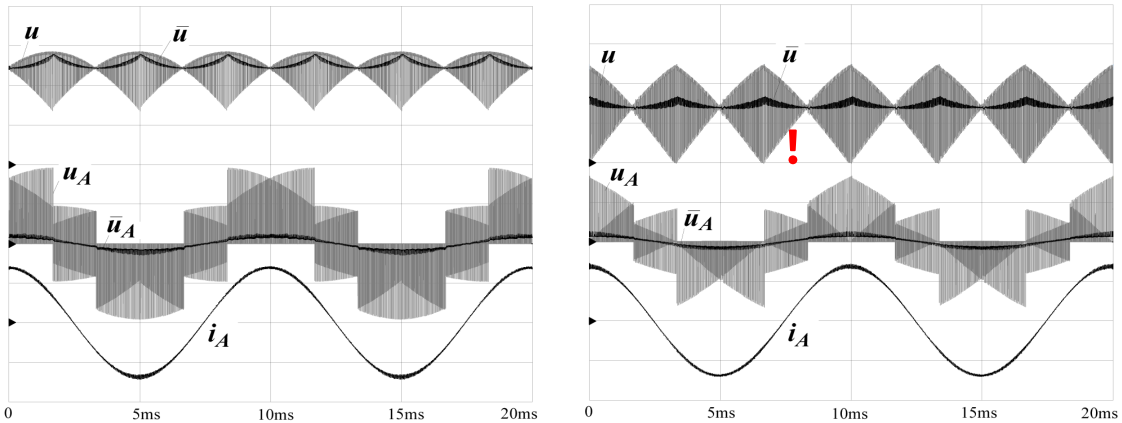

Input Current Generation

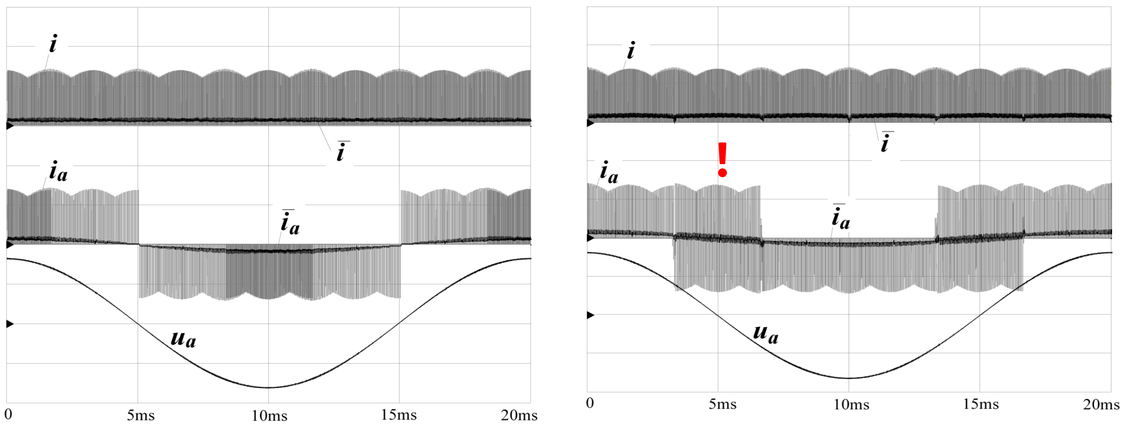

Alternative Modulation Schemes (4)

▶ LV vs. HV Modulation

Switching Losses

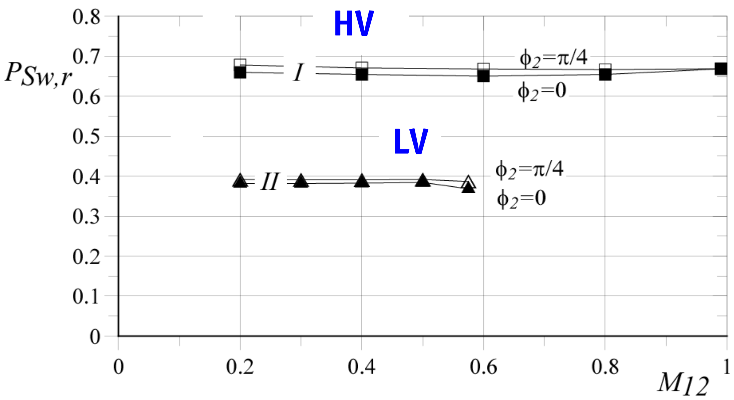

Reduction of Switching Losses
to approx. 58%

Output Common Mode Voltage

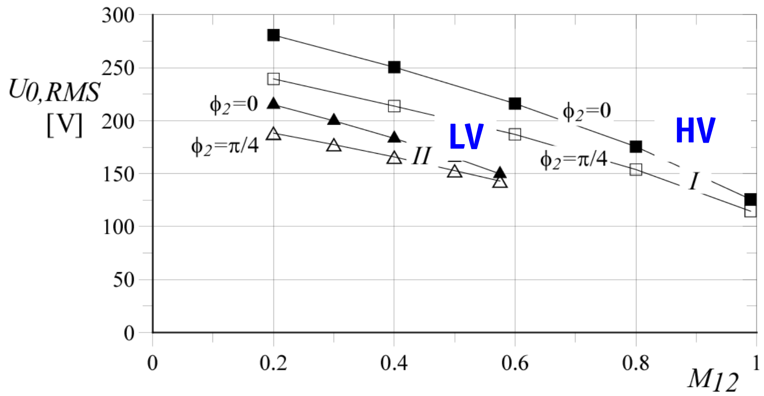

Output Common Mode Voltage reduced
to approx. 75%

Alternative Modulation Schemes (5)

▶ LV vs. HV Modulation

Input Voltage Ripple

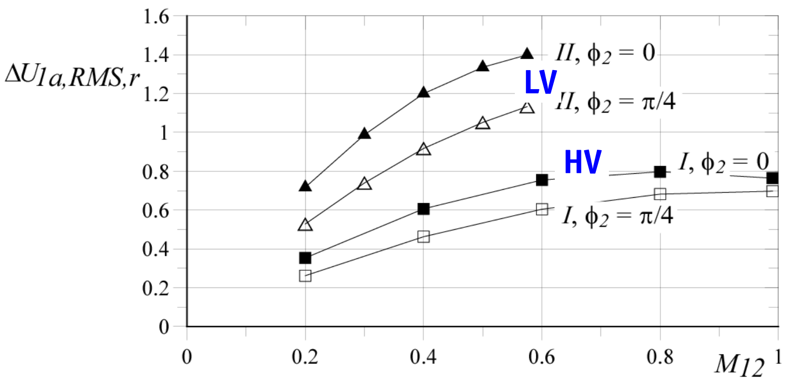

Output Current Ripple

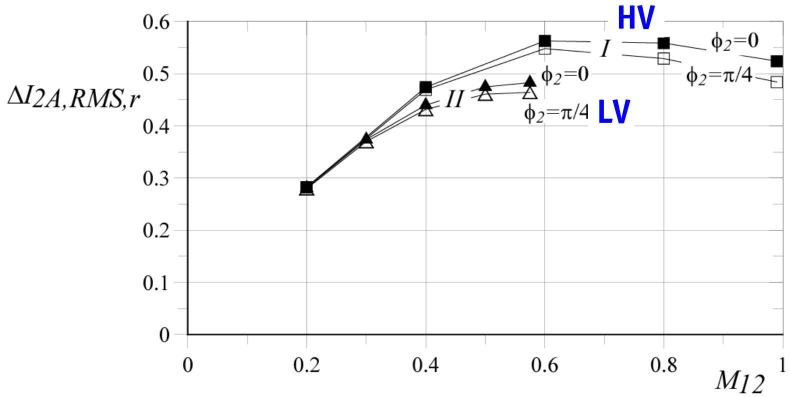

Current Stresses

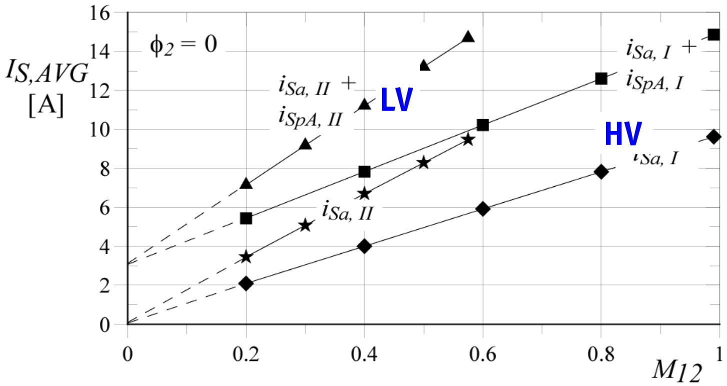

- Input Voltage Ripple Doubles
- Output Current Ripple Slightly Reduced
- For given $\hat{U}_2$ (M_{12}) the Component Current Stress are Increasing (Conduction Losses)

Alternative Modulation Schemes (6)

► Three-Level Medium Voltage Modulation

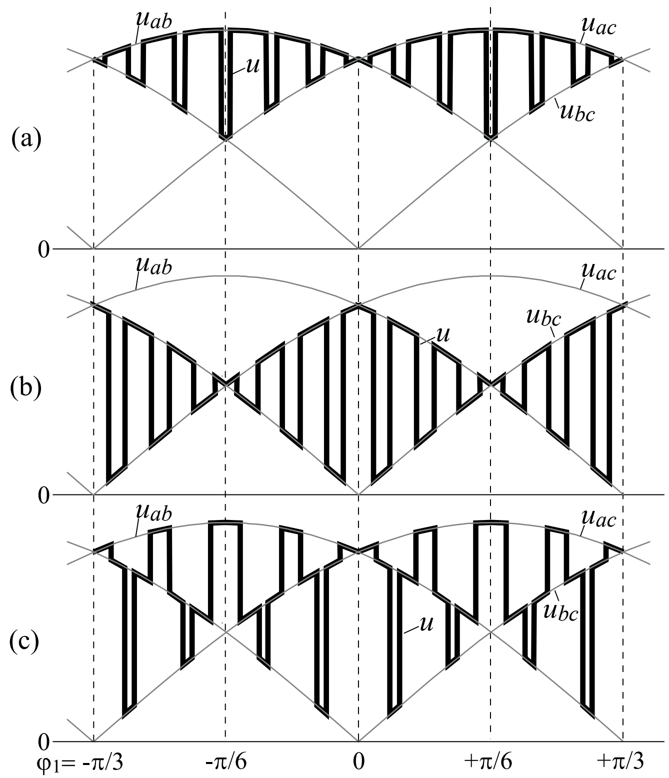

High Output Voltage Modulation (HVM)

$$\hat{U}_2 = 0 \ldots \frac{\sqrt{3}}{2} \cdot \hat{U}_1$$

Low Output Voltage Modulation (LVM)

$$\hat{U}_2 = 0 \ldots \frac{1}{2} \cdot \hat{U}_1$$

Three-Level Modulation

$$\hat{U}_2 = \frac{1}{2} \ldots \frac{\sqrt{3}}{2} \cdot \hat{U}_1$$

Weighted Combination of HVM and LVM

Sparse Matrix Converter - SMC

Topology Derivation
Bidirectional / Unidirectional Converter
Experimental Results

Classification of Three-Phase AC-AC Converters

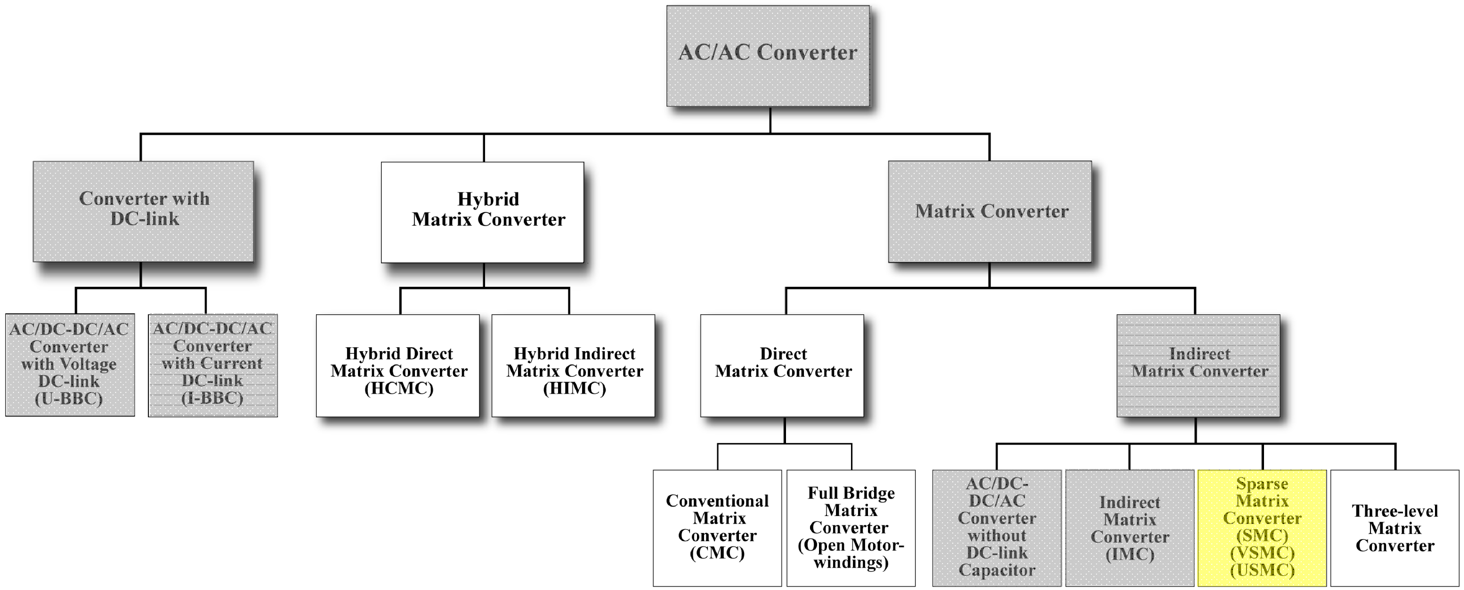

- *Sparse Matrix Converter*

Sparse Matrix Converter

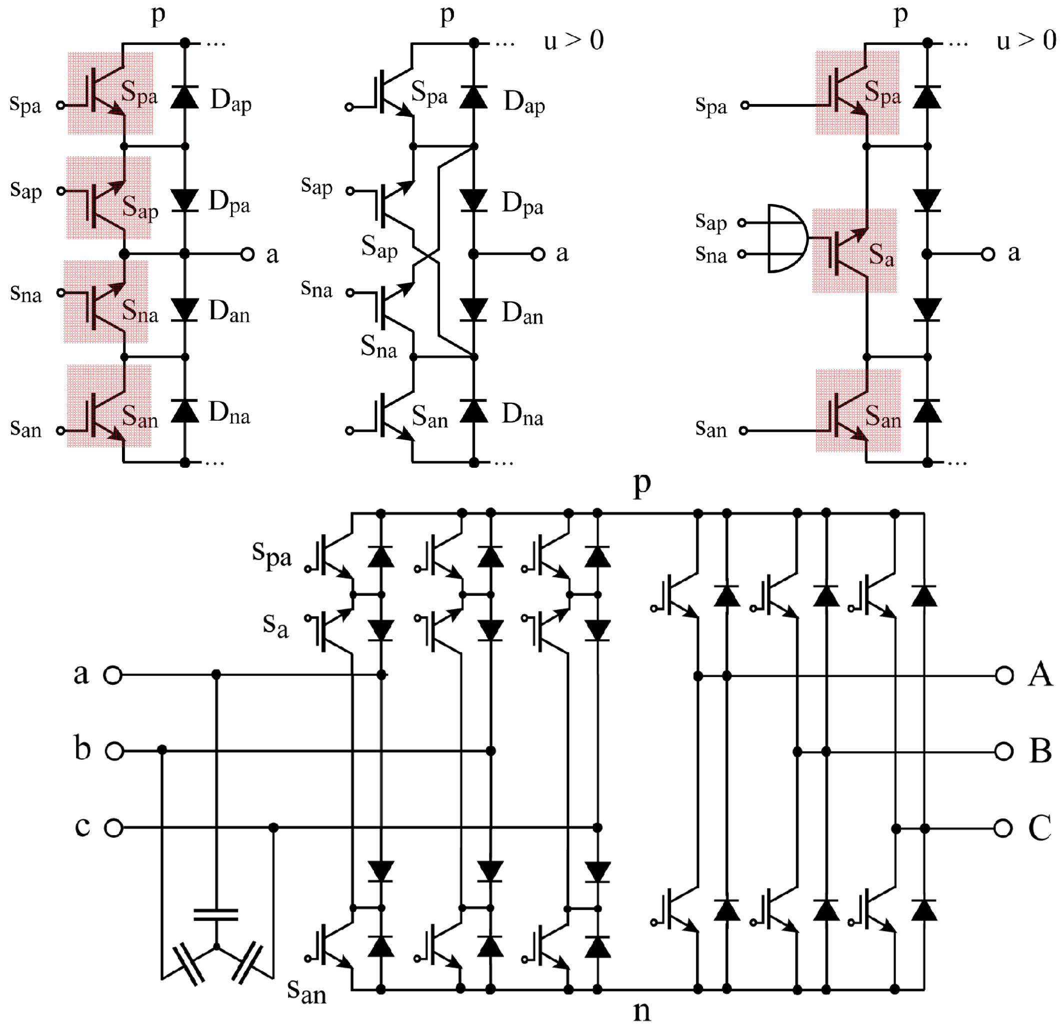

ETH Zurich

- ***15 Transistors***
- ***18 Diodes***

All-SiC-Sparse Matrix Converter

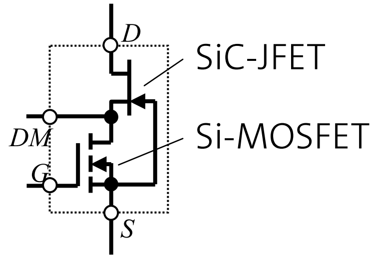

Switching Frequency 150kHz
Output Power 2.5kW@10kW/dm^3

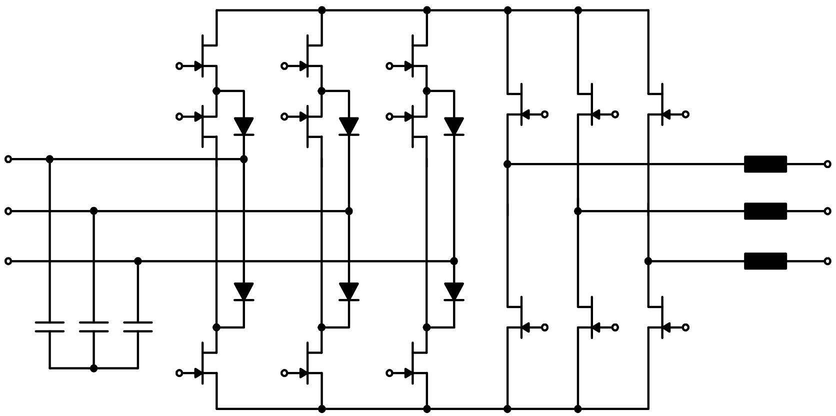

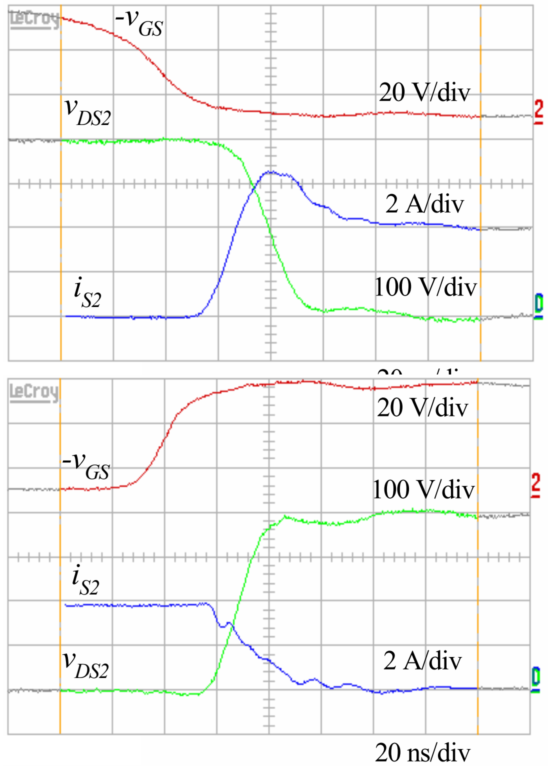

All-SiC-Sparse Matrix Converter

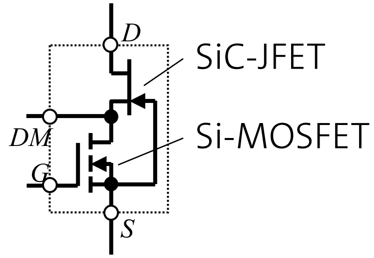

Switching Frequency 150kHz
Output Power 2.5kW@10kW/dm^3

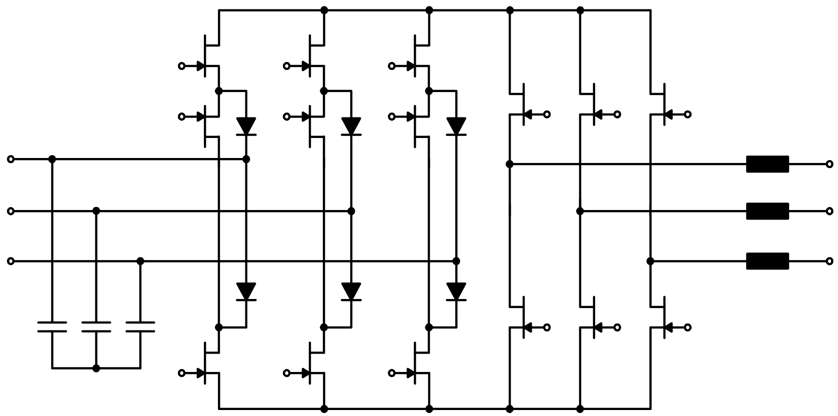

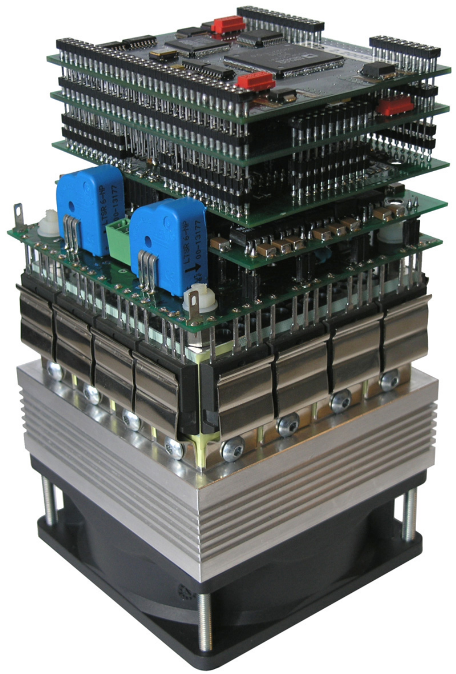

Ultra Sparse Matrix Converter

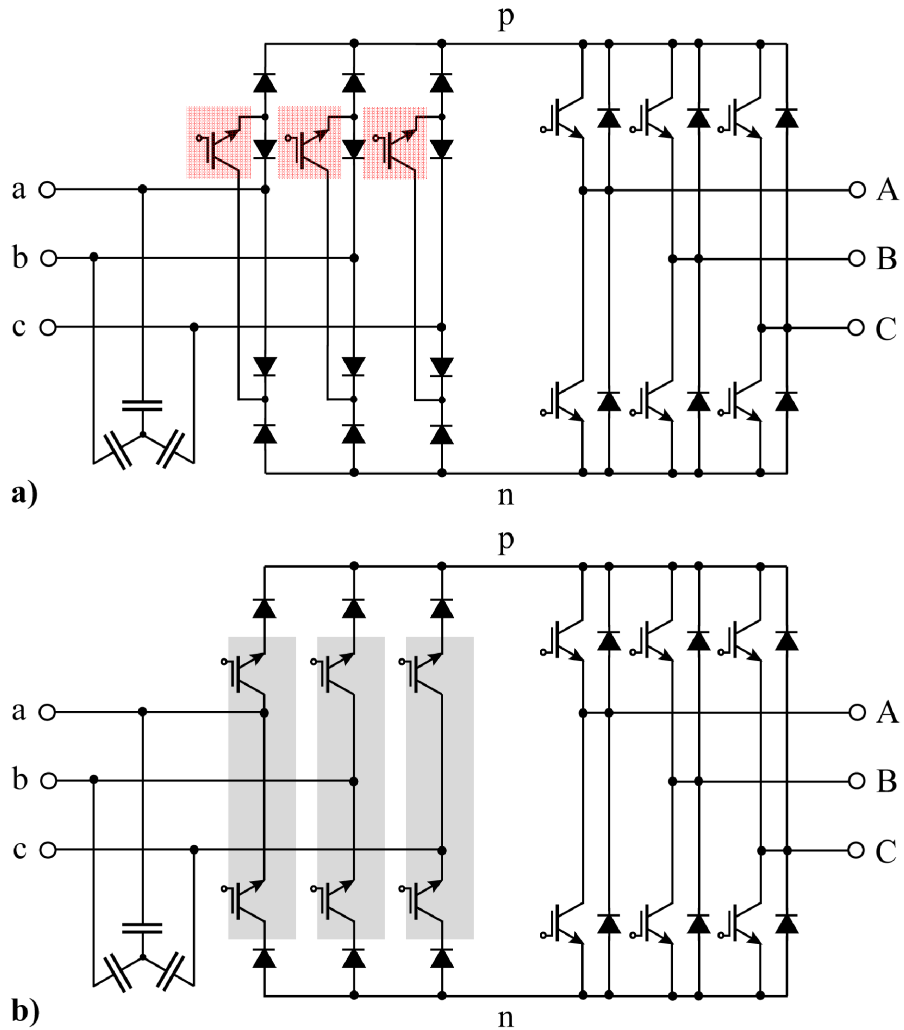

ETH Zurich
T. Lipo [13, 20]

- *9 Transistors*
- *18 Diodes*

Ultra-Sparse Matrix Converter

U_1 = 3-Φ 400V/50Hz
U_2 = 3-Φ 0...340V / 0...200Hz
P = 5.5kVA

f = 25kHz (Rect.) / 50kHz (Inv.)

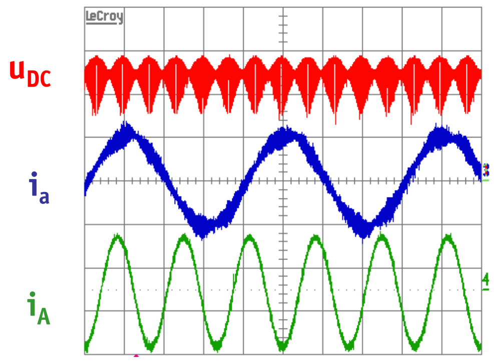

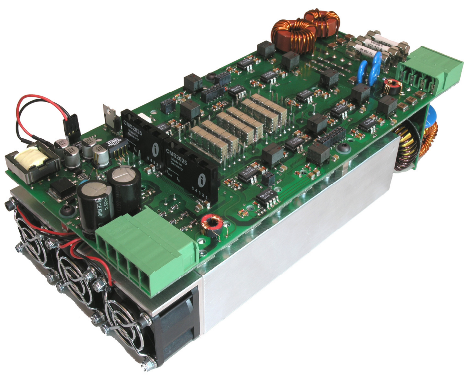

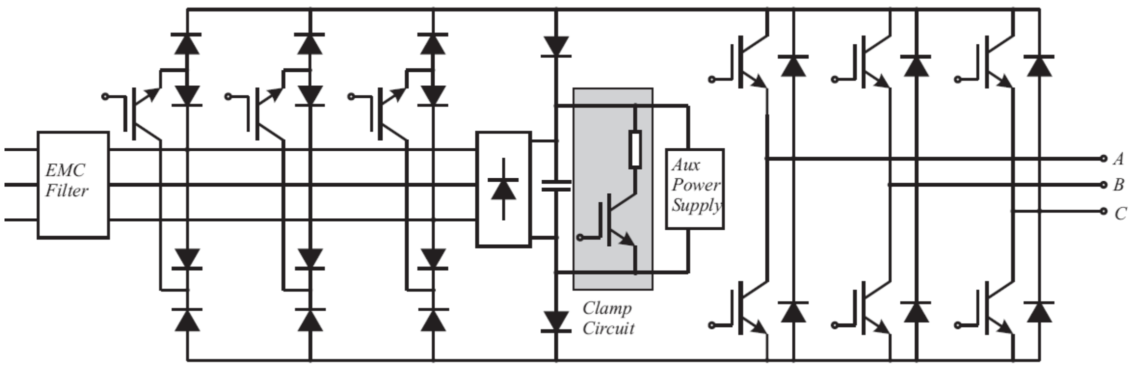

!

IMC - Extensions

Three-Level
Hybrid

Classification of Three-Phase AC-AC Converters

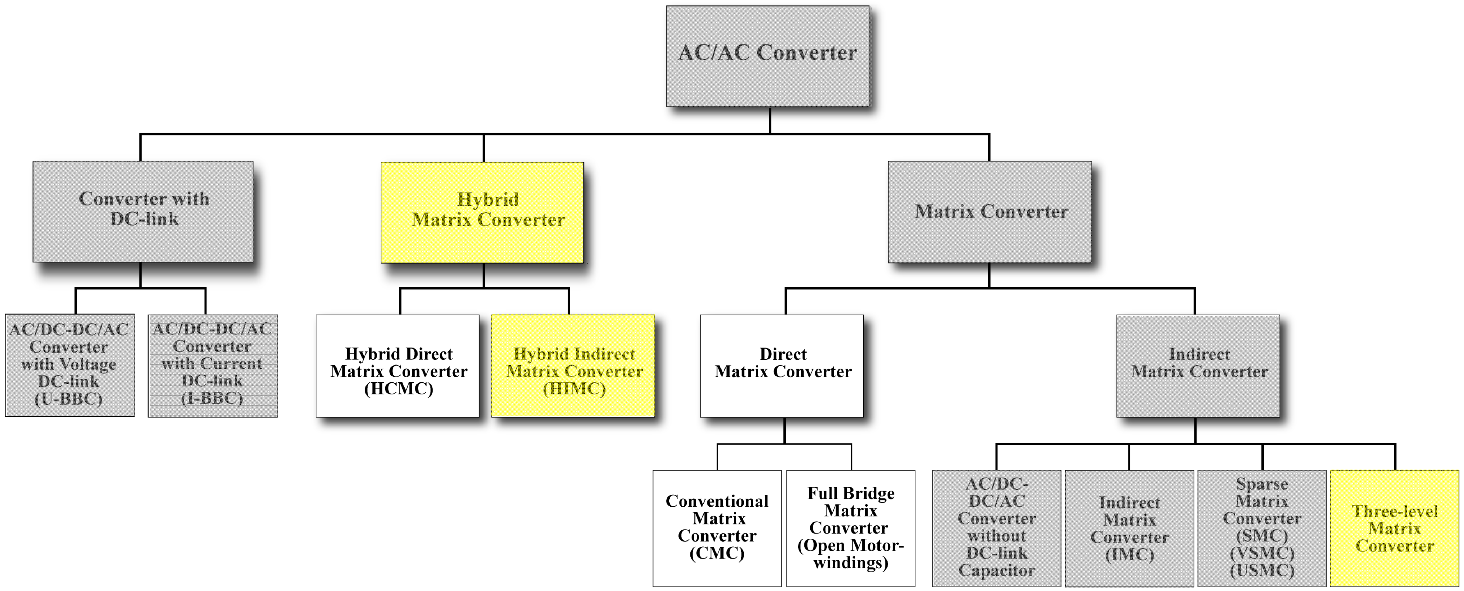

- *Three-Level IMC*
- *Hybrid IMC*

Three-Level Matrix Converter

- *Bidirectional Converter*

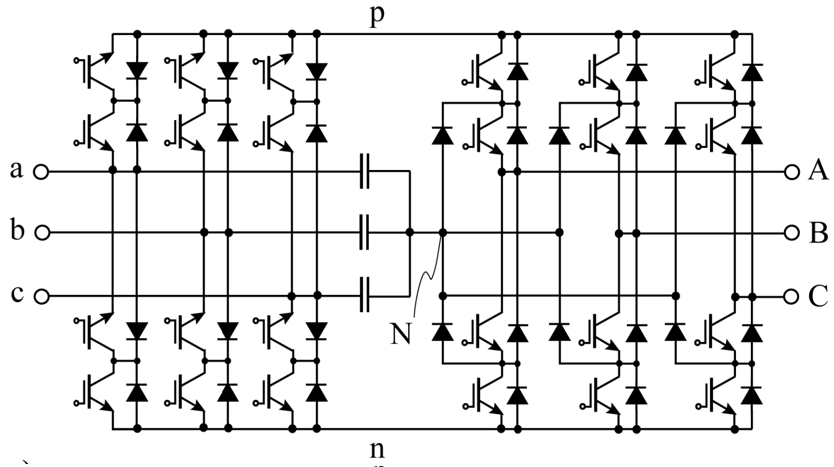

- *Unidirectional Converter*

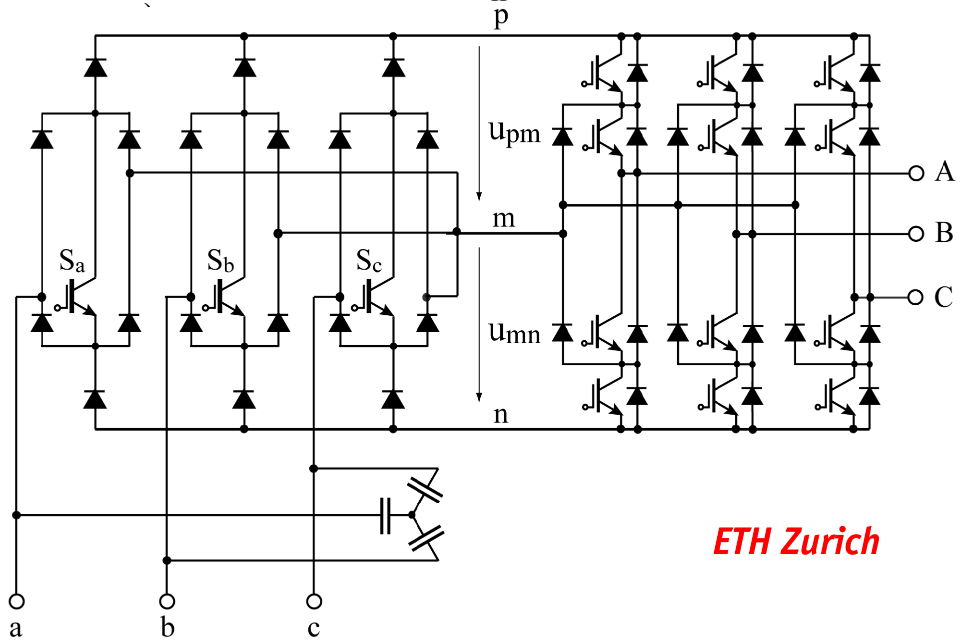

ETH Zurich

Three-Level Matrix Converter

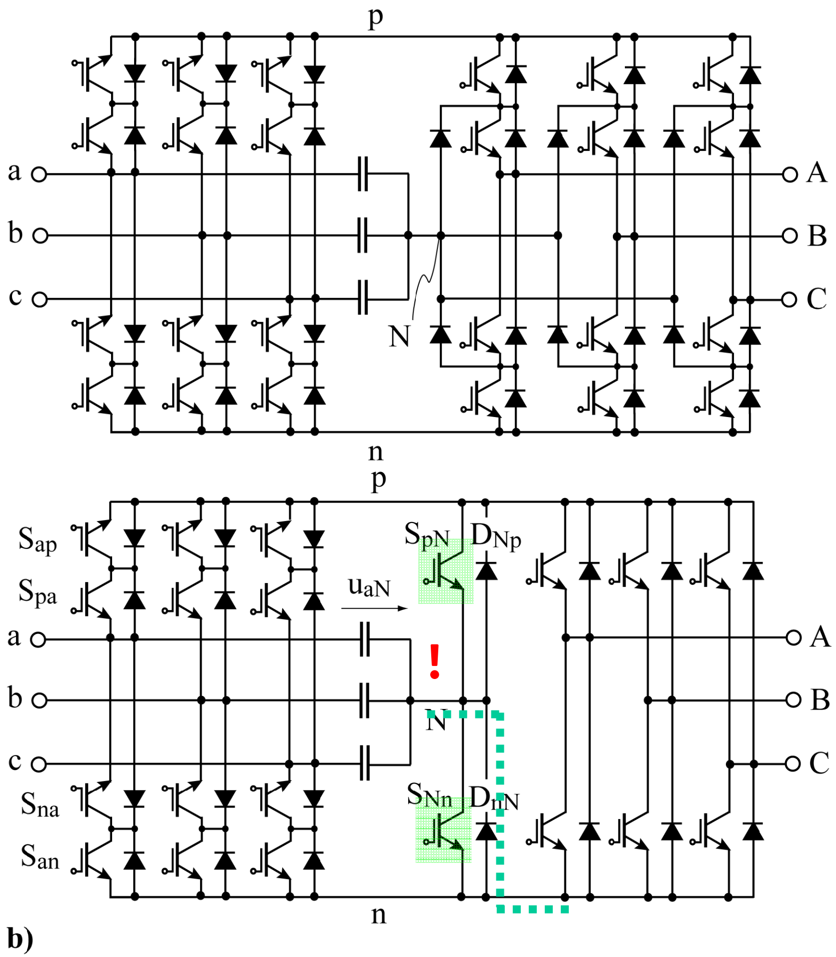

Ch. Klumpner [23, 24]

Hybrid IMC

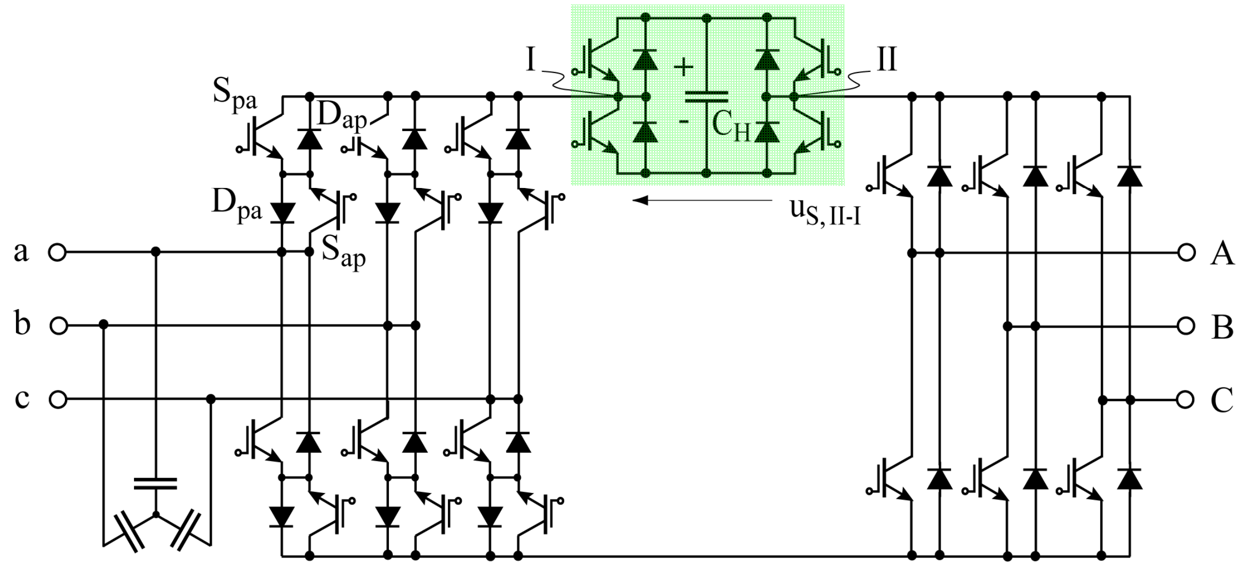

Ch. Klumpner [5, 6]

Conventional Matrix Converter - CMC

Modulation
Multi-Step Commutation

Classification of Three-Phase AC-AC Converters

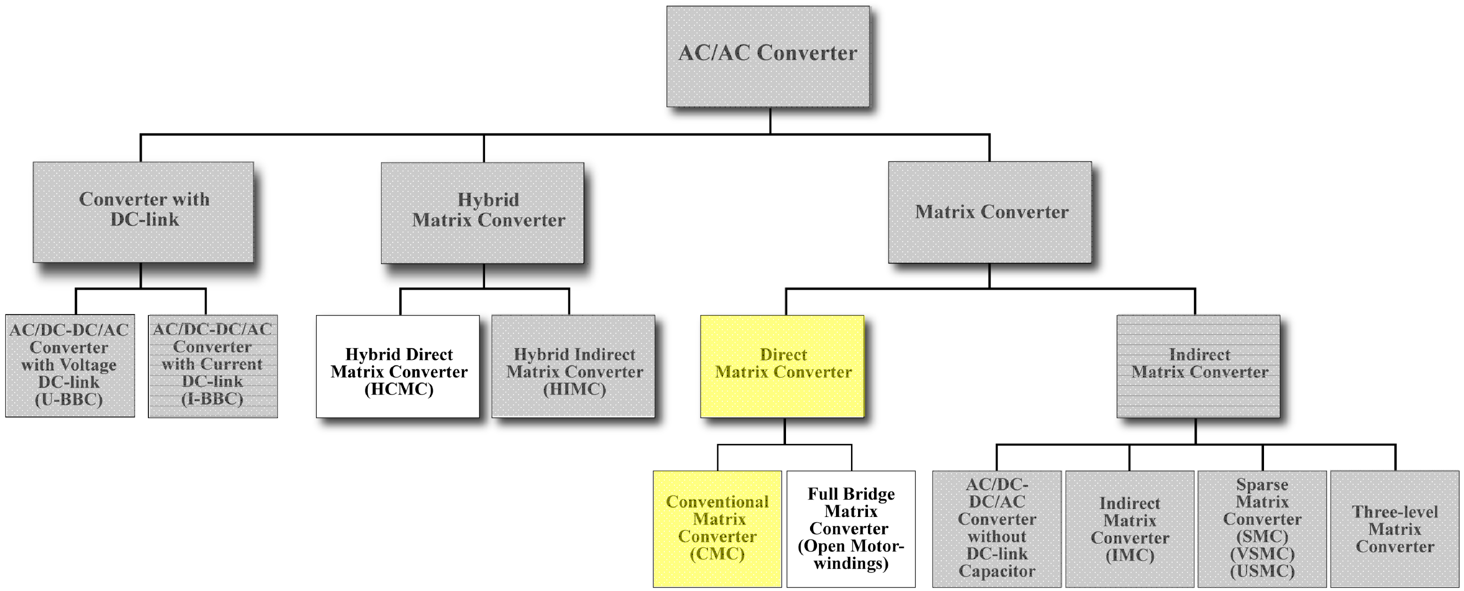

- *Conventional Matrix Converter*

Conventional Matrix Converter - CMC

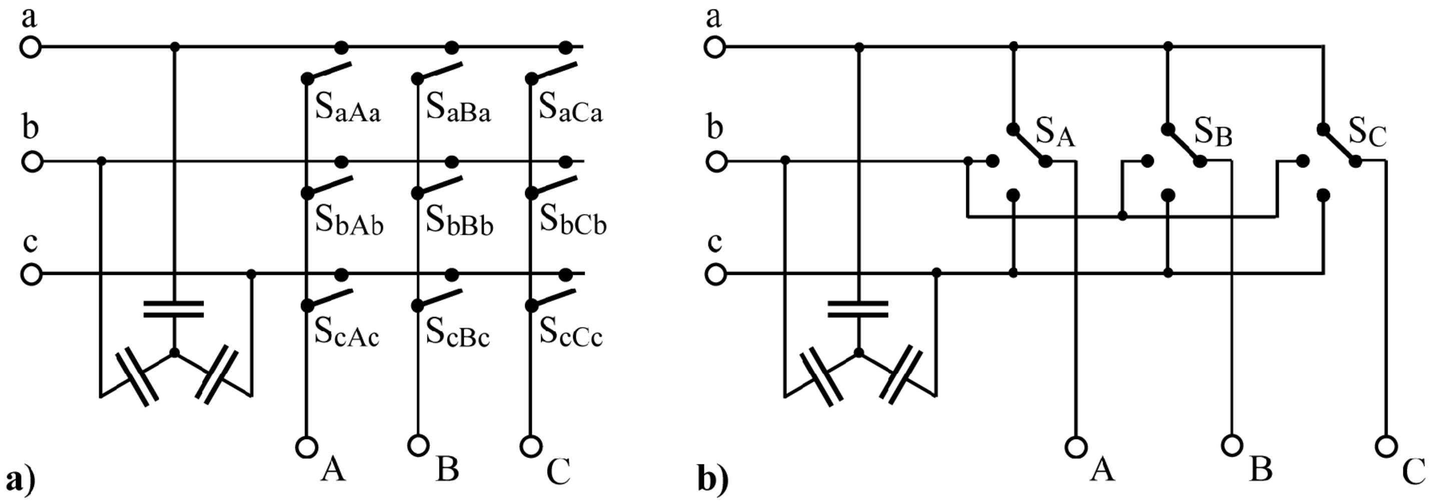

► *Quasi Three-Level Characteristic*

CMC Classification of Switching States

Group I *Freewheeling States*	(aaa)	(bbb)	(ccc)	
Group II *Generating Stationary Output Voltage and Input Current Space Vectors*	(cca)	(ccb)	(aab)	$u_{AB} = 0$
	(aac)	(bbc)	(bba)	$u_{AB} = 0$
	(acc)	(bcc)	(baa)	$u_{BC} = 0$
	(caa)	(cbb)	(abb)	$u_{BC} = 0$
	(cac)	(cbc)	(aba)	$u_{CA} = 0$
	(aca)	(bcb)	(bab)	$u_{CA} = 0$
Group III *Generating Rotating Space Vectors*	(abc)	(cab)	(bca)	*Positive Sequence*
	(acb)	(cba)	(bac)	*Negative Sequence*

CMC Rotating Space Vectors

Positive Sequence Switching States

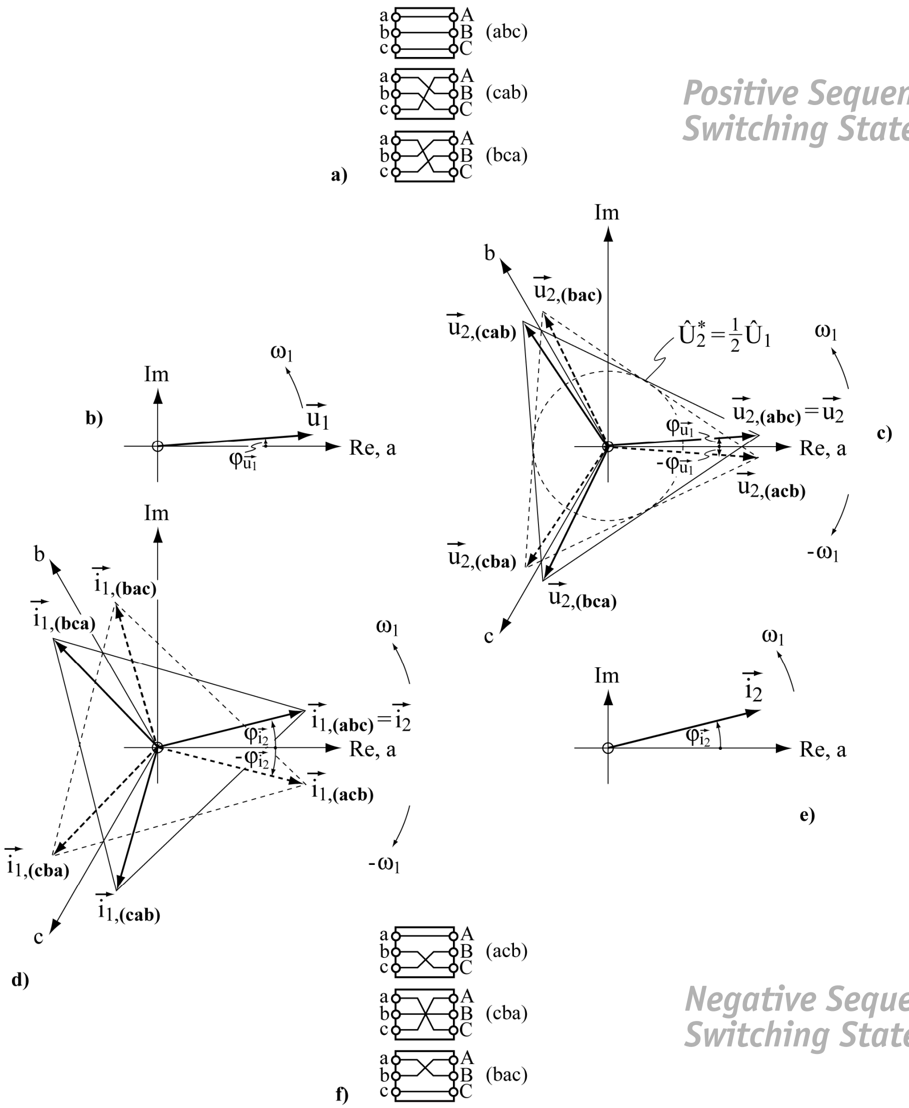

Negative Sequence Switching States

CMC Stationary Space Vectors

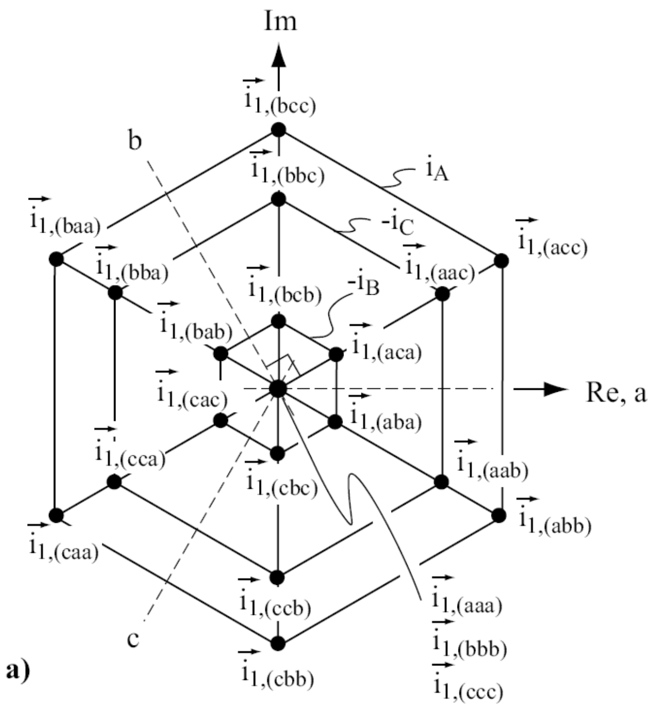

Input Current Space Vectors

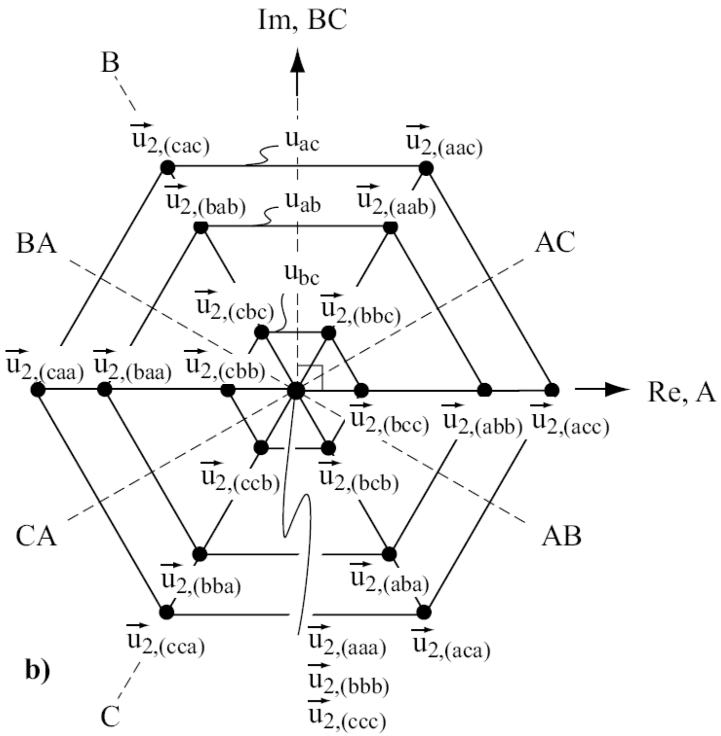

Output Voltage Space Vectors

CMC/IMC Relation (1)

Correspondence of Switching States

$$\vec{u}_{2,(acc)} = \vec{u}_{2,(ac)(pnn)}$$

$$\vec{i}_{1,(acc)} = \vec{i}_{1,(ac)(pnn)}$$

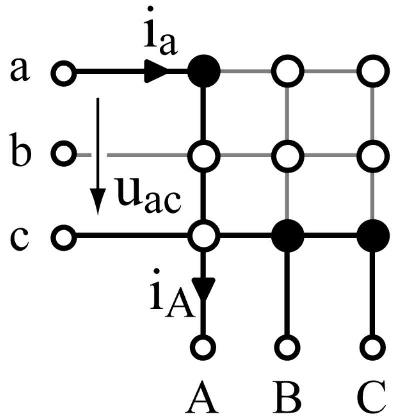

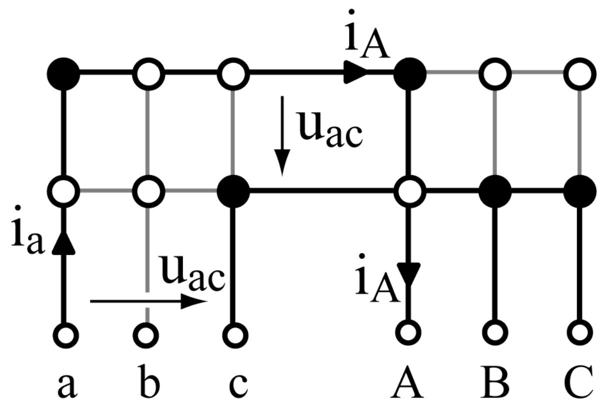

► *Indirect Space Vector Modulation*

P. Ziogas [12]
L. Huber / D. Borojevic

CMC/IMC Relation (2)

Matrix Representation of Voltage and Current Conversion

- **CMC**

$$\begin{pmatrix} u_A \\ u_B \\ u_C \end{pmatrix} = \begin{pmatrix} s_{aAa} & s_{bAb} & s_{cAc} \\ s_{aBa} & s_{bBb} & s_{cBc} \\ s_{aCa} & s_{bAb} & s_{cCc} \end{pmatrix} \cdot \begin{pmatrix} u_a \\ u_b \\ u_c \end{pmatrix} = \underline{\underline{S}}_{CMC,U} \begin{pmatrix} u_a \\ u_b \\ u_c \end{pmatrix}$$

$$\begin{pmatrix} i_a \\ i_b \\ i_c \end{pmatrix} = \underline{\underline{S}}_{CMC,I} \begin{pmatrix} i_A \\ i_B \\ i_C \end{pmatrix}$$

$$\underline{\underline{S}}_{CMC,I} = \underline{\underline{S}}^T_{CMC,U}$$

- **IMC**

$$\begin{pmatrix} u_A \\ u_B \\ u_C \end{pmatrix} = \begin{pmatrix} s_{pA} & s_{An} \\ s_{pB} & s_{Bn} \\ s_{pC} & s_{Cn} \end{pmatrix} \cdot \begin{pmatrix} u_p \\ u_n \end{pmatrix} = \underline{\underline{S}}_{WR,U} \begin{pmatrix} u_p \\ u_n \end{pmatrix}$$

$$\begin{pmatrix} u_p \\ u_n \end{pmatrix} = \begin{pmatrix} s_{apa} & s_{bpb} & s_{cpc} \\ s_{ana} & s_{bnb} & s_{cnc} \end{pmatrix} \cdot \begin{pmatrix} u_a \\ u_b \\ u_c \end{pmatrix} = \underline{\underline{S}}_{GR,U} \begin{pmatrix} u_a \\ u_b \\ u_c \end{pmatrix}$$

$$\underline{\underline{S}}_{IMC,I} = \underline{\underline{S}}^T_{IMC,U}$$

CMC/IMC Relation (3)

$$\underline{\underline{S}}_{CMC,U} \equiv \underline{\underline{S}}_{IMC,U}$$

$$\underline{\underline{S}}_{IMC,U} = \underline{\underline{S}}_{WR,U}\,\underline{\underline{S}}_{GR,U} = \begin{pmatrix} s_{pA} & s_{An} \\ s_{pB} & s_{Bn} \\ s_{pC} & s_{Cn} \end{pmatrix} \cdot \begin{pmatrix} s_{apa} & s_{bpb} & s_{bpb} \\ s_{ana} & s_{bnb} & s_{cnc} \end{pmatrix}$$

$$\begin{pmatrix} s_{aAa} & s_{bAb} & s_{cAc} \\ s_{aBa} & s_{bBb} & s_{cBc} \\ s_{aCa} & s_{bCb} & s_{cCc} \end{pmatrix}$$

$$\equiv \begin{pmatrix} s_{apa}s_{pA} + s_{ana}s_{An} & s_{bpb}s_{pA} + s_{bnb}s_{An} & s_{cpc}s_{pA} + s_{cnc}s_{An} \\ s_{apa}s_{pB} + s_{ana}s_{Bn} & s_{bpb}s_{pB} + s_{bnb}s_{Bn} & s_{cpc}s_{pB} + s_{cnc}s_{Bn} \\ s_{apa}s_{pC} + s_{ana}s_{Cn} & s_{bpb}s_{pC} + s_{bnb}s_{Cn} & s_{cpc}s_{pC} + s_{cnc}s_{Cn} \end{pmatrix}$$

Example

$$\vec{u}_{2,(acc)} = \vec{u}_{2,(ac)(pnn)}$$

$$\vec{i}_{1,(acc)} = \vec{i}_{1,(ac)(pnn)}$$

$$\underline{\underline{S}}_{CMC,U} = \begin{pmatrix} 1 & 0 \\ 0 & 1 \\ 0 & 1 \end{pmatrix} \cdot \begin{pmatrix} 1 & 0 & 0 \\ 0 & 0 & 1 \end{pmatrix} = \begin{pmatrix} 1 & 0 & 0 \\ 0 & 0 & 1 \\ 0 & 0 & 1 \end{pmatrix}$$

CMC/IMC Relation (4)

$\varphi_{\vec{u}_2^*} \in [0, \pi/6]$

Correspondence of Switching States

- **IMC**

$$\ldots|_{t_\mu = 0} \quad (ac)(pnn) - (ac)(ppn) - (ac)(ppp) - (ab)(ppp) - (ab)(ppn) - (ab)(pnn)|_{t_\mu = T_P/2}$$
$$(ab)(pnn) - (ab)(ppn) - (ab)(ppp) - (ac)(ppp) - (ac)(ppn) - (ac)(pnn)|_{t_\mu = T_P} \quad \cdots$$

- **CMC**

$$\ldots|_{t_\mu = 0} \quad (acc) - (aac) - (aaa) - (aaa) - (aab) - (abb)|_{t_\mu = T_P/2}$$
$$(abb) - (aab) - (aaa) - (aaa) - (aac) - (acc)|_{t_\mu = T_P} \quad \cdots$$

$\varphi_{\vec{u}_2^*} \in [\pi/6,\ \pi/3]$

- **IMC**

$$\ldots|_{t_\mu = 0} \quad (ac)(ppn) - (ac)(pnn) - (ac)(nnn) - (ab)(nnn) - (ab)(pnn) - (ab)(ppn)|_{t_\mu = T_P/2}$$
$$(ab)(ppn) - (ab)(pnn) - (ab)(nnn) - (ac)(nnn) - (ac)(pnn) - (ac)(ppn)|_{t_\mu = T_P} \quad \cdots$$

- **CMC**

$$\ldots|_{t_\mu = 0} \quad (aac) - (acc) - (ccc) - (bbb) - (abb) - (aab)|_{t_\mu = T_P/2}$$
$$(aab) - (abb) - (bbb) - (ccc) - (acc) - (aac)|_{t_\mu = T_P} \quad \cdots$$

CMC/IMC Relation (5)

$\varphi_{\vec{u}_2^*} \in [0, \pi/6]$

$\varphi_{\vec{u}_2^*} \in [\pi/6, \pi/3]$

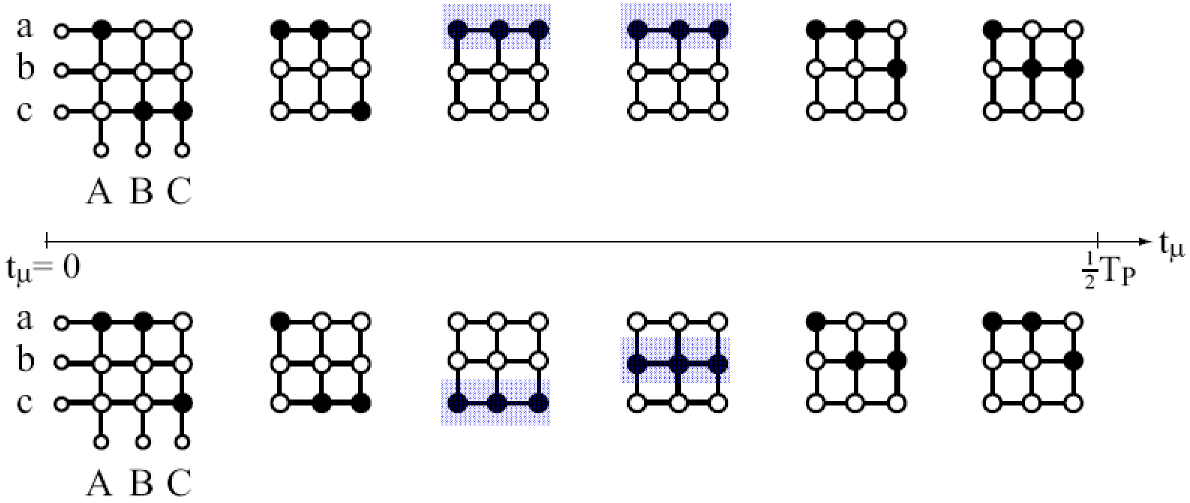

$\varphi_{\vec{u}_2^*} \in [0, \pi/3]$

$$\ldots|_{t_\mu = 0} \quad (acc) - (aac) - (aaa) - (aaa) - (aab) - (abb)|_{t_\mu = T_P/2}$$
$$(abb) - (aab) - (aaa) - (aaa) - (aac) - (acc)|_{t_\mu = T_P} \quad \ldots$$

CMC Multi-Step Commutation

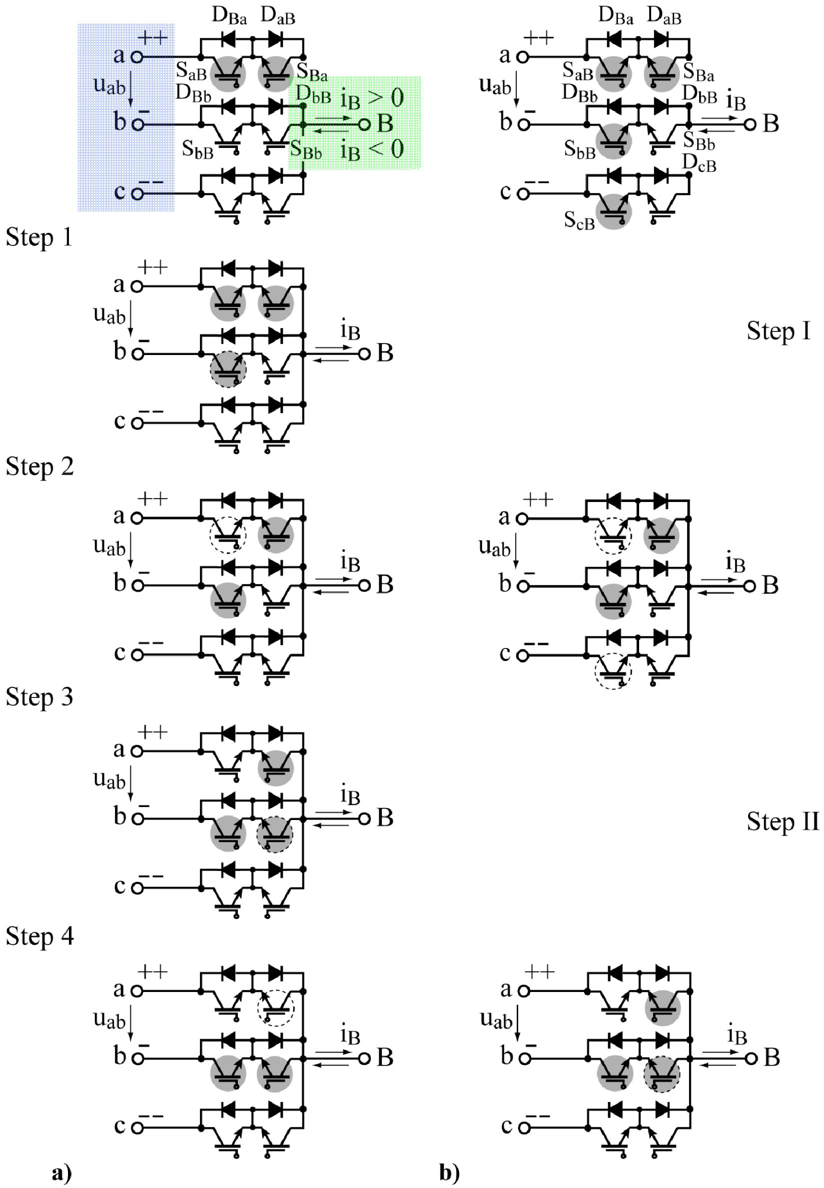

J. Oyama / T. Lipo
N. Burany
P. Wheeler
W. Hofmann

- *Four-Step Commutation*
- *Two-Step Commutation*

4-Step Commutation of CMC (1)

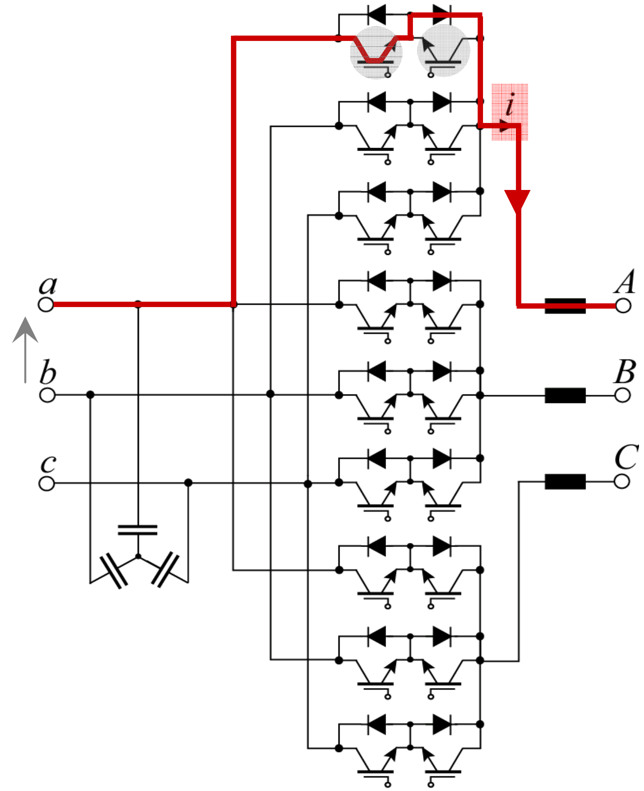

Constraints

- No Short Circuit of Mains Phases
- No Interruption of Load Current

Example: $i > 0$, $u_{ab} < 0$, $aA \rightarrow bA$

4-Step Commutation of CMC (2)

1st Step: Off

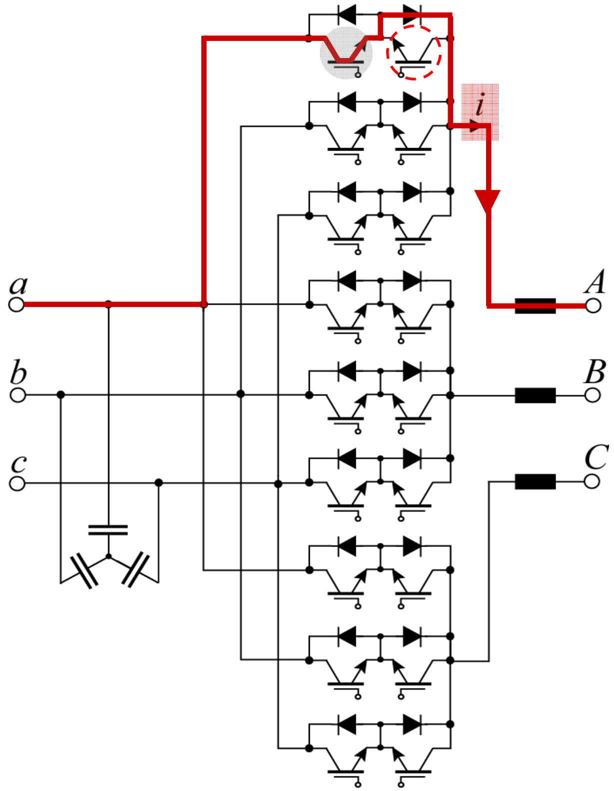

Constraints

- No Short Circuit of Mains Phases
- No Interruption of Load Current

Example: $i > 0,\ u_{ab} < 0,\quad aA \rightarrow bA$

4-Step Commutation of CMC (3)

1st Step: Off
2nd Step: On

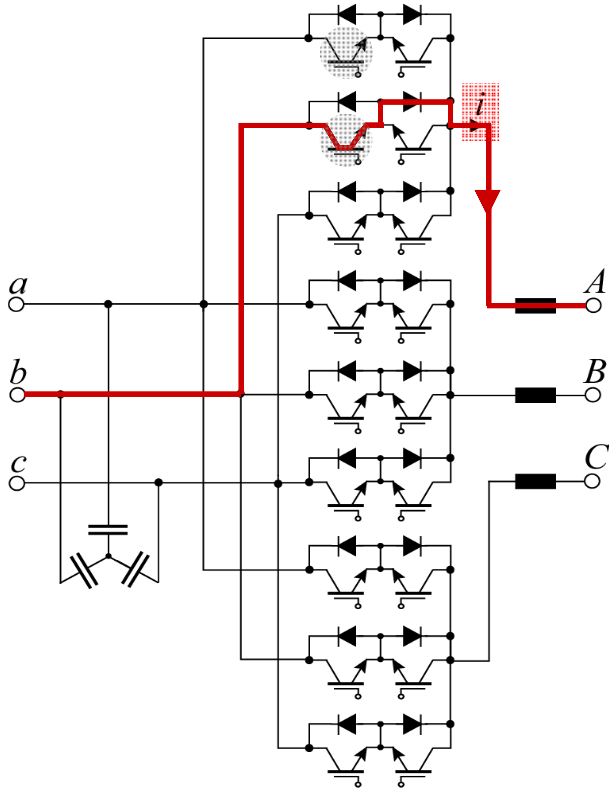

Constraints

- No Short Circuit of Mains Phases
- No Interruption of Load Current

Example: $i > 0,\ u_{ab} < 0,\quad aA \rightarrow bA$

4-Step Commutation of CMC (4)

1st Step: Off
2nd Step: On
3rd Step: Off

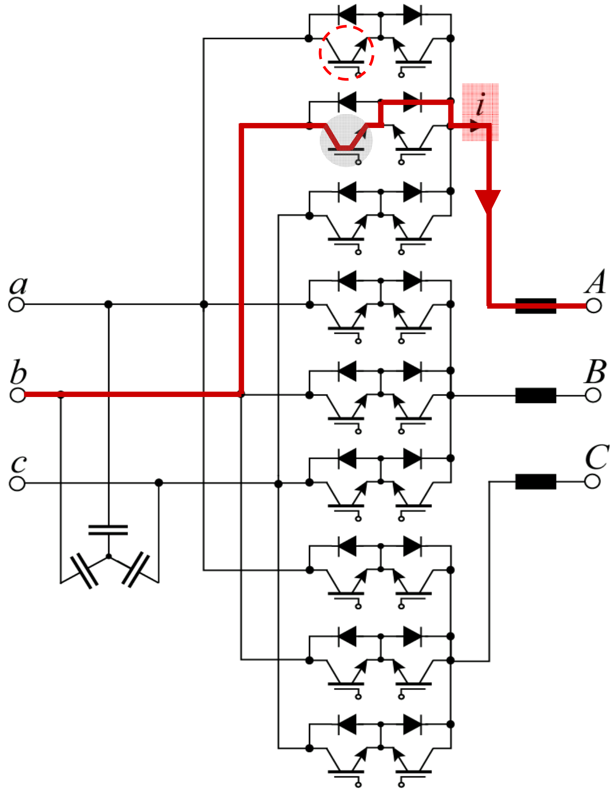

Constraints

- No Short Circuit of Mains Phases
- No Interruption of Load Current

Example: $i > 0,\ u_{ab} < 0,\quad aA \rightarrow bA$

4-Step Commutation of CMC (5)

1st Step: Off
2nd Step: On
3rd Step: Off
4th Step: On

Sequence Depends on
Direction of Output Current !

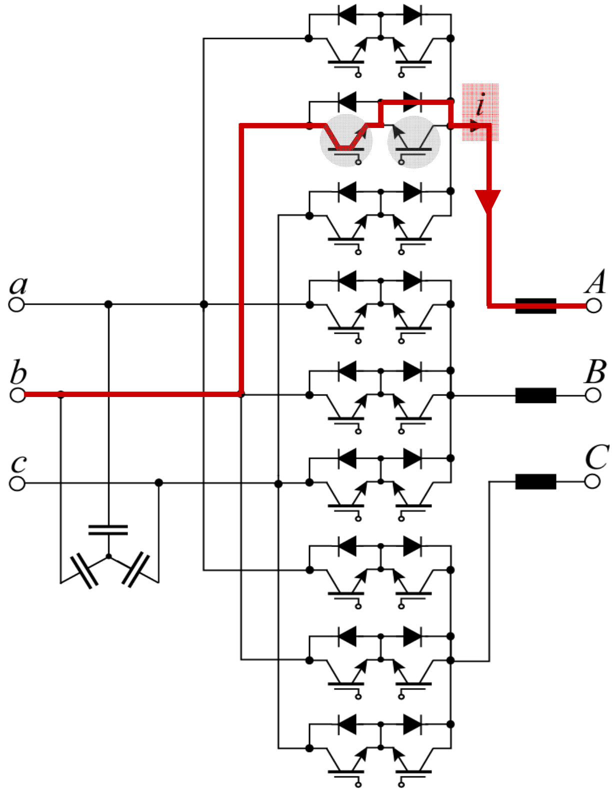

Constraints

- No Short Circuit of Mains Phases
- No Interruption of Load Current

Example: $i > 0,\ u_{ab} < 0, \quad aA \rightarrow bA$

CMC - Extensions

Multi-Level
Full-Bridge

Classification of Three-Phase AC-AC Converters

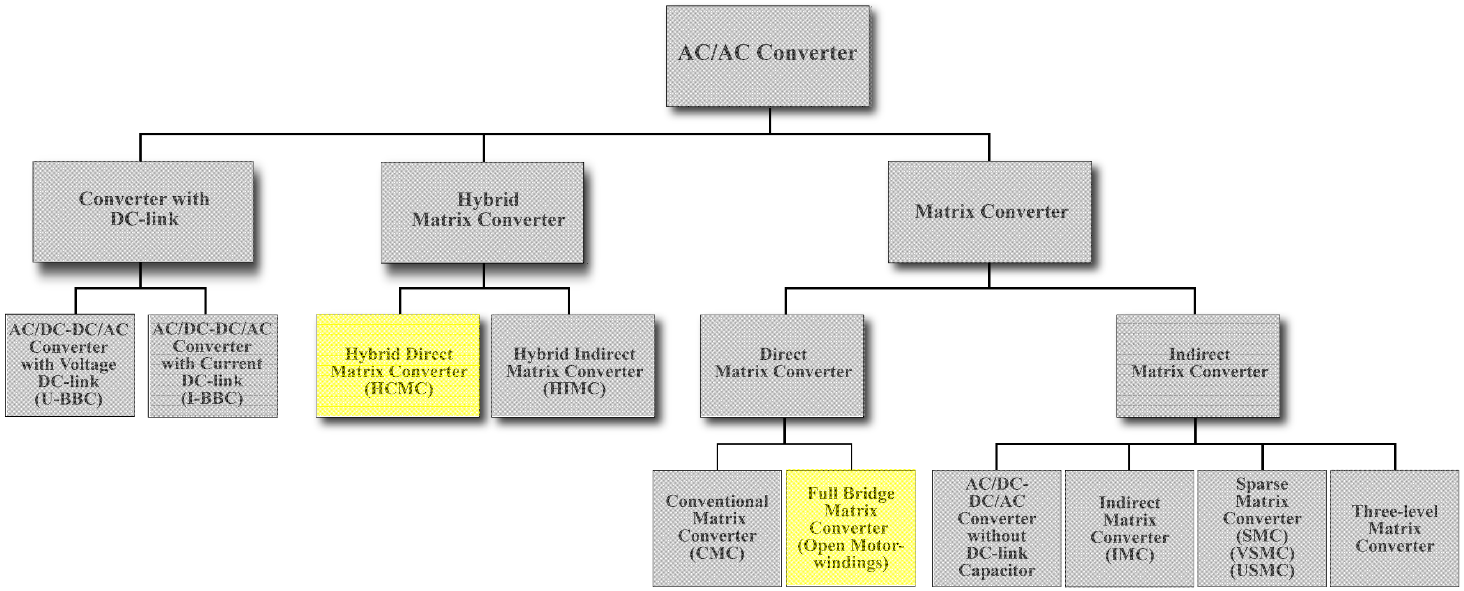

- *Hybrid CMC*
- *Full-Bridge CMC*

Hybrid CMC

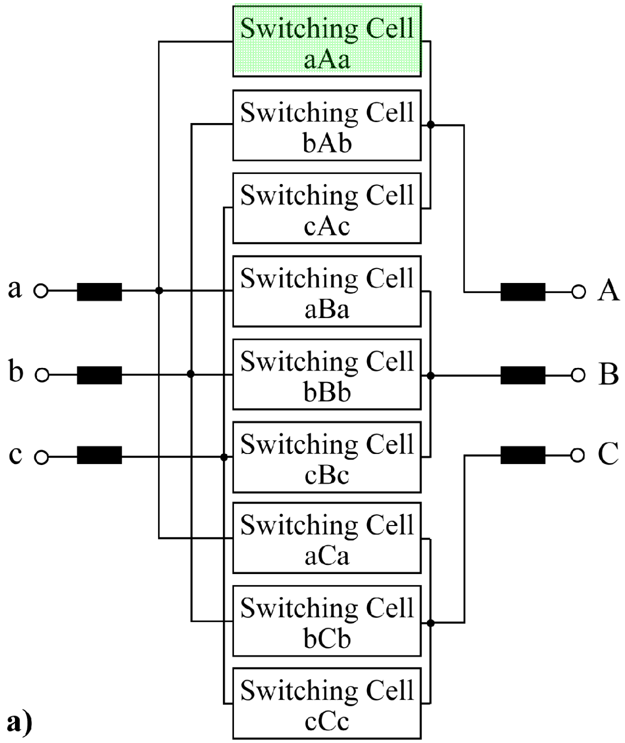

a)

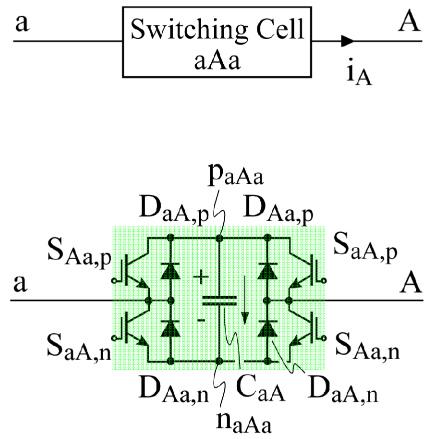

b)

B. Erickson

Full-Bridge CMC / IMC

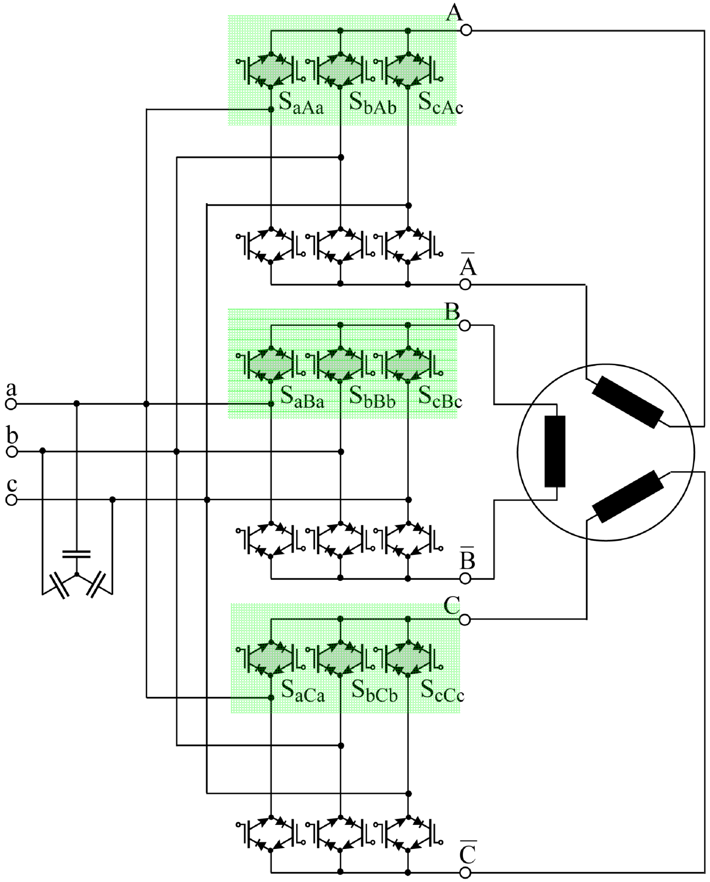

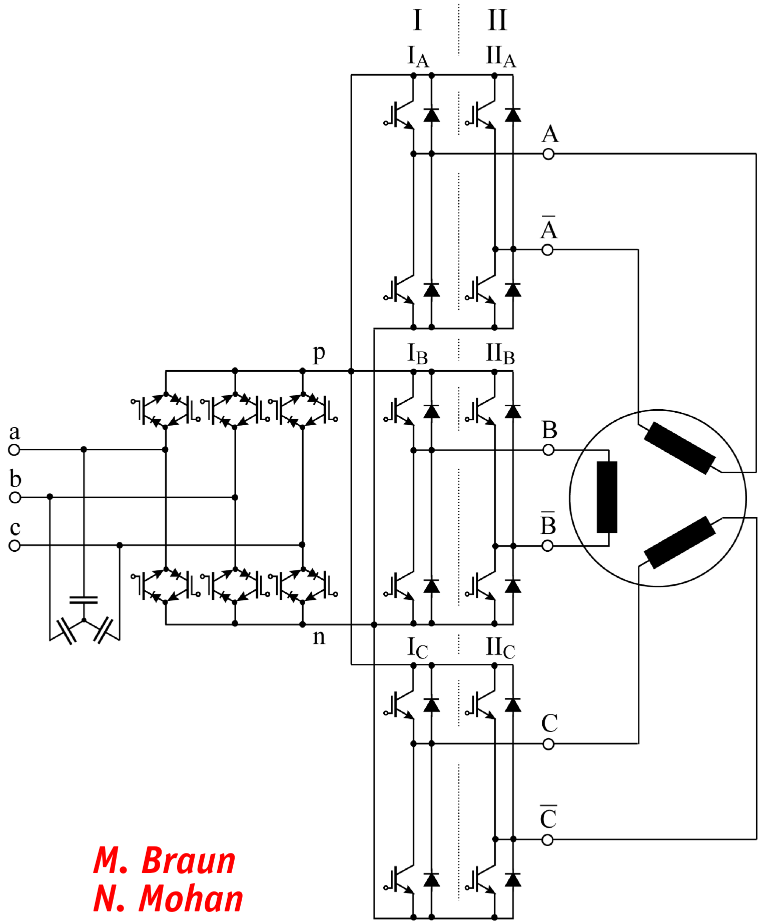

M. Braun
N. Mohan

Coffee Break !

Comparative Evaluation

DC Link Converters
Matrix Converters

Comparative Evaluation

- *Define Application / Mission Profile*
  - *M/n Operating Rage (Continuous / Overload Requirement)*
  - *Torque at Standstill*
  - *Motor Type*
  - *etc.*

- *Compare Required Total Silicon Area* (T_j< 150°C, T_c=80°C)
  - *Guarantee Optimal Partitioning of Si Area between IGBTs and Diodes*

- *Semiconductor Type / Data*
- *Thermal Properties*
- *EMI Specs*
- *Converter Type*
- *Modulation Scheme*
- *etc.*

- *M/n Operating Range*
- *Mission Profile*
- *etc.*

Virtual Converter Evaluation Platform

- *Total Si Area*
- *Operating Efficiency*
- *Average Mission Efficiency*
- *Total Mission Energy Losses*
- *EMI Filter Volume*
- *Costs*

Semiconductor Characteristics

- 4^{th} Generation Si IGBT (T & FS IGBT 4)
- EMCON4 Diode
- $T_{j,max}$ = 175°C

$T_j \leq$ 150°C
T_S = 80°C

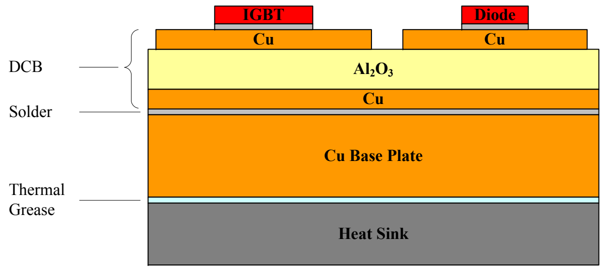

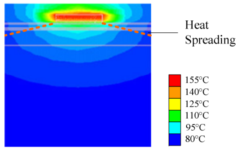

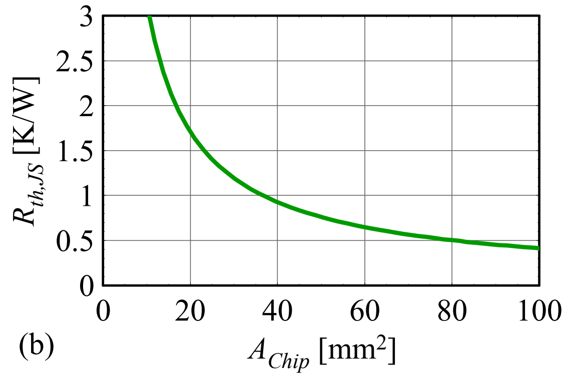

(b)

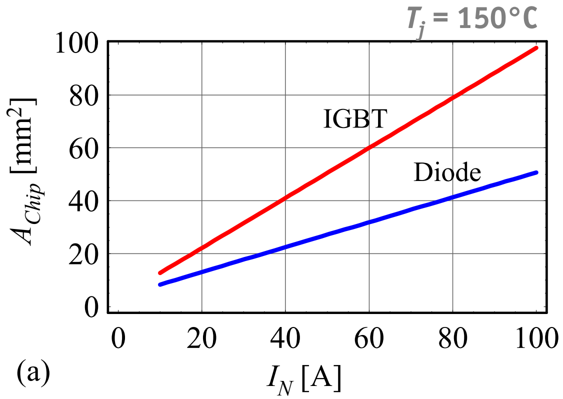

(a)

Turn-on Switching Loss Energy

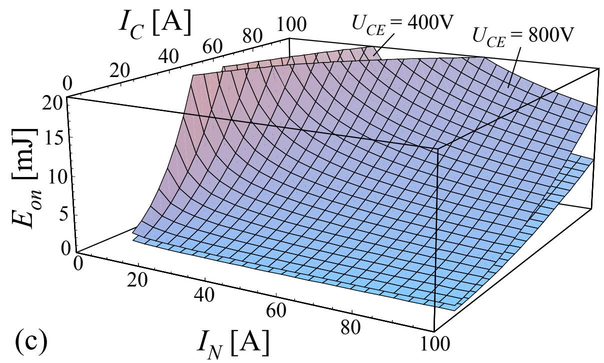

(c)

Thermal Resistance vs. Chip Area
Switching Losses vs. Switched Current / Voltage

Drive Specification

230 V, 50 Hz
15 kVA @ 90% of Max. Output Voltage
8 kHz / 24 kHz
PMSM
0...150 Hz

OP1	Nominal Output Frequency f_{2N}
OP2	$f_2 = f_1$, Mains Frequency
OP3	Close to Stand-still ($f_2 \approx 0$), Voltage Transfer Ratio $M_{12} = 0.02$

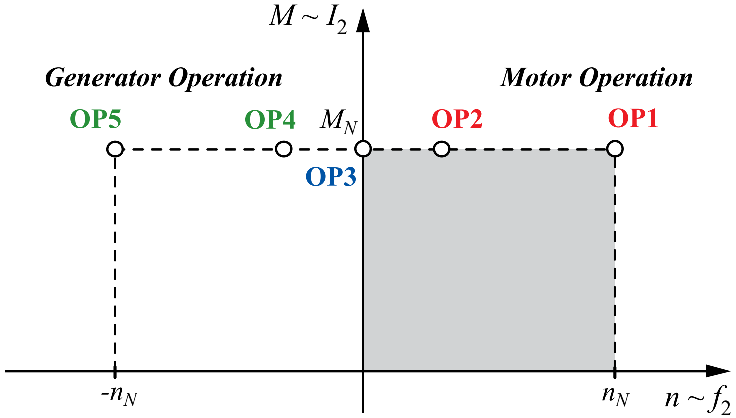

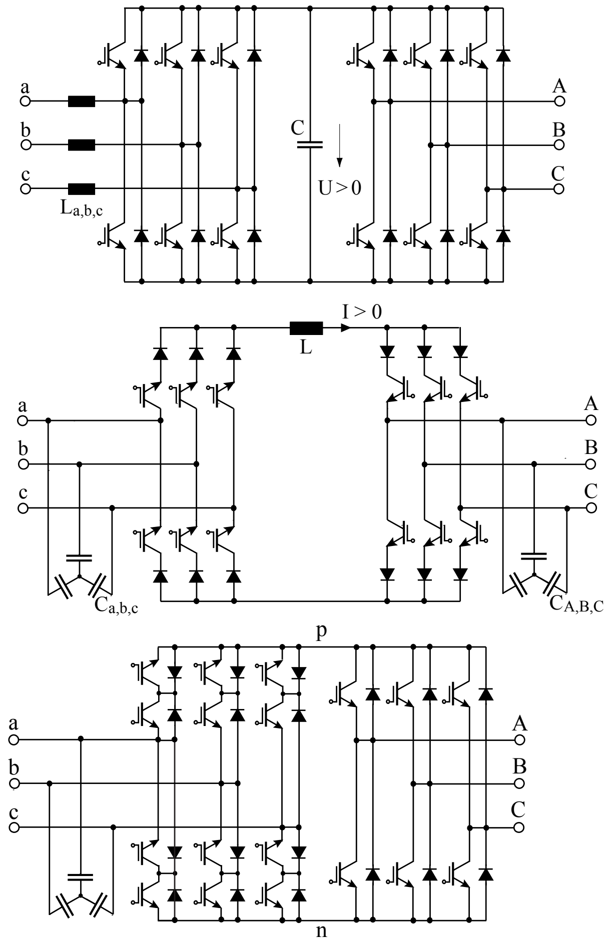

Results for OP1

f_S= 8 kHz f_S= 24 kHz

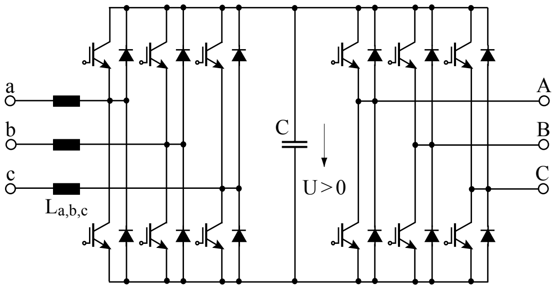

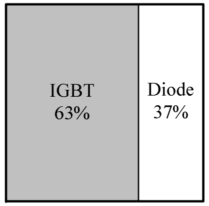

$A_{Chip} = 3.3\ \text{cm}^2$
$\eta_{OP1} = 95.7\%$

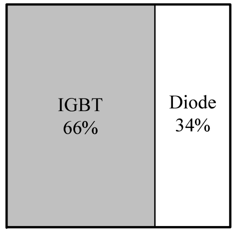

$A_{Chip} = 4.3\ \text{cm}^2$
$\eta_{OP1} = 94.4\%$

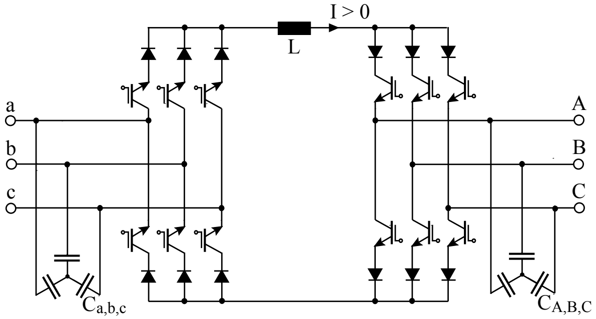

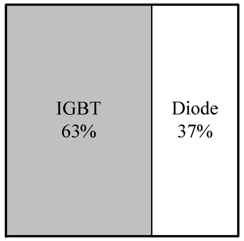

$A_{Chip} = 4.7\ \text{cm}^2$
$\eta_{OP1} = 94.0\%$

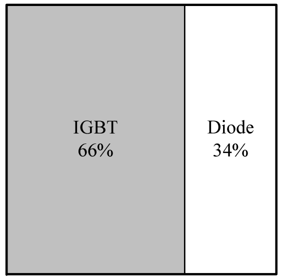

$A_{Chip} = 6.3\ \text{cm}^2$
$\eta_{OP1} = 92.3\%$

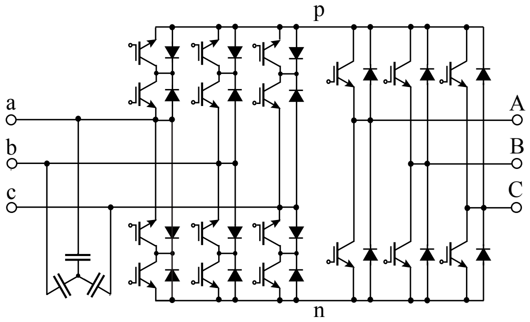

$A_{Chip} = 5.6\ \text{cm}^2$
$\eta_{OP1} = 95.3\%$

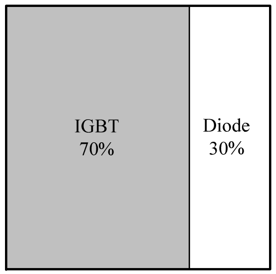

$A_{Chip} = 6.0\ \text{cm}^2$
$\eta_{OP1} = 94.8\%$

Results for OP3 ! & OP1

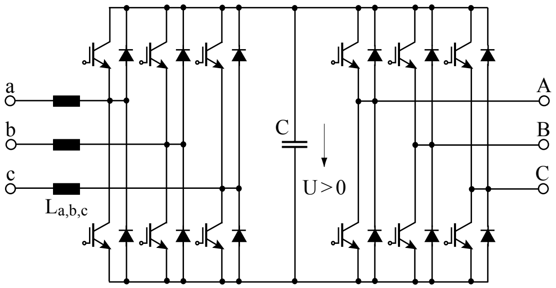

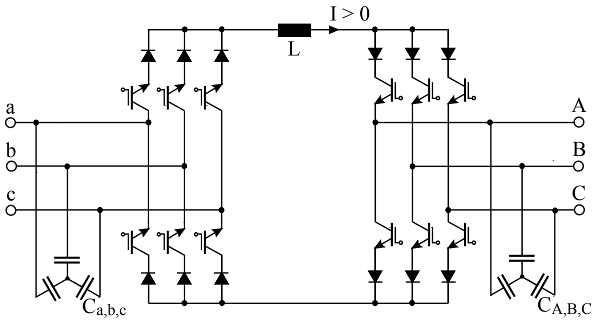

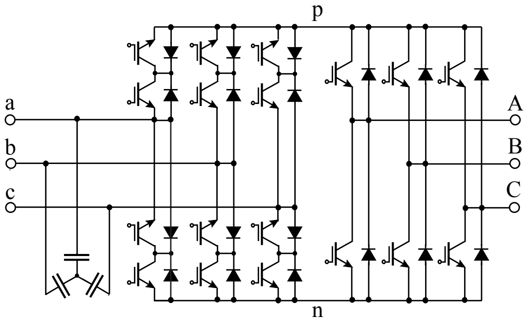

f_S= 8 kHz

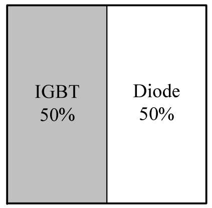

A_{Chip} = 4.8 cm^2

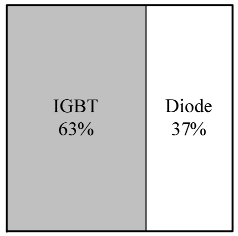

A_{Chip} = 6.3 cm^2

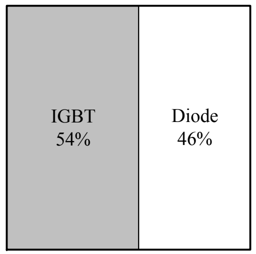

A_{Chip} = 7.5 cm^2

f_S= 24 kHz

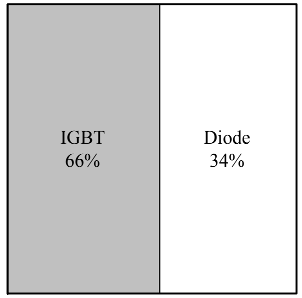

A_{Chip} = 10.3 cm^2

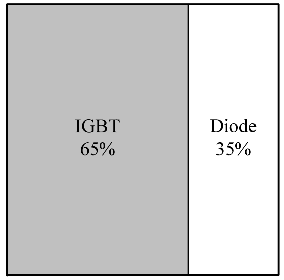

A_{Chip} = 9.2 cm^2

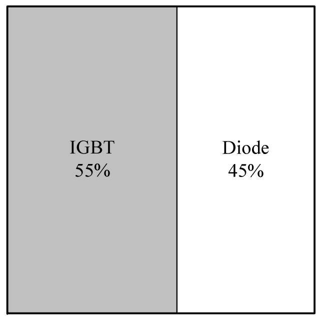

A_{Chip} = 11.7 cm^2

Efficiency vs. Switching Frequency

OP1 @ P_{2N} = 15 kVA

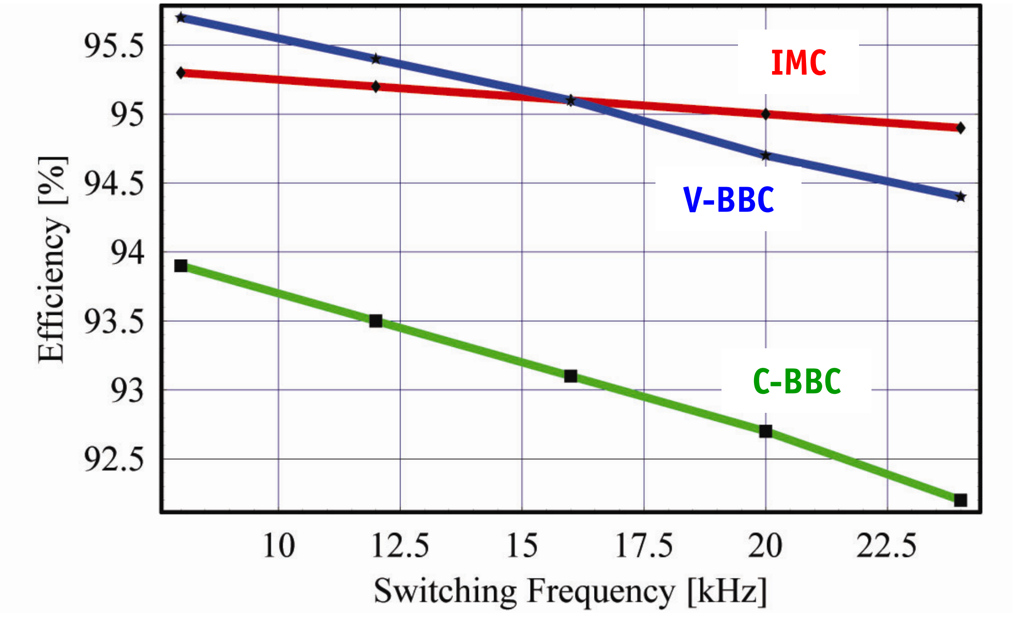

► **High Efficiency of IMC at High Switching Frequencies**

Control Porperties of AC-AC Converters

! *Uncontrolled Input Filter*

DC-DC Equivalent Circuits

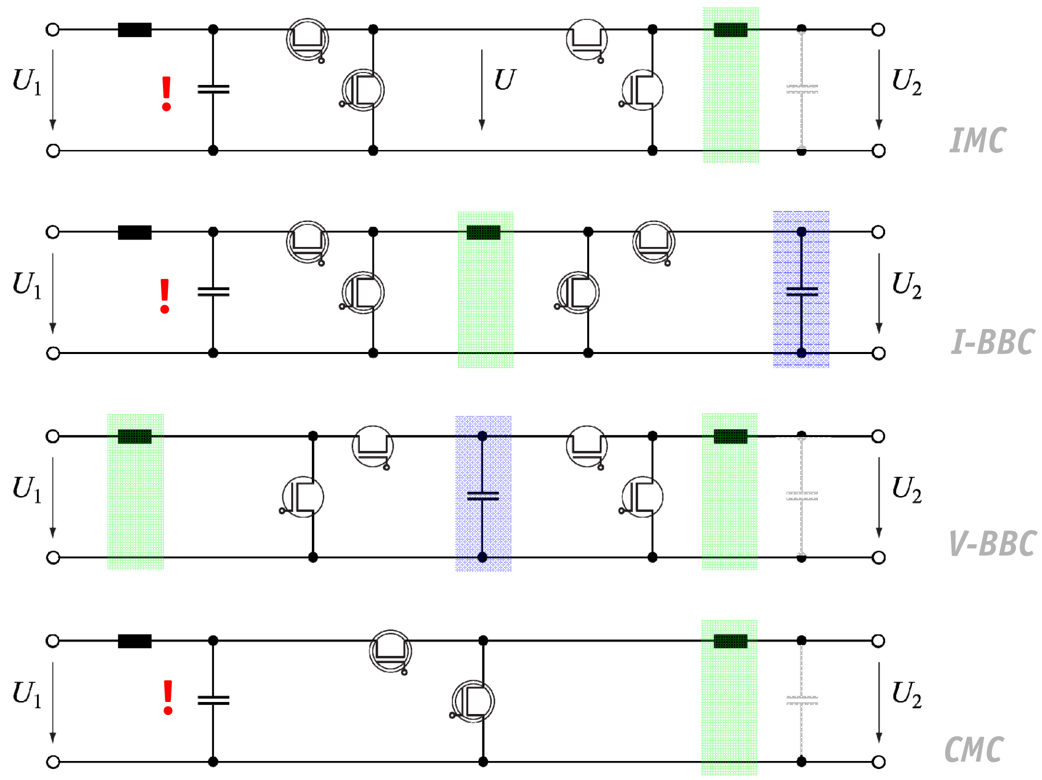

Conclusions

Conclusions (1)

- *MC is NOT an All-SiC Solution*
  - *Industry Engineers Missing Experience*
  - *86% Voltage Limit / Application Specific Motor / Silicon Area*
  - *Limited Fault Tolerance*
  - *Braking in Case of Mains Failure*
  - *Costs and Complexity Challenge*
  - *Voltage DC Link Converter could employ Foil Capacitors*

- *MC does NOT offer a Specific Advantage without Drawback*

- *EMI Filter*
- *Clamp Circuit*

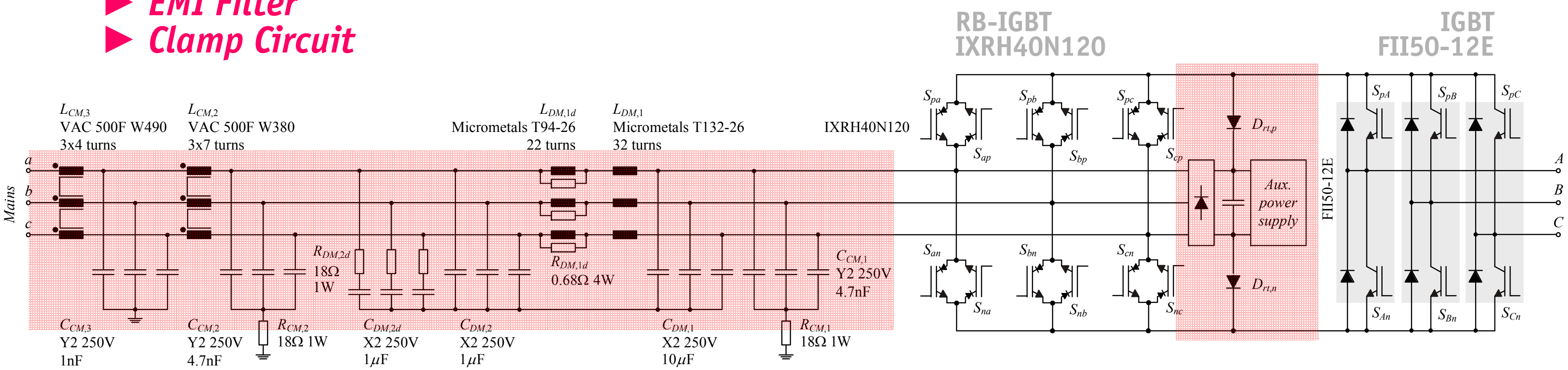

Three-Phase DM/CM Noise Separation

Three-Phase PWM Rectifier Noise Characteristic

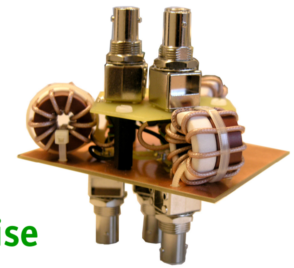

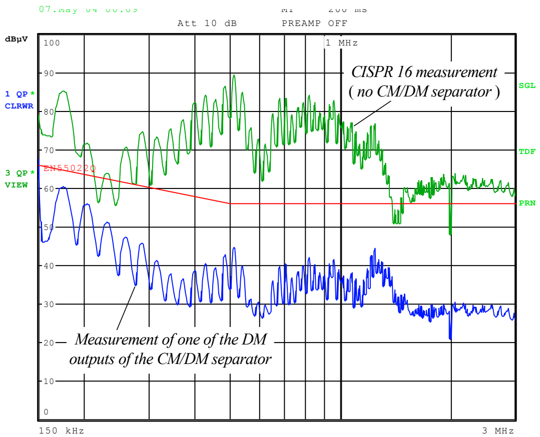

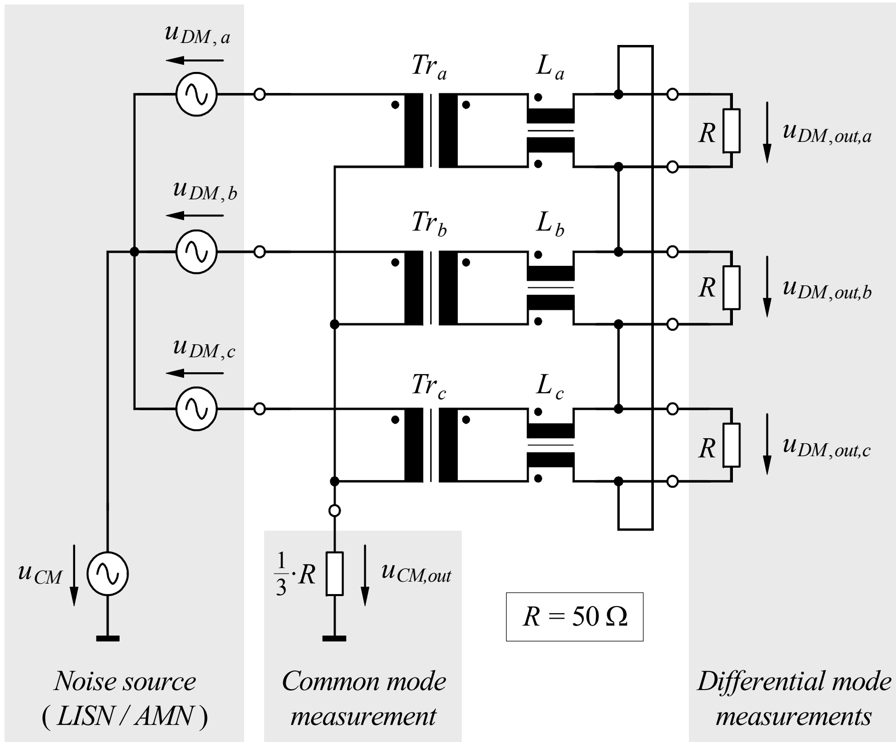

Hype Cycle of Technologies

-Gartner Group

2005
- ***Hybrid Matrix Converter***
- ***More Complicated Topologies***
- ***Refinements***

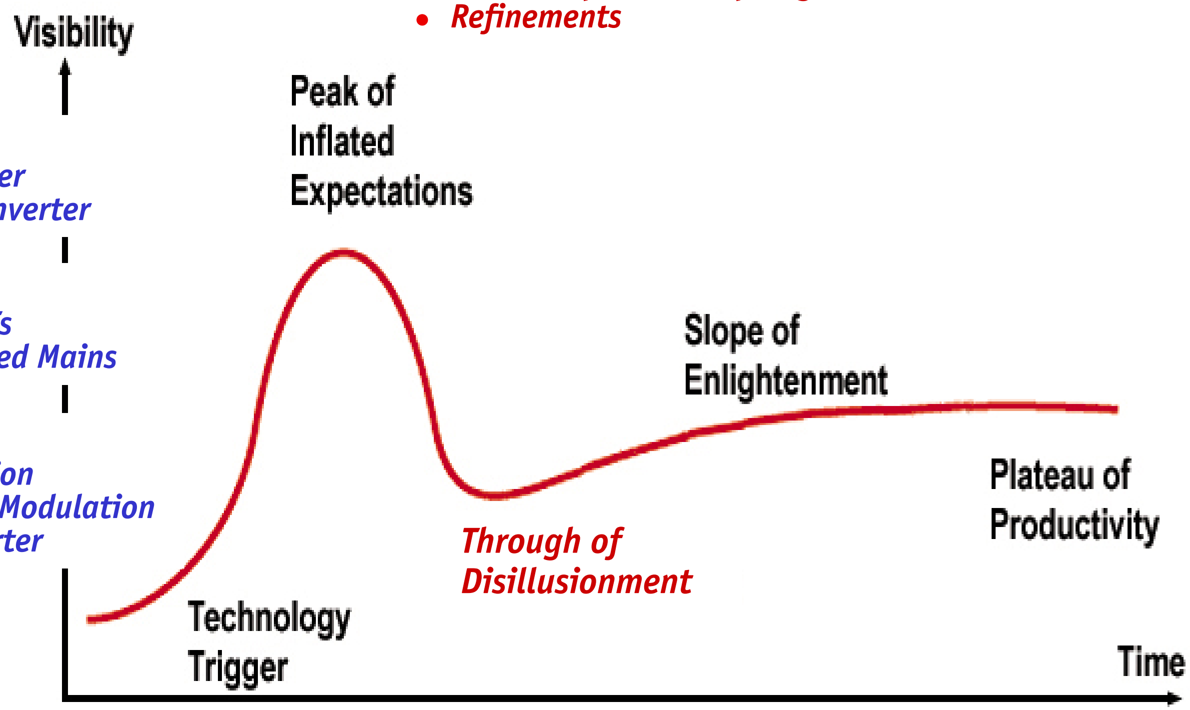

2000
- ***Sparse Matrix Converter***
- ***Three-Level Matrix Converter***

1995
- ***Reverse Blocking IGBTs***
- ***Handling of Unbalanced Mains***

1990
- ***Multi-Step Commutation***
- ***Indirect Space Vector Modulation***
- ***Indirect Matrix Converter***

1970´s
- ***Invention of Matrix Converter Topology***

Conclusions (2)

- *Research MUST Address Comprehensive System Evaluations*
  - *MC Promising for High Switching Frequency*
  - *Consider Specific Application Areas*
  - *Consider Life Cycle Costs*
  - *etc.*
- *V-BBC will be Tough Competitor anyway*
- *F^3E Might Offers a Good Compromise*
- *Integration of Functions Nearly ALWAYS Requires a Trade-off*

References (1)

[1] **I. Takahashi and Y. Itoh,** "*Electrolytic Capacitor-Less PWM Inverter,*" in *Proc. IPEC*, Tokyo, Japan, April 2–6, 1990, pp. 131–138.
[2] **K. Kuusela, M. Salo, and H. Tuusa,** "*A Current Source PWM Converter Fed Permanent Magnet Synchronous Motor Drive with Adjustable DC-Link Current*," in Proc. NORPIE, Aalborg, Denmark, June 15–16, 2000, pp. 54–58.
[3] **M. H. Bierhoff and F. W. Fuchs,** "*Pulse Width Modulation for Current Source Converters – A Detailed Concept*," in Proc. 32nd IEEE IECON, Paris, France, Nov. 7–10, 2006.
[4] **R. W. Erickson and O. A. Al-Naseem,** "*A New Family of Matrix Converters*," in Proc. 27th IEEE IECON, Denver, CO, Nov. 29–Dec. 2, 2001, vol. 2, pp. 1515–1520.
[5] **C. Klumpner and C. I. Pitic,** "*Hybrid Matrix Converter Topologies: An Exploration of Benefits*," in Proc. 39th IEEE PESC, Rhodos, Greece, June 15–19, 2008, pp. 2–8.
[6] **C. Klumpner,** "*Hybrid Direct Power Converters with Increased/Higher than Unity Voltage Transfer Ratio and Improved Robustness against Voltage Supply Disturbances*," in Proc. 36th IEEE PESC, Recife, Brazil, June 12–16, 2005, pp. 2383–2389.
[7] **L. Gyugyi, B. R. Pelly,** "*Static Power Frequency Changers – Theory , Performance, & Application*," New York: J. Wiley, 1976.
[8] **W. I. Popow,** "*Der zwangskommutierte Direktumrichter mit sinusförmiger Ausgangsspannung*," Elektrie 28, no. 4, pp. 194–196, 1974.
[9] **K. K. Mohapatra and N. Mohan,** "*Open-End Winding Induction Motor Driven with Matrix Converter for Common-Mode Elimination*," in Proc. PEDES, New Delhi, India, Dec. 12–15, 2006.
[10] **M. Braun and K. Hasse,** "*A Direct Frequency Changer with Control of Input Reactive Power*," in Proc. 3rd IFAC Symp., Lausanne, Switzerland, 1983, pp. 187–194.
[11] **D. H. Shin, G. H. Cho, and S. B. Park,** "*Improved PWM Method of Forced Commutated Cycloconverters*," in Proc. IEE, vol. 136, pt. B, no. 3, pp. 121–126, 1989.

References (2)

[12] **P. D. Ziogas, Y. Kang, and V. R. Stefanovic,** "*Rectifier-Inverter Frequency Changers with Suppressed DC Link Components*," IEEE Trans. Ind. Appl., vol. IA-22, no. 6, pp. 1027–1036, 1986.
[13] **S. Kim, S. K. Sul, and T. A. Lipo,** "*AC/AC Power Conversion Based on Matrix Converter Topology with Unidirectional Switches*," IEEE Trans. Ind. Appl., vol. 36, no. 1, pp. 139–145, 2000.
[14] **K. G¨opfrich, C. Rebbereh, and L. Sack,** "*Fundamental Frequency Front End Converter (F3E)*," in Proc. PCIM, Nuremberg, Germany, May 20–22, 2003, pp. 59–64.
[15] **B. Piepenbreier and L. Sack,** "*Regenerative Drive Converter with Line Frequency Switched Rectifier and Without DC Link Components*," in Proc. 35th IEEE PESC, Aachen, Germany, June 20–25, 2004, pp. 3917–3923.
[16] **J. Holtz and U. Boelkens,** "*Direct Frequency Converter with Sinusoidal Line Currents for Speed-Variable AC Motors*," IEEE Trans. Ind. Electron., vol. 36, no. 4, pp. 475–479, 1989.
[17] **K. Shinohara, Y. Minari, and T. Irisa,** "*Analysis and Fundamental Characteristics of Induction Motor Driven by Voltage Source Inverter without DC Link Components (in Japanese)*," IEEJ Trans., vol. 109-D, no. 9, pp. 637–644, 1989.
[18] **L. Wei and T. A. Lipo,** "*A Novel Matrix Converter Topology with Simple Commutation*," in Proc. 36th IEEE IAS, Chicago, IL, Sept. 30–Oct. 4, 2001, vol. 3, pp. 1749–1754.
[19] **J. W. Kolar, M. Baumann, F. Stögerer, F. Schafmeister, and H. Ertl,** "*Novel Three-Phase AC-DC-AC Sparse Matrix Converter, Part I - Derivation, Basic Principle of Operation, Space Vector Modulation, Dimensioning, Part II - Experimental Analysis of the Very Sparse Matrix Converter*," in Proc. 17th IEEE APEC, Dallas, TX, March 10–14, 2002, vol. 2, pp. 777–791.
[20] **L. Wei, T. A. Lipo, and H. Chan,** "*Matrix Converter Topologies with Reduced Number of Switches*," in Proc. VPEC, Blacksburg, VA, April 14–18, 2002, pp. 125–130.
[21] **F. Schafmeister,** "*Sparse und Indirekte Matrix Konverter*," PhD Thesis no. 17428, ETH Zurich, 2007.
[22] **J. W. Kolar, F. Schafmeister, S. D. Round, and H. Ertl,** "*Novel Three-Phase AC-AC Sparse Matrix Converters*," Trans. Power Electron., vol. 22, no. 5, pp. 1649–1661, 2007.

References (3)

[23] M. Y. Lee, P. Wheeler, and C. Klumpner, "*A New Modulation Method for the Three-Level-Output-Stage Matrix Converter*," in Proc. 4th PCC, Nagoya, Japan, April 2–5, 2007.
[24] C. Klumpner, M. Lee, and P. Wheeler, "*A New Three-Level Sparse Indirect Matrix Converter*," in Proc. IEEE IECON, 2006, pp. 1902–1907.
[25] M. Baumann and J. W. Kolar, "*Comparative Evaluation of Modulation Methods for a Three Phase / Switch Buck Power Factor Corrector Concerning the Input Capacitor Voltage Ripple*," in Proc. 32th IEEE PESC, Vancouver, Canada, June 17–21, 2001, vol. 3, pp. 1327–1333.
[26] J. W. Kolar, H. Ertl, and F. C. Zach, "*Power Quality Improvement of Three-Phase AC-DC Power Conversion by Discontinuous-Mode 'Dither'-Rectifier Systems*," in Proc. 6th Int. (2nd European) Power Quality Conf. (PQ), Munich, Germany, Oct. 14–15, 1992, pp. 62–78.
[27] J. Oyama, T. Higuchi, E. Yamada, T. Koga, and T. A. Lipo, "*New Control Strategy for Matrix Converter*," in Proc. 20th IEEE PESC, Milwaukee, WI, June 26–29, 1989, vol. 1, pp. 360–367.
[28] Burany, N., "*Safe Control of Four-Quadrant Switches*," in Conf. Rec. IEEE IAS, San Diego, CA, Oct. 1–5, 1989, pp. 1190–1194.
[29] M. Ziegler and W. Hofmann, "*A New Two Steps Commutation Policy for Low Cost Matrix Converter*," in Proc. 41st IEEE PCIM, Nuremberg, Germany, June 6–8, 2000, pp. 445–450.
[30] W. Hofmann and M. Ziegler, "*Schaltverhalten und Beanspruchung bidirektionaler Schalter in Matrixumrichtern*," ETG/VDE Fachbericht 88 der Fachtagung Bauelemente der Leistungselektronik, Bad Nauheim, Germany, April 23–24, 2002, pp. 173–182.
[31] M. Venturini, "*A New Sine Wave In, Sine Wave Out Conversion Technique Eliminates Reactive Elements*," in Proc. Powercon 7, San Diego, CA, 1980, pp. E3-1–E3-15.
[32] J. W. Kolar and F. C. Zach, "*A Novel Three-Phase Utility Interface Minimizing Line Current Harmonics of High-Power Telecommunications Rectifier Modules*," Trans. Ind. Electron., vol. 44, no. 4, pp. 456–467, 1997.
[33] J. W. Kolar, U. Drofenik, and F. C. Zach, "*VIENNA Rectifier II - A Novel Single-Stage High-Frequency Isolated Three-Phase PWM Rectifier System*," Trans. Ind. Electron., vol. 46, no. 4, pp. 674 – 691, 1999.

References (4)

[34] **K. Mino, Y. Okuma, and K. Kuroki,** "*Direct-Linked-Type Frequency Changer Based on DC-Clamped Bilateral Switching Circuit Topology*," Trans. Ind. Electron., vol. 34, no. 6, pp. 1309–1317, 1998.

[35] **D. Casadei, G. Serra, G., A. Tani, and P. Nielsen,** "*Performance of SVM Controlled Matrix Converter with Input and Output Unbalanced Condition*," in Proc. 6th European Conf. on Power Electron. and Appl. (EPE), Sevilla, Spain, Sept. 19–21, 1995, vol. 2, pp. 628–633.

[36] **Schafmeister, F., Baumann, M., and Kolar, J.W.,** "*Analytically Closed Calculation of the Conduction and Switching Losses of Three-Phase AC-AC Sparse Matrix Converters*," Proc. of the 10th International Power Electronics and Motion Control Conference, Dubrovnik, Croatia, Sept. 9 - 11, CD-ROM, ISBN: 953-184-047-4 (2002).

[37] **Schafmeister, F., Herold, S., and Kolar, J.W.,** "*Evaluation of 1200V-Si-IGBTs and 1300V-SiC-JFETs for Application in Three-Phase Very Sparse Matrix AC-AC Converter Systems*," Proc. of the 18th Annual IEEE Applied Power Electronics Conference and Exposition, Miami Beach (Florida), USA, February 9 – 13, Vol. 1, pp. 241 - 255 (2003).

[38] **Kolar, J.W., and Schafmeister, F.,** "*Novel Modulation Schemes Minimizing the Switching Losses of Sparse Matrix Converters,*" Proc. of the 29th Annual Conference of the IEEE Industry Electronics Society, Roanoke (VA), USA, Nov. 2 - 6, pp. 2085 - 2090 (2003).

[39] **Heldwein, M.L. , Nussbaumer, T. , and Kolar, J.W.,** "*Differential Mode EMC Input Filter Design for Three-Phase AC-DC-AC Sparse Matrix PWM Converters*," Proc. of the 35th IEEE Power Electronics Specialists Conference, Aachen, Germany, June 20 - 25, CD-ROM, ISBN: 07803-8400-8 (2004).

[40] **Heldwein, M.L. , Nussbaumer, T. , Beck, F., and Kolar, J.W.,** "*Novel Three-Phase CM/DM Conducted Emissions Separator*," Proc. of the 20th Annual IEEE Applied Power Electronics Conference and Exposition, Austin (Texas), USA, March 6 - 10, Vol. 2, pp. 797 - 802 (2005).

[41] **Friedli, T., Heldwein, M.L., Giezendanner, F., and Kolar, J. W.,** "*A High Efficiency Indirect Matrix Converter Utilizing RB-IGBTs*," Proc. of the 37th Power Electronics Specialists Conference, Jeju, Korea, June 18 - 22, CD ROM, ISBN: 1-4244-9717-7, (2006).

References (5)

[42] **Round, S., Schafmeister, F., Heldwein, M.L., Pereira, E., Serpa, L., and Kolar, J.W.,** "*Comparison of Performance and Realization Effort of a Very Sparse Matrix Converter to a Voltage DC Link PWM Inverter with Active Front End*," IEEJ Transactions of the Institute of Electrical Engineers of Japan, Volume 126-D, Number 5, May 2006, pp. 578 - 588.

[43] **Friedli, T., Round S.D., Hassler D., Kolar J.W.,** "*Design and Performance of a 200 kHz All-SiC Current Source Converter*", Proc. Industrial Applications Society IAS'08, Edmonton, Canada, Oct. 5-9, 2008.

Thank You !